Investigations into the utility of aminoboronates as bifunctional catalysts

Giles, Richard Lloyd

Investigations into the utility of aminoboronates as bifunctional catalysts

A thesis submitted to the University of Durham for the degree of Doctor of Philosophy

Richard Lloyd Giles

Department of Chemistry, Durham

2006

Preface

To the best of my knowledge, the research described in this thesis is entirely original except where due reference is made and has not been previously submitted in support of an application for any other degree or qualification at this or any other university or institute of learning.

R. L. Giles

Durham, 7th April 2006

To Monica

Contents

i	Acknowledgements			11
ii	Abstract			13
iii	Abbreviations list			14
1	Introduction			21
	1.1	Background		21
	1.2	Mode of action		21
		1.2.1	Lewis acid - Lewis base systems	23
			1.2.1.1 Carbonyl reduction	23
			1.2.1.2 Alkylations, alkynylations and allylations	27
			1.2.1.3 Cyanations	30
			1.2.1.4 β-lactam synthesis	33
		1.2.2	H-bonding - functional group	34
			1.2.2.1 Bifunctional thioureas	35
			1.2.2.2 Reduction	38
		1.2.3	Metal - H-bonding	39
			1.2.3.1 Asymmetric allylic alkylation	39
			1.2.3.2 Asymmetric cyclopropanation	40
		1.2.4	Metal - reactive ligand	41
			1.2.4.1 Aldol	41
			1.2.4.2 Epoxidation	43
		1.2.5	Nucleophilic Lewis base - functional group	45
			1.2.5.1 Proline-based enamine catalysts	45
			1.2.5.2 Aza-Bayliss-Hillman	49
	1.3	Conclusions – Introduction		51

2 Results and discussion 52
2.1 Aims and overview of the project 52
2.2 Catalyst design 53
2.3 Catalyst synthesis and structure 54
2.3.1 *N,N*-Dialkylbenzylamine-2-boronic acid series and related structures 55
2.3.1.1 Directed *o*-lithiation methodology 56
2.3.1.2 Reductive amination methodology 60
2.3.1.3 Spectroscopy of *N,N*-dialkylbenzyl amine-2-boronic acids 66
2.3.1.4 Fluorinated derivatives 68
2.3.1.5 Bromo-(*S,S*)-(-)-bis(α-methylbenzyl) amine]-*N*-benzamides – Miyaura methodology 70
2.3.1.6 Summary – *N,N*-Dialkylbenzylamine -2-boronic acid series 76
2.3.2 Quinoline-8-boronic acid series 77
2.3.3 2-Phenylpyridine-2'-boronic acid series 79
2.3.4 1-Dimethylaminonaphthalene-8-boronic acid series 82
2.3.4.1 Directed *o*-lithiation methodology 82
2.3.4.2 Fluorinated derivative 84
2.3.4.3 Spectroscopy 85
2.3.4.4 Summary – *N,N*-Dimethylnaphthyl-1-amine-8-boronic acid series 89
2.3.5 *N,N*-Dimethylaniline-2-boronic acid series 90
2.3.6 Aniline-3-boronic acid series 91
2.3.7 Guanidinobenzene-3-boronic acid series 92
2.3.8 Conclusions – Synthesis 93
2.4 Complexation studies of arylboron difluorides 96
2.5 Catalyst *vs.* Reaction screening 100

2.5.1 Automated methods - Liquid Handling workstation 100
2.5.2 Multi-reaction screening 102
2.5.3 Phenylacetylene and benzaldehyde 109
2.5.4 Nitro-aldol and aldol reactions 109
2.5.5 Conclusions – Catalyst *vs.* Reaction screening 110
2.6 Direct amide bond formation 111
2.6.1 Introduction – Direct amide bond formation 111
2.6.2 Identification of catalysts 114
2.6.3 Substrate range 117
2.6.4 Optimisation of conditions 118
2.6.4.1 Solvent 119
2.6.4.2 Reaction molarities 120
2.6.4.3 Dehydration method 121
2.6.4.4 Summary – Optimisation of conditions 122
2.6.5 Effect of molecular sieves 122
2.6.6 Rate determination 124
2.6.6.1 Methodology 124
2.6.6.2 Experimental set-up 126
2.6.6.3 Results – Rate determination 127
2.6.7 Deboronation studies 136
2.6.8 Initiation temperature determination 139
2.6.9 Amide bond cleavage 140
2.6.10 Direct ester bond formation 141
2.6.11 Conclusions – Direct amide bond formation 142
2.7 Concluding remarks 148
2.8 Further work 149

3 Experimental 151
3.1 General experimental details 151
3.2 Catalyst synthesis and structure 152
3.2.1 Synthesis of *N,N*-bis-((S)-α-methylbenzyl)benzamide 211 152
3.2.2 Synthesis of *N,N*-bis-((S)-α-methylbenzyl)benzylamine 227 153
3.2.3 Synthesis of *N,N*-diisopropylbenzyl amine-2-boronic acid 206 154
3.2.4 Synthesis of *N*-morpholinobenzylamine-2-boronic acid 235 155
3.2.5 Synthesis of *N*-methyl-*N*-((R)-α-methyl benzyl)benzylamine-2-boronic acid 236 156
3.2.6 Synthesis of Hydrogen *N,N*-diisopropyl-benzylamine-2-trifluoroborate 239 157
3.2.7 Synthesis of 2-bromo-*N,N*-bis-((S)-α-methylbenzyl)benzamide 248 158
3.2.8 Synthesis of 3-bromo-*N,N*-bis-((S)-α-methylbenzyl)benzamide 250 159
3.2.9 Synthesis of hydrogen quinoline-8-trifluoroborate 254 160
3.2.10 Synthesis of 2-phenylpyridine 258 161
3.2.11 Synthesis of dimethyl-[8-(diisopropyl oxyborolyl)-naphthalen-1-yl]amine 271 161
3.2.12 Synthesis of 1,3,5-tris(1-*N,N*-dimethyl amino)-8-naphthylboroxine 270 163
3.2.13 Synthesis of dimethyl-[8-(4,4,5,5-tetramethyl-[1,3,2]dioxaborolan-2-yl)-amine 272 163
3.2.14 Synthesis of *N,N*-dimethyl-[8-(difluoro borolyl)-naphthalen-1-yl]-amine 273 164

3.2.15 Synthesis of 3-(4,4,5,5-tetramethyl-[1,3,2]dioxaborolan-2-yl)-phenylamine 280 165
3.2.16 Synthesis of hydrogen 3-aminobenzenetrifluoroborate 281 166
3.3 Complexation studies of fluorinated boron Lewis acids 167
3.3.1 Synthesis of potassium *o*-nitrobenzenetrifluoroborate 290 168
3.3.2 Representative procedure for NMR shift experiments 168
3.4 Catalyst *vs* Reaction screening 168
3.4.1 Microdart operation 168
3.5 Direct amide bond formation 170
3.5.1 Synthesis of *N*-methylbenzylamine benzoate 333 170
3.5.2 Representative procedures – Amide bond forming experiments 170
3.5.2.1 Synthesis of *N*-benzyl-4-phenyl butyramide 332 171
3.5.2.2 Synthesis of *N*-4-phenylbutyl benzamide 341 172
3.5.2.3 Synthesis of *N*-4-phenylbutyl-4-phenylbutyramide 342 172
3.5.2.4 Synthesis of *N*-morpholino benzamide 343 173
3.5.2.5 Synthesis of *N*-morpholino-4-phenylbutyramide 344 173
3.5.2.6 Synthesis of *N*-benzylbenzamide 328 174
3.5.2.7 Synthesis of *N*-morpholinotrimethyl acetamide 376 174

3.5.2.8 Synthesis of *N*-benzyltrimethyl acetamide 377 174
3.5.3 Direct amide bond formation – Kinetics experiments 175
3.5.3.1 Representitive procedure – Amide bond forming kinetics experiments 175
3.5.4 Deboronation studies 175
3.5.5 Initiation temperature determination 178

4 References 180

Appendixes – Supplied on attached CD-ROM

Appendix A	**Crystallographic data**
Appendix B	**HPLC data and calculations for amide bond formation experiments**

i Acknowledgements

First and foremost I would like to offer my sincere thanks to Dr. Andy Whiting, my supervisor, for his advice, encouragement, support and optimism, which have been invaluable during this project.

I would like to thank Dr. Gillian Smith for lending a fresh perspective to the project, for injecting her infectious enthusiasm into the work and for making my time in her group so enjoyable.

I have been privileged work in two fantastic groups during these studies; in the Whiting group in Durham and in Gill Smith's group in Tonbridge. Thanks go to Drs. Hayley Wan, John Hannan, Alan Bowden, Leonard Patrick, Carl Thirsk, David Jay, Thorben Schütz, Christophe Grosjean and Damien Hérault who have always been ready to contribute their considerable wit and wisdom to all aspects of the work. Thanks also to Steve Twiddle, Alex Blatch, Kenny Arnold and Sam Coghlan who have provided much fun and laughter. Other friends with whom I have shared this journey include Milena Trmcic, John Henry, Chris Murray, Simon Walton, Caroline Bridgends, Johnathan Knowles, Chris Hargreaves, Matt Cartwright, Karel Aelvoet, Barney Squires, Mike Kingswood, Mark Armitage, Hannah Wankling, Mike Hope and last but not least Jelena Trmcic.

None of this research would have been possible without the considerable help and support of the technical staff at both Durham and Tonbridge. Thanks go to Dr. Alan Kenwright and his NMR group for the excellent service they provide, Drs. Mike Probert and Andrei Batsanov for crystal structures, Dr. Mike Jones and the EPSRC service at Swansea for mass spectrometry and Dr. John Warren and his analytical group at Tonbridge. Thanks also go to Elizabeth Wood, Jimmy Lincoln and Tony Baxter in stores for helping the smooth running of the project and the Durham glassblowers Peter Coyne and Malcolm Richardson for their craftsmanship.

Funding for this research was supplied by EPSRC and GlaxoSmithKline.

Finally I would like to acknowledge my family who have supported me through the toughest parts of my life in the past four years of this work.

ii Abstract

This project has been concerned with identification and refinement of any bifunctional catalytic properties of arylaminoboronic acids and derivatives. Stage one of the project was directed towards the design, synthesis and structural understanding of several series of novel and interesting bifunctional boronic acids and derivatives, including the *N,N*-dialkylbenzylamine-2-boronic acid series and the 1-dimethylaminonaphthene-8-boronic acid series. Stage two involved the high-throughput testing of potential catalysts. Direct amide bond formation (i.e. directly from carboxylic acid and amine) was identified from stage two as an interesting reaction and was investigated further in stage three of the project. *N,N*-Diisopropylamine-2-boronic acid was found to be an effective catalyst for this reaction. In this area in particular we made many exciting and sometimes surprising findings: the thermal direct amide bond forming reaction is effective under certain circumstances, the current industry standard catalyst - 3,4,5-trifluorobenzeneboronic acid - appears to deboronate under some of the published reaction conditions, and boric acid is frequently more effective than the significantly more expensive boronic acid catalysts for the direct amide bond forming reaction.

iii Abbreviations List

‡	Transition state
Ac	Acyl
acac	Acetylacetone or acetylacetonide (where counterion)
a.k.a.	Also known as
approx.	Approximately
aq.	Aqueous
Ar	Generic aryl group
B	Base
BINOL	1,1'-Bi-2,2'-naphthol
BINOLAM	1,1'-Bi-(bis(3,3'-diethylaminomethylene))-2,2'-naphthol
Bn	Benzyl
b.p.	Boiling point
br	Broad
^{t}Bu	*tert*-Butyl

^{n}Bu	Straight chain-butyl
^{s}Bu	*sec*-Butyl
ca.	*Circa*, about (Latin)
calcd	Calculated
Cat.	Catalyst
Cats.	Catalysts
CBS	Corey-Bakshi-Shibata
CN	Cyano, nitrile
Cpd.	Compound
DAIB	(-)-3-*exo*-(Dimethylamino)isobornenol
DCM	Dichloromethane
d.e.	Diastereomeric excess
DEAD	Diethylazodicarboxylate
dil.	Dilute
DMAP	*N*,*N*-Dimethyl-4-aminopyridine
DMF	*N*,*N*-Dimethylformamide
DMPU	*N*,*N*'-Dimethyl-*N*,*N*'-propylene urea

DMSO	Dimethylsulfoxide
DPPF	1,1'-Bis(diphenylphosphino)ferocene
Dr.	Doctor
d.r.	Diastereomeric ratio
E	Electrophile
e.e.	Enantiomeric excess
e.g.	*Exampli gratia*, for example (Latin)
eq.	Equivalents
ESMS	Electrospray mass spectrometry
$ESMS^+$	Electrospray mass spectrometry positive ion current
$ESMS^-$	Electrospray mass spectrometry negative ion current
esp.	Especially
Et	Ethyl
et al.	*Et alii / et aliae*, and others (Latin)
EWG	Electron withdrawing group
FG	functional group

FTIR	Fourier transform infra red
h	Hours
H-bonding	Hydrogen-bonding
HPLC	High performance liquid chromatography, (a.k.a. high pressure liquid chromatography)
HPLC-MS	High performance liquid chromatography with mass spectrometric analysis
HPLC-UV	High performance liquid chromatography with ultraviolet light absorbance analysis
HPLC-UV/MS	High performance liquid chromatography with ultraviolet light absorbance and mass spectrometric analysis
HRMS	High resolution mass spectrometry
i.e.	*Id est*, that is to say (Latin)
IR	Infra red (light)
k	Rate constant
LA	Lewis acid
LB	Lewis base
LTMP	Lithium 2,2,6,6-tetramethylpiperidine
m	Mass

M	Metal
Me	Methyl
min	Minutes
mol	Mole
Mol.	Molecular (esp. preceding sieves)
m.p.	Melting point
MS	Mass spectrometric analysis
m/z	Mass charge ratio
NMR	Nuclear magnetic resonance
Nu	Nucleophile
Ph	Phenyl
PMP	*p*-Methoxyphenol
ppm	Parts per million
^{i}Pr	*iso*-Propyl
R	Generic organic structure
R_L	Large generic organic structure
R_S	Small generic organic structure

r.t.	Room temperature
S	Substrate
s	Strong
sat.	Saturated
Tf	Triflic, trifluoroacyl
TFA	Trifluoroacetic acid
THF	Tetrahydrofuran
TLC	Thin layer chromatography
TMEDA	Tetramethylethylenediamine
TMS	Trimethylsilyl or tetramethylsilane (esp. w.r.t. NMR)
TMSCl	Trimethylsilylchloride
TMSCN	Trimethylsilylcyanide
TMSOMe	Trimethylsilylmethoxide
Tol.	Toluene
Ts	Tosyl, toluenesulfonyl
UV	Ultraviolet (light)

Vis.	Visible (light)
vs.	Versus
w.r.t.	With respect to
w/v	Weight/volume ratio
X	Unspecified atom
Y	Unspecified atom
z	Charge

1 Introduction

1.1 Background

Organic chemists have long wondered at enzymatic systems where complex transformations are achieved catalytically, often with great stereoselectivity, diastereoselectivity, regioselectivity and chemoselectivity.[1] It is well understood that enzymes generally act by the synergistic action of a combination of well placed, but often unspectacular functional groups. However, most synthetic catalytic systems developed to date use the principle of activation of a single substrate or dual activation of two substrates at the same centre.[2, 3] This is usually achieved by utilising transition metal complexes, whereas metals are present in only about half of known enzyme active sites.

Recently, the development of bifunctional catalysts[4-7] and enzyme mimics[8-10] has created a collection of small molecules analogous to enzymes. The purpose of this introduction is to survey the area of small molecule bifunctional catalysis, concentrating on successful, homogeneous, enantioselective and regioselective reactions where something is understood about the mechanism of the reaction and bifunctionality is clearly demonstrated. Discussions of hetero- and homo-bimetallic catalysts[11-13] are not included except where hydrogen is the metal. Although these areas are well studied, such compounds were not investigated as part of this project.

1.2 Mode of Action

The majority of traditional monofunctional chiral catalysts function in one of the two following ways:

1) The catalyst will bind or react with the substrate, simultaneously activating it and inducing a chiral environment, allowing a second

reagent to attack in a stereoselective manner. e.g. Chiral DMAP derivatives.[14]

2) The single centre binds two or more substrates stereoselectively in the correct orientation to form bonds. This intra-molecularisation of the reaction on a chiral / stereo-controlled framework allows the reaction to proceed selectively. e.g. Heck reaction.[15]

Bifunctional catalysis involves a mechanism in which the two functional groups of a catalyst molecule are involved in the rate-determining step. The synergistic action of the groups increases the reaction rate to a greater degree than either functionality alone, or both functionalities together in the same reaction but in separate molecules.

In this introduction the bifunctional catalysts under review are organised into five classes (Figure 1):

1) Catalysts which activate and direct the reagents utilising a Lewis acidic metal and a Lewis base.
2) Catalysts which activate and direct the reagents utilising hydrogen bonding and a non-metal functional group.
3) Catalysts which activate and direct the reagents utilising a Lewis acidic metal and a H-bonding functional group.
4) Catalysts in which a metallic site first interacts with a substrate before a site on the ligand performs a chemical reaction.
5) Catalysts which activate and direct the reagents utilising a nucleophilic Lewis base and a non-metal functional group.

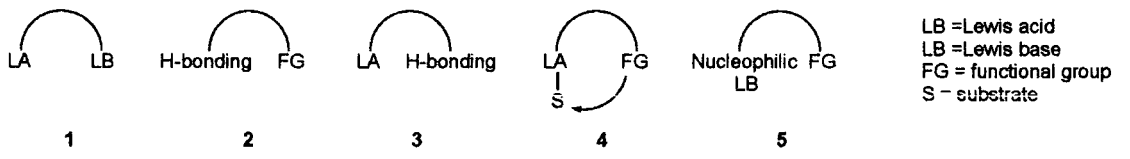

Figure 1: Modes of action of bifunctional catalysts.

Where there is overlap and a catalyst may be included in more than one class, the principal binding and activation step shall define the class.

1.2.1 Lewis acid - Lewis base systems

A common motif in bifunctional catalysis is the Lewis acid – Lewis base system. Commonly a Lewis acid will bind the substrate, simultaneously activating it and inducing chirality, then a Lewis base will activate and deliver a second reagent to the available face of the substrate.

1.2.1.1 Carbonyl reduction

Perhaps the most famous and ground-breaking demonstration of the power of bifunctional catalysis is the Corey-Bakshi-Shibata (CBS) reaction, the catalytic enantioselective reduction of ketones first reported in 1987.[16-20] Following on from work by Itsuno and Hirao,[21, 22] Corey *et al.* discovered that oxazaborolidines of type **6** mediated the enantioselective catalytic reduction of ketones.

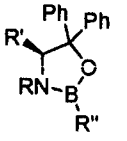

6

A classic CBS reaction is shown in equation 1 and proposed mechanism is as follows. (Scheme 1).

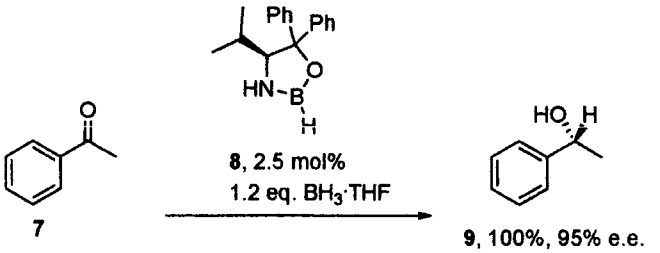

7 **9**, 100%, 95% e.e.

Equation 1: CBS oxazaborolidine-catalysed reduction with borane.

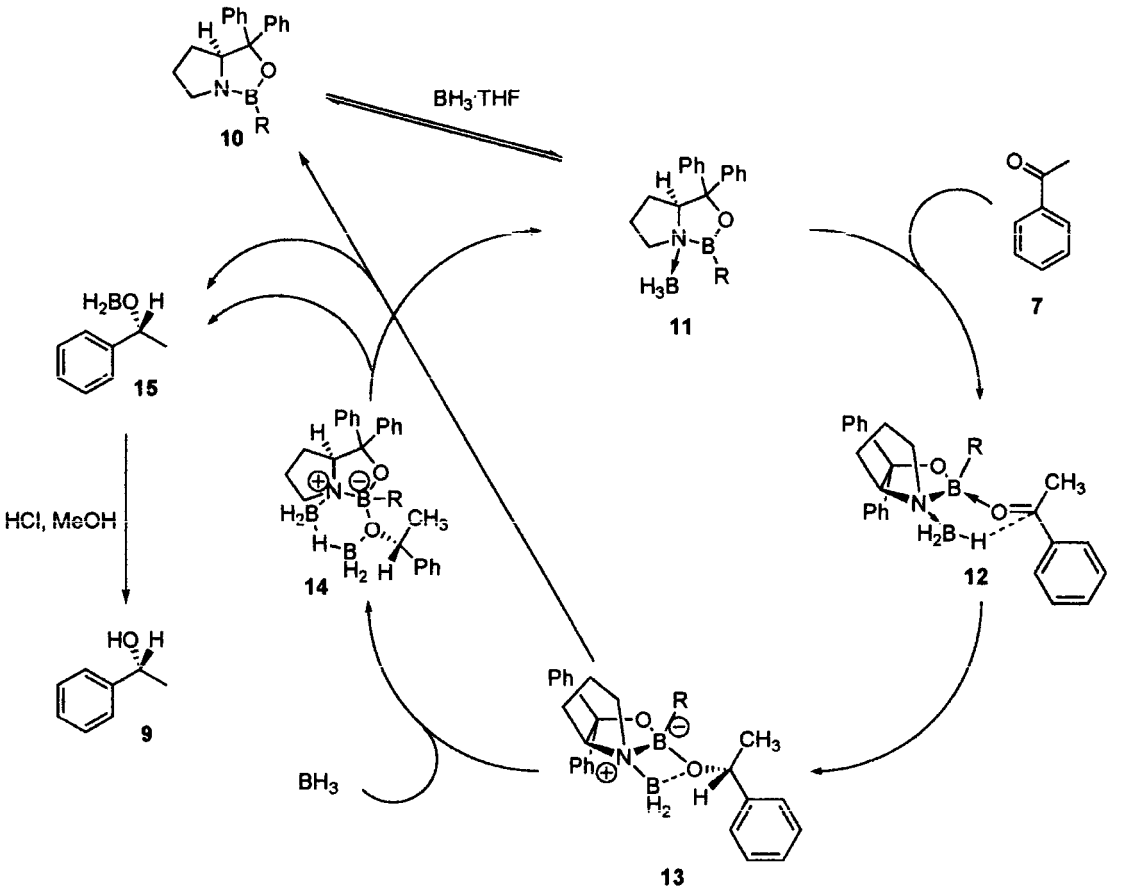

Scheme 1: Proposed reaction mechanism of the CBS reaction.

The first step of the reaction is thought to be the reversible coordination of borane by the lone pair of nitrogen on the sterically available face of the oxazaborolidine **10**. This would increase the negative charge on this boron, activating it as a hydride donor and strongly increase the Lewis acidity of the endocyclic boron. The endocyclic boron of **11** then binds to the lone pair of ketone **7** in the least sterically demanding conformation **12**, thus simultaneously aligning and activating the coordinated ketone for *si*-face hydride transfer *via* a six-membered transition state to form **13**. Two pathways have been proposed for dissociation of the intermediate **13**: 1) reaction of the alkoxide ligand with the *N*-bound BH_2 of **13** to regenerate **10** by cycloelimination, 2) addition of borane to **13** to generate a six-membered BH_3 bridged species **14**. Decomposition regenerates catalyst-BH_3 complex **11** and the borinate **15**. Hydrolysis of the reaction mixture generates the enantioenriched alcohol **9**.

Demonstrated here is an excellent example of the principle of simultaneous binding and activation of two separate reagents on a tightly defined chiral template in order to achieve a highly enantioselective reaction.

This highly successful reaction has been well developed from the original conditions to give a widely applicable method for the synthesis of secondary alcohols and also amines from imines, typically with good to excellent e.e.s (>90%).[16] The CBS reaction can be regarded historically as one of the most successful examples of bifunctional catalysis.

Sibi and Cook *et al.* have reported bifunctional borane complexes **16-20** for the enantioselective reduction of ketones.[23] The yields and e.e.s for the enantioselective reduction of acetophenone are indicated beneath each complex (Scheme 2). Complexes **17**, **19** and **20** with basic side-arms were found to produce lower e.e.s and yields than the parent compound **16**. Complexes **18** and **19**, with no basic group on the side-arm and a distal basic group respectively, were found to produce the worst results. The postulated transition state **21** for this system suggests activation and delivery of the borane by the basic side-chain. This suggests that the arrangement of the Lewis acidic and basic groups in the CBS oxazaborolidines is superior to side-arm delivery.

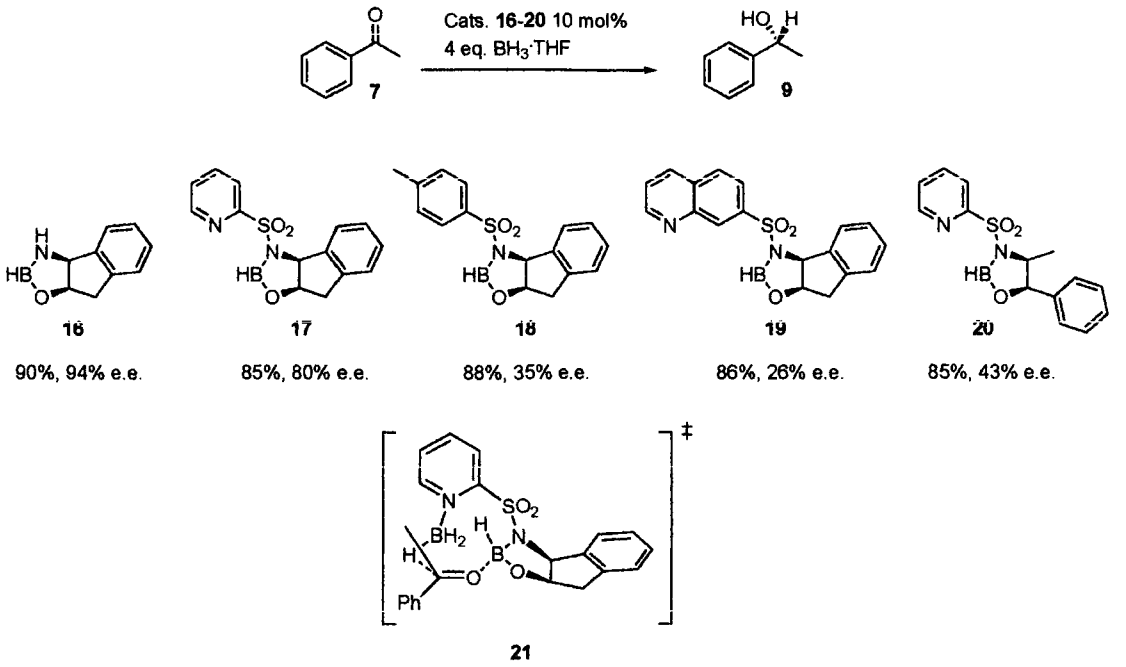

Scheme 2: Sibi and Cook oxazaborolidine-catalysed reduction with borane.

The chiral phosphinamide-mediated enantioselective borane reduction of ketones has been investigated by Wills *et al.* and shown to produce chiral secondary alcohols with modest e.e.s.[24] The postulated mechanism of this process involves a bifunctionally catalytic system. A modification of the phosphinamide strategy saw the introduction of a side-chain hydroxyl group to produce molecules such as **23**, which greatly increased the efficacy of the reaction (Equation 2).[25-27] The active complex is formed when the side-arm of **23** reacts with borane to produce a R-O-BH_2 Lewis acidic site with a secondary interaction with the basic phosphinamide oxygen, which defines a well-ordered chiral template. In the transition-state **25** the Lewis acidic R-O-BH_2 site coordinates the ketone with the *re*-face exposed to hydride attack from the borane, which is coordinated to the Lewis basic phosphinamide oxygen.

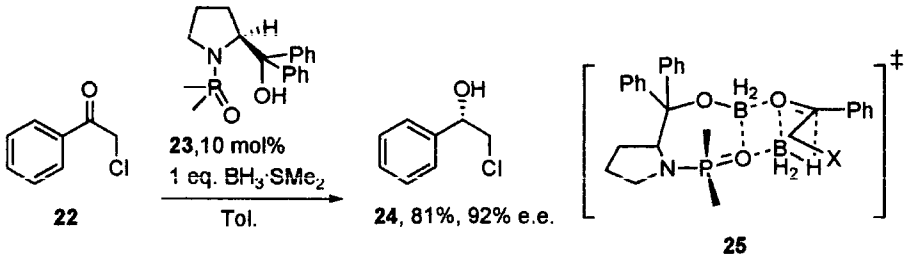

Equation 2: Chiral phosphinamide-catalysed reduction with borane.

1.2.1.2 Alkylations, alkynylations and allylations

Alkylzinc reagents are similar to borane in that as neutral planar compounds they are unreactive, but complexation to a pair of Lewis basic centres creates a reactive species. In the case of dialkylzinc reagents, coordination to a bidentate Lewis basic ligand results in a *pseudo*-tetrahedral complex. The resultant increased electron density on the zinc activates the metal as an alkyl donor. Noyori *et al.* pioneered the use of β-dialkylamino alcohols such as (-)-3-*exo*-(dimethylamino)isobornenol (DAIB) **27** for the enantioselective addition of dialkylzincs to aldehydes. An example from the first report is shown in equation 3.[28]

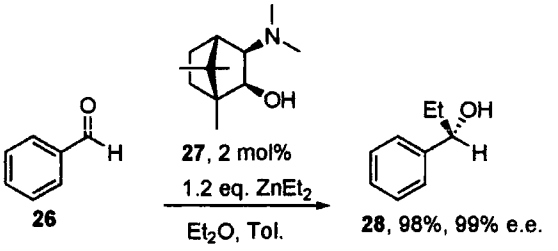

Equation 3: DAIB-catalysed addition of dimethylzinc to benzaldehyde.

The reaction has been developed and optimised[29] and the mechanism rigorously investigated.[30-37] The first step of the postulated mechanism (Scheme 3) is reaction of the dimethylzinc with the DAIB alcohol **29**, with loss of methane and coordination of the trialkylamino group. This is followed by coordination of an extra equivalent of dimethylzinc to a lone pair of the oxygen and the stereoselective coordination of the aldehyde to give intermediate **30**. The complexation of the second aldehyde oxygen lone pair to the

neighbouring zinc activates the metal as an alkyl donor and the methyl group is delivered stereoselectively to the carbonyl *via* transition state **31**. The intermediate is recycled by the addition of dimethylzinc to release the product **33**, which is readily hydrolysed to the alcohol.

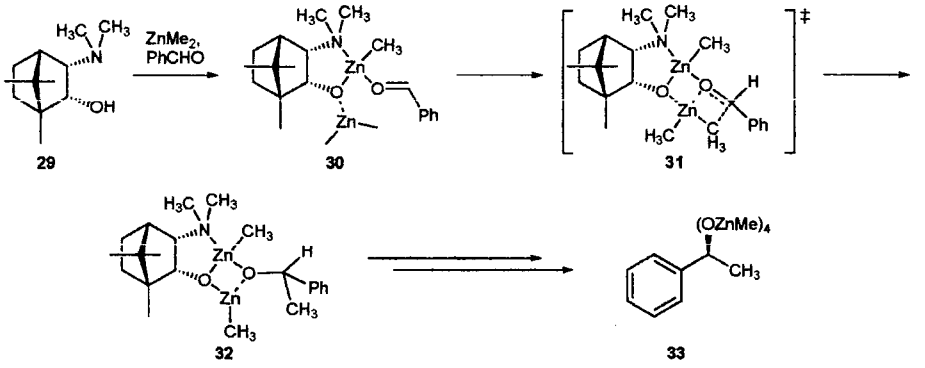

Scheme 3: Mechanism of DAIB-catalysed addition of diethylzinc to benzaldehyde.

Notable developments of this strategy are shown in equations 4 and 5.

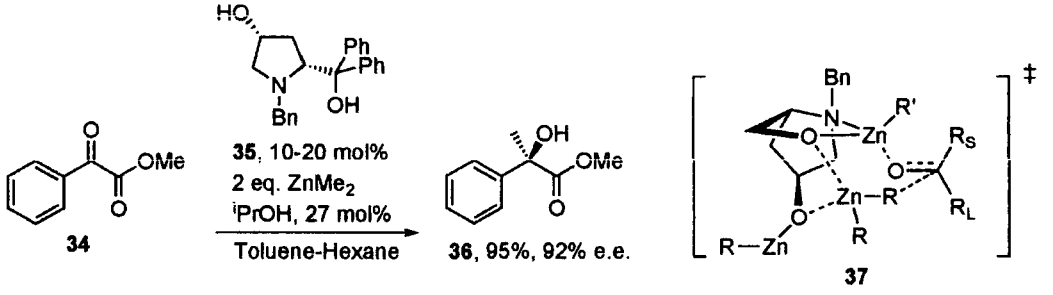

Equation 4: Asymmetric alkylation of α-ketoesters

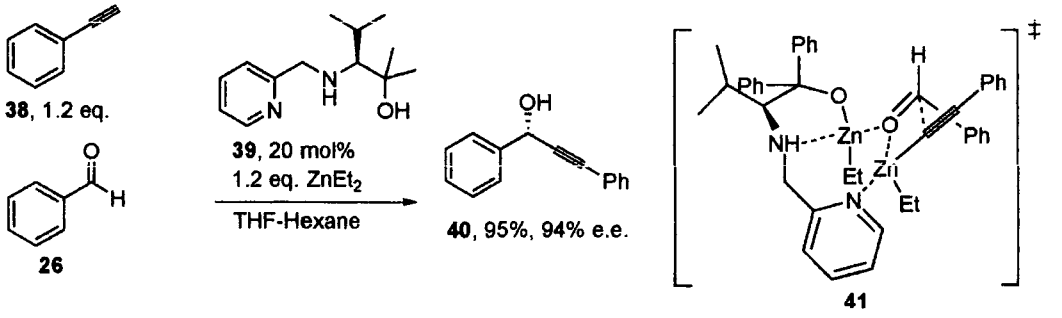

Equation 5: Asymmetric alkynylation of aldehydes.

Shibasaki *et al.* have reported tridentate ligand **35** for the alkylation of α-ketoesters with good to excellent asymmetric induction (Equation 4).[38] This strategy provides a sterically well-defined transition state **37**. Wang *et al.* have reported the utility of ligand **39** for the asymmetric alkynylation of aldehydes with good to excellent e.e.s (Equation 5).[39] In this reaction a quantity of alkyl,alkynylzinc **42** is formed, which is more reactive than dialkylzinc in this system. The pyridyl side-arm helps to deliver the mixed zinc reagent **42** to the *si*-face of the ketone *via* transition state **41**. Other attempts at introducing the zinc-alkylating agent using a side-arm have been less successful.[39, 40]

42

Carreira *et al.* have reported a system based on trialkylaluminium which is perhaps the closest analogue of the CBS system (Equation 6).[41] Aluminium is directly under boron in group III of the Periodic Table and, like borane, coordination of trialkylaluminium to a single Lewis base produces an 'ate'-complex with greatly increased nucleophilicity. The bifunctional system generated by the complexation of TiF to the diol **44** generates a Lewis acid-Lewis base system. In the postulated mechanism, **46**, a fluorine lone pair coordinates to the Lewis acidic trimethylaluminium, thus activating the aluminium as a methylating agent, whilst coordination of the aldehyde **43** to titanium activates the carbonyl to nucleophilic attack. The reaction proceeds with moderate enantioselectivity (up to 83% e.e.).

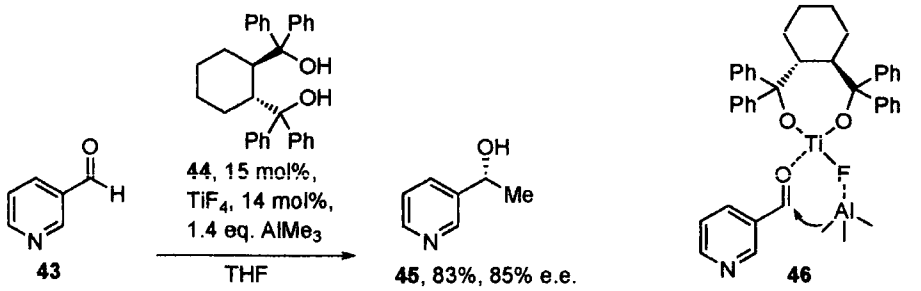

Equation 6: Titanium fluoride-based asymmetric methylation.

1.2.1.3 Cyanations

Asymmetric cyanation reactions have been a particular success story of bifunctional catalysis. Shibasaki *et al.* pioneered compounds such as **47** (Equation 7) with a Lewis acid and two pendant side-arms.[42] Under optimised conditions which include the addition of an achiral phosphine oxide additive, excellent yields and very good to excellent e.e.s are observed for the asymmetric cyanosilylation of aldehydes.[43, 44]

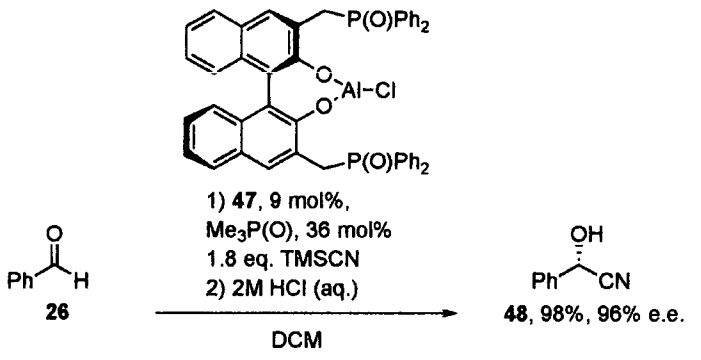

Equation 7: Aluminium-catalysed asymmetric cyanosilylation.

This process is believed to proceed through the following mechanism (Scheme 4): Coordination of the phosphine oxide **49** and the aldehyde **50** to form the pentavalent aluminium species **51** that places the aldehyde at the apical site close to the side-arm phosphine oxide. Interaction of the side-arm phosphine oxide with TMSCN to form the pentavalent silicon species activates the silicon for cyanide transfer to the *re*-face of the aldehyde to form

the (*S*)-enantiomer **53**, and transfer of the TMS group to oxygen releases the product **54** from the catalyst. The O-silylated product is hydrolysed by treatment with hydrochloric acid.

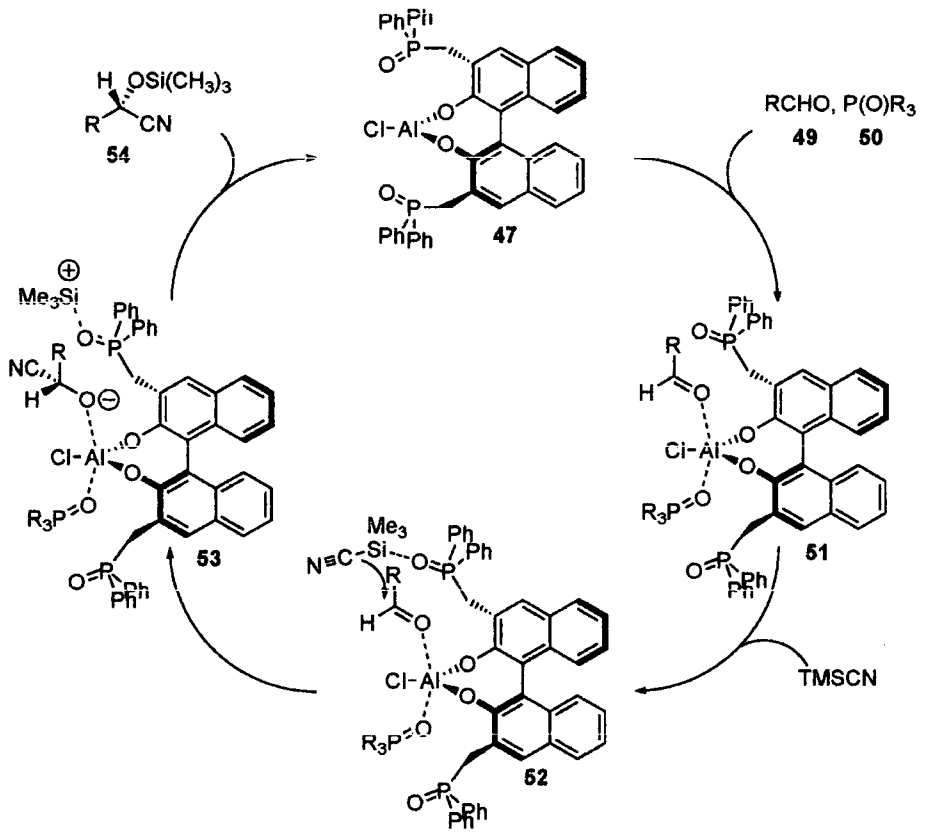

Scheme 4: Postulated catalytic cycle aluminium-catalysed asymmetric cyanosilylation.

Shibasaki has shown the catalytic cyanosilylation reaction to be a good generally applicable reaction which has found utility in additions to imines[45] and as a polymer-supported version.[46]

Extensions of the BINOL-plus-side-arm Lewis base cyanation strategy have seen the development by Saá *et al.* of an aluminium-BINOLAM **55** system that has the advantage of being recyclable. This complex has found utility for cyanosilylation (Equation 8),[47, 48] cyanoformylation[49] and cyanophosphorylation (Equation 9),[50] in the latter two reactions the direct formation of O-protected products is possible. The asymmetric Reissert

reaction has also been reported by Shibasaki *et al.*, allowing the enantioselective construction of quaternary carbon centres (Equation 10).[51-53]

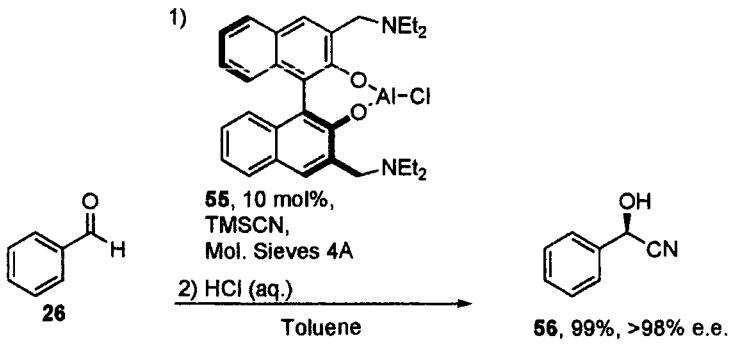

Equation 8: Aluminium-catalysed cyanation.

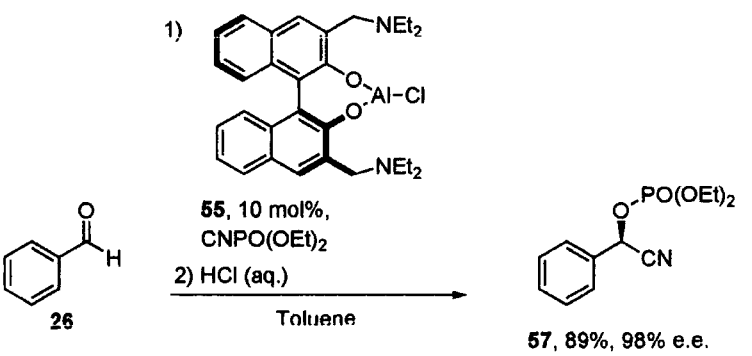

Equation 9: Aluminium-catalysed cyanophosphorylation.

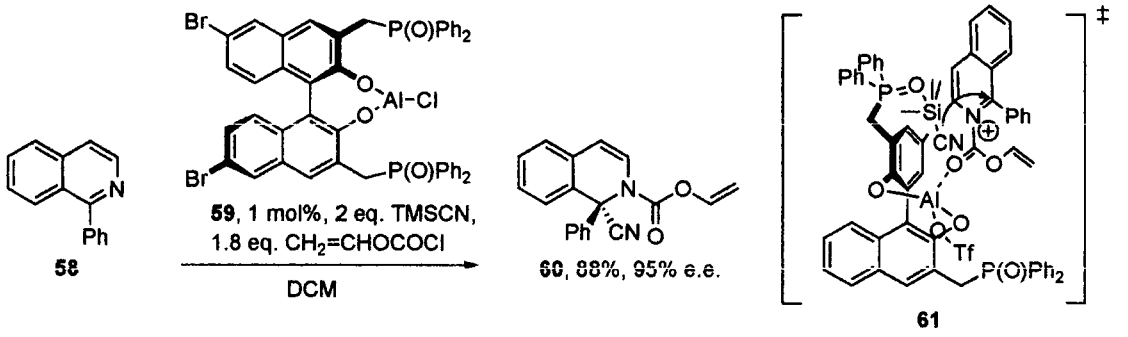

Equation 10: Aluminium-catalysed Reissert reaction.

Other successful systems for the Lewis acid – Lewis base strategy for asymmetric cyanation reaction have been developed. Feng *et al.* have reported titanium-centred systems with pendent *N*-oxides for the cyanosilylation of ketones.[54-56] Notable in this area is the peptide base system developed by Snapper and Hoveyda *et al.*, who reported the titanium-

catalysed enantioselective cyanation of imines[57-60] (Equation 11) and the aluminium-catalysed enantioselective cyanation of ketones and aldehydes.[61] The ligands for this process are peptide-based entities such as **63**.

In the postulated mechanism, hydrogen cyanide interacts with the amide oxygen to be delivered in tautomeric form to the imine in its energetically favoured conformation *via* transition state **65**.

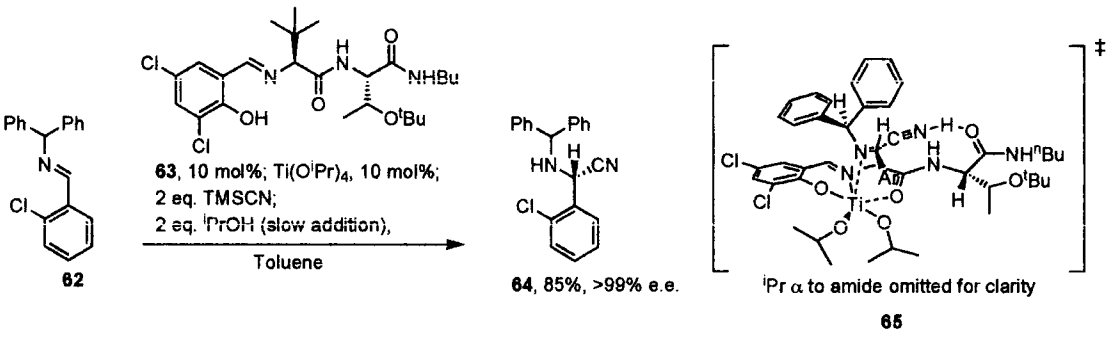

Equation 11: Titanium-catalysed Strecker reaction.

1.2.1.4 β-lactam synthesis

Lectka *et al.* initially demonstrated that benzoylquinine-type compounds were effective for the stereoselective synthesis of β-lactams with moderate yields and good e.e.s (45-65%, 95-99% e.e., 25-99:1 d.r.) (Equation 12).[62]

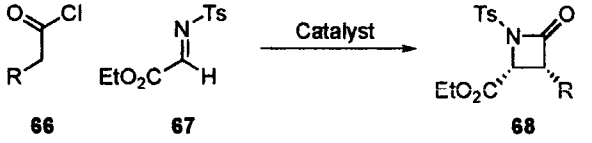

Equation 12: β-lactam synthesis.

However, it was discovered that compound **70** (Scheme 5) produced superior results (95%, 98% e.e., 60:1 d.r.).[63] A bifunctional mechanism is thought to be in operation in this case.[64-66]

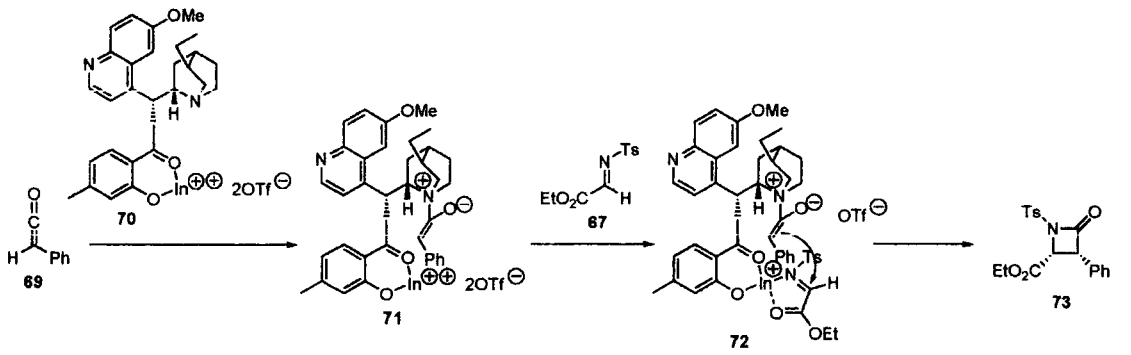

Scheme 5: Postulated mechanism for β-lactam synthesis.

The first step involves attack of the nucleophilic nitrogen to form the enolate intermediate **71**, assisted by reaction of the indium with the phenylketene **69**. Coordination of the imine **67** to the indium sets up the stereochemistry for the rate-determining C-C bond-forming step. Transacylation regenerates the catalyst and forms the product.

1.2.2 H-bonding - functional group

In modern organic synthesis carbonyls are commonly activated by interaction with Lewis acids. Coordination of oxygen lone pairs to the Lewis acid reduces the electron density at the oxygen and lowers the energy of the lowest unoccupied molecular orbital, the C=O π^* orbital, activating the carbonyl to nucleophilic attack at carbon. The hard Lewis basic lone pairs of oxygen are well matched to hard Lewis acids, which produce particularly effective activation. The proton is the smallest possible Lewis acid. Protic catalysis activates many C-C bond-forming reactions, but is incompatible with many nucleophiles, for example cyanides, enolates and enamines. In weak acid catalysis[67-70] the proton transfer may only occur in the transition state, or the catalyst may act to stabilise the transition state by hydrogen bonding. These weaker acids are often compatible with the common nucleophiles and represent a separate class of catalysis.

The H-bonding - functional group series of catalysis is a relatively new addition to bifunctional catalysis. However, its similarity to Lewis acid - Lewis

base catalysis leads to its ability to catalyse many of the same reactions and has brought the area to prominence.

1.2.2.1 Bifunctional thioureas

Takemoto *et al.*, Jacobsen *et al.* and many other groups have developed urea-based catalysts of the general structure illustrated below (Figure 2).

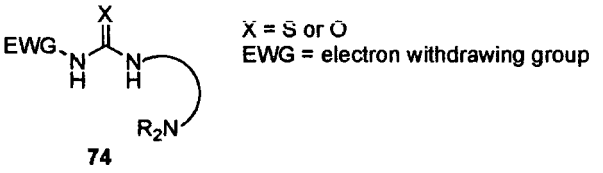

Figure 2: Generalised structure urea-based catalysts.

These structures take advantage of the potential for ureas to H-bond via two hydrogens to carbonyls, imines and nitro groups, further polarising the functional group bonds and activating the substrates, within a chiral environment, to nucleophilic attack, or to deprotonation in the case of alkyl-nitro compounds (Scheme 6).

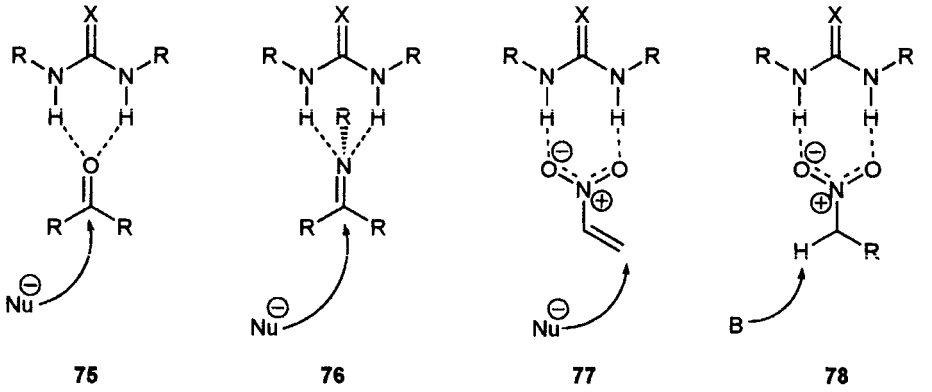

Scheme 6: Urea H-bonding interaction with a carbonyl, an imine, a nitro-olefin and an alkyl-nitro compound.

In the case of Michael addition of 1,3-dicarbonyls to nitro-olefins (Equation 13),[71] the following mechanism has been proposed (Scheme 7).[72]

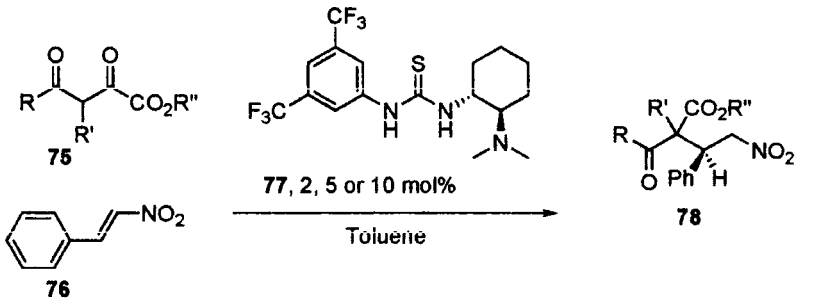

Equation 13: Bifunctional thiourea-catalysed Michael addition to nitro-olefins.

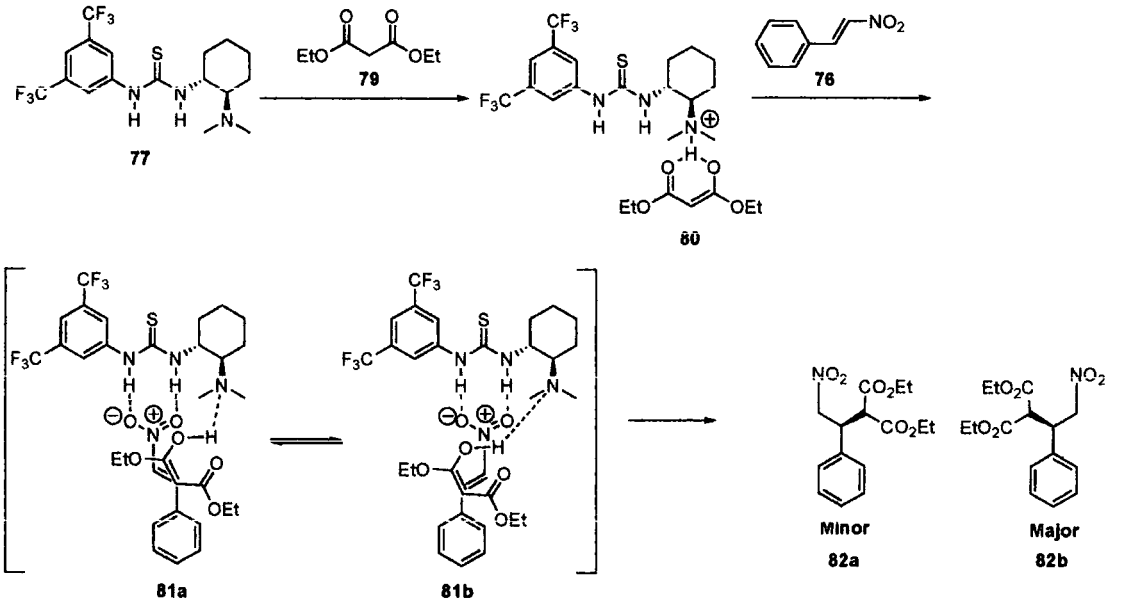

Scheme 7: Proposed reaction mechanism for Michael additions of malonate.

The tertiary amine of **77** deprotonates an acidic proton of the malonate **79** to form the H-bond-stabilised intermediate **80**. The nitro-olefin **76** then coordinates to the urea moiety via its two δ negative oxygen atoms to lead to the two energetically favoured transition states **81a** and **81b**. Transition state **81b** is thought to be the lowest energy of the two transition states and thus leads to the major product of the reaction **82b**.

Reactions of this type have been shown to generate products of up to 93% e.e. In the reaction of prochiral keto-esters moderate to high diastereomeric ratios were achieved, up to 20:1 with 90% e.e. for the major diastereoisomer.

In this example of bifunctional catalysis, the pendant basic group delivers a prochiral nucleophile onto a prochiral Michael acceptor. An H-bonding interaction serves to activate and define the orientation of the Michael acceptor within the chiral template to allow diastereoselective and enantioselective bond formation

Bifunctional compounds of type **74** have been shown to be effective, producing good to excellent e.e.s in enantioselective Michael addition of nitromethane (Equation 14),[73] Michael additions of arylthiols,[74] asymmetric aza-Henry reactions (Equation 15),[75] cascade Michael additions,[76] dynamic kinetic resolution of azlactones (Equation 16),[77, 78] in the acyl-Pictet-Spengler reaction (Equation 17)[79] and in cyanations including the asymmetric Strecker using HCN (Equation 18).[80, 81]

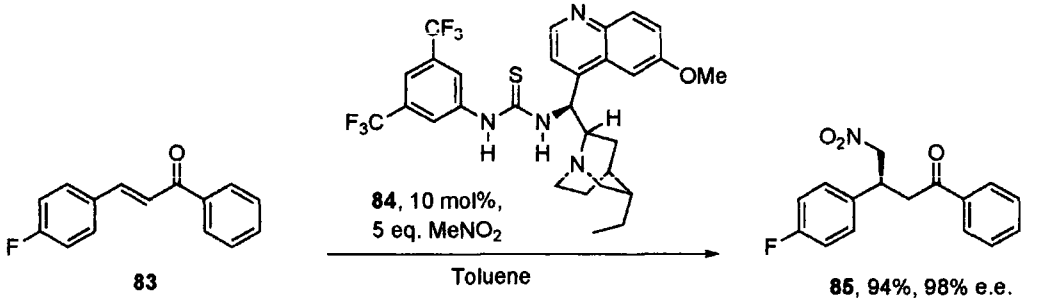

Equation 14: Bifunctional thiourea-catalysed Michael addition.

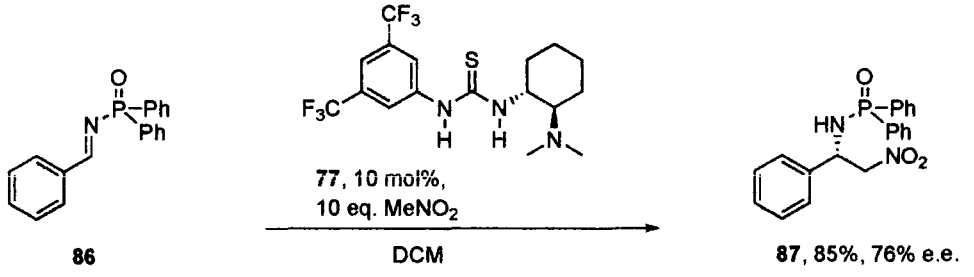

Equation 15: Bifunctional thiourea-catalysed aza-Henry reaction.

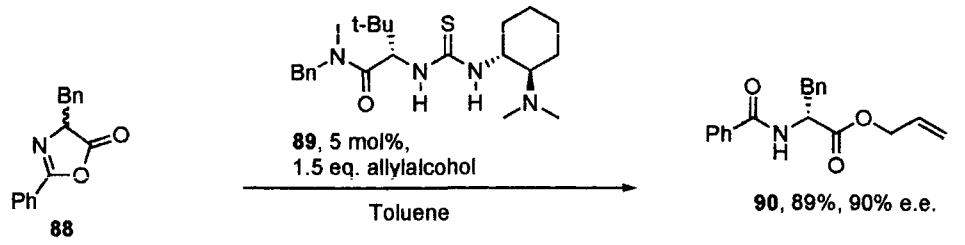

Equation 16: Bifunctional thiourea-catalysed dynamic kinetic resolution of azlactones.

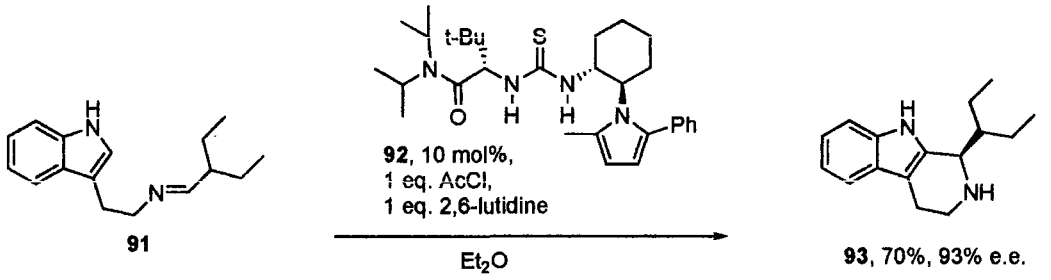

Equation 17: Bifunctional thiourea-catalysed acyl-Pictet-Spengler reaction.

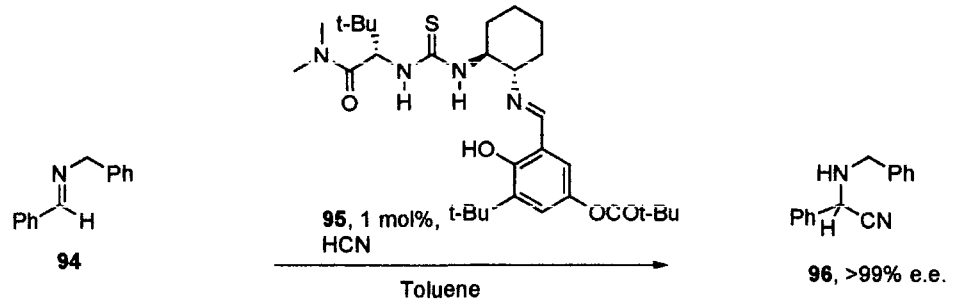

Equation 18: Bifunctional thiourea-catalysed cyanation.

1.2.2.2 Reduction

Malkov *et al.* have reported the asymmetric reduction of ketimines with trichlorosilane (Equation 19).[82] The organocatalytic valine-derived catalyst is thought to act *via* a H-bond-stabilised transition state with secondary π-π interactions as illustrated in **100**. It would however appear that H-bonding is the major factor as toluene is also an effective solvent. Being aromatic, toluene would have been expected to weaken the π-π interactions in the

transition state, but the reaction proceeds with an increase in yield and no loss of e.e.

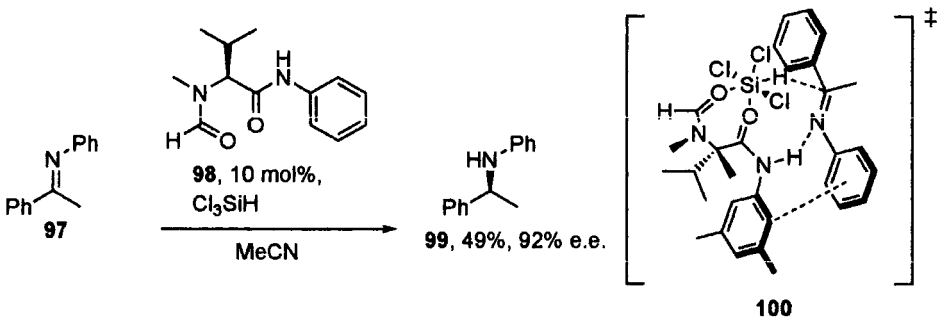

Equation 19: Asymmetric reduction of ketimines with trichlorosilane.

1.2.3 Metal-H-bonding

The metal-H-bonding class of catalysts is considered separately from the metal-metal systems (excluded from this introduction), as compounds of the type synthesised in this project have the potential to act by this mechanism.

1.2.3.1 Asymmetric allylic alkylation

One of the first reports of bifunctional catalysis came from Hayashi *et al.*, who first synthesised palladium complexes such as **103** in 1986. Complex **103** was effective for the asymmetric allylic alkylation reaction (Equation 20).[83 87] In the postulated reaction mechanism, palladium complex **103** reacts with the allylic acetate **102** to form a π-allylpalladium intermediate, which stereoselectively delivers an enolate nucleophile using a chiral H-bonding side-arm, as illustrated in figure 3.

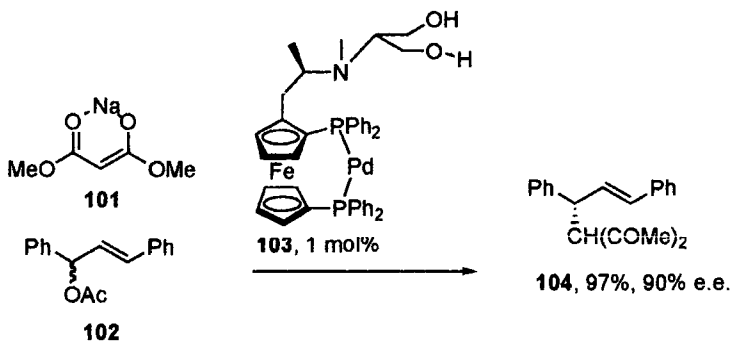

Equation 20: Palladium-catalysed asymmetric allylation.

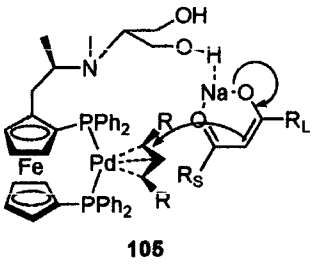

105

Figure 3: Mechanism palladium-catalysed asymmetric allylation.

1.2.3.2 Asymmetric cyclopropanation

Reiser *et al.* have reported the catalytic asymmetric cyclopropanation of furans with **108**, a copper-centred C_2-symmetric catalyst with tosyl-protected secondary amine side-arms (Equation 21).[88] The postulated transition state **110** of the reaction suggests that H-bonding of the secondary amine on the side-arm to the ester carbonyl of furan **107** orientates the molecule for reaction with the copper carbene. The steric interactions with the carbene ester group are avoided in the transition state by directed approach from the underside of the carbene. This results in **109** being the major product of the reaction.

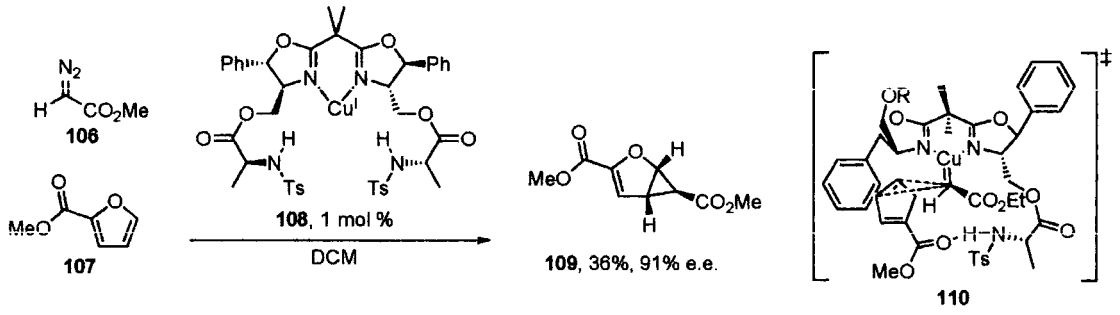

Equation 21: Reiser *et al.* asymmetric cyclopropanation.

1.2.4 Metal - reactive ligand

This is a rare class of bifunctional catalysts in which a substrate reacts first with a metal centre before a site on the ligand performs a chemical reaction. By intramolecularising these two stages the overall reaction rate is increased.

1.2.4.1 Aldol

In work presumably following-on from the synthesis of **103** for the asymmetric allylic alkylation reaction, Hayashi, Ito *et al.* also produced complex **113** for the catalytic asymmetric aldol reaction (Equation 22).[89]

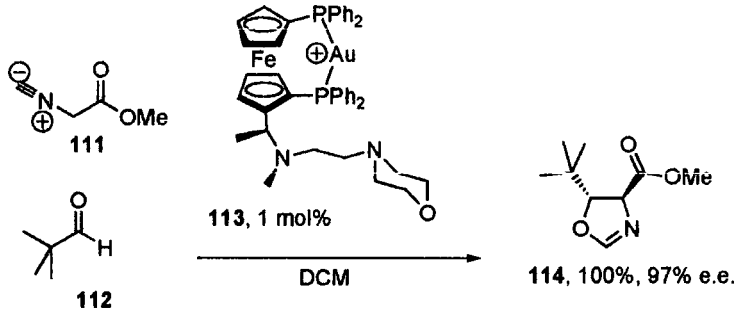

Equation 22: Gold-catalysed asymmetric aldol reaction.

In the proposed reaction mechanism[90-93] (Scheme 8) the isocyanoacetamide **115** coordinates the gold centre. The morpholino side-chain then deprotonates the coordinated isocyanoacetamide to form an enolate **116** stabilised and orientated by H-bonding **116**, thus differentiating the two

prochiral faces of the enolate. Ketone **118** then coordinates the gold centre with the R group orientated to minimise steric interaction thereby positioning itself for *si*-face enolate attack via transition state **119**. The dissociation and subsequent cyclisation yields 5-alkyl-2-oxazoline-4-carboxylate **120** with high diastereoselectivity and enantioselectivity.

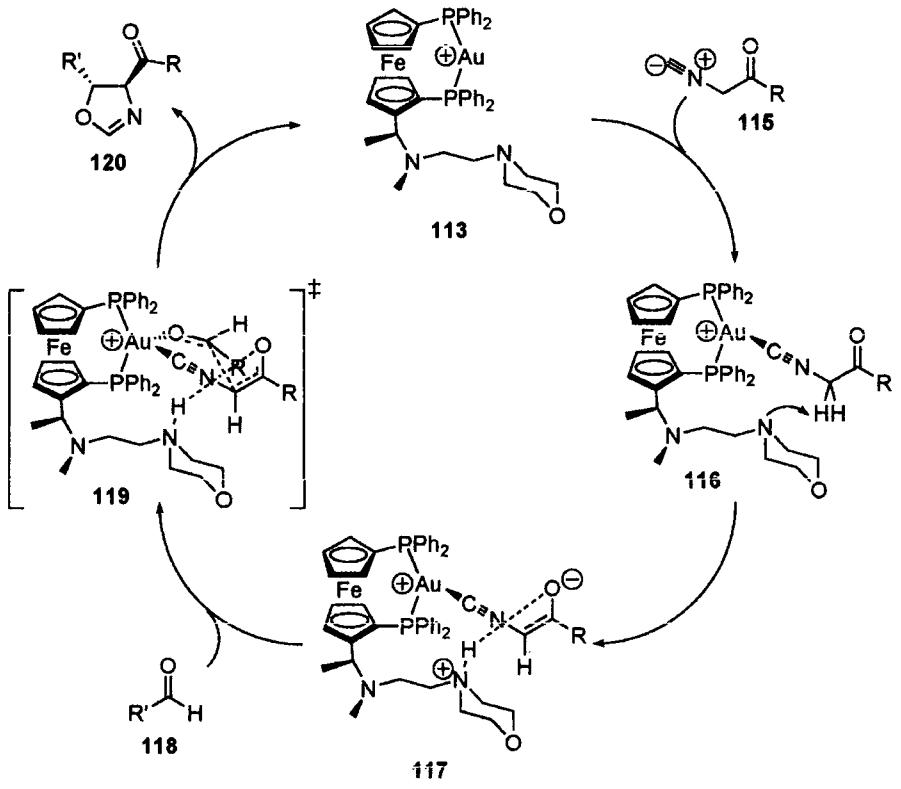

Scheme 8: Proposed reaction mechanism of the gold-catalysed asymmetric aldol reaction.

The gold-catalysed asymmetric aldol reaction has been optimised for isocyanoacetates and isocyanoacetamides,[94] including Weinreb amides (Equation 23).[90] The methodology has also been extended to (isocyanomethyl)phosphonates (Equation 24).[95, 96]

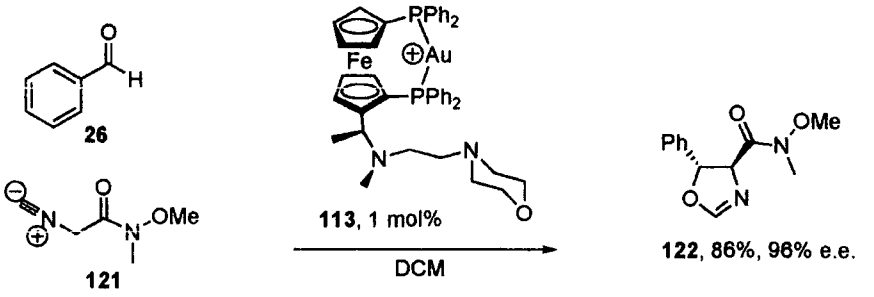

Equation 23: Gold-catalysed asymmetric aldol reaction.

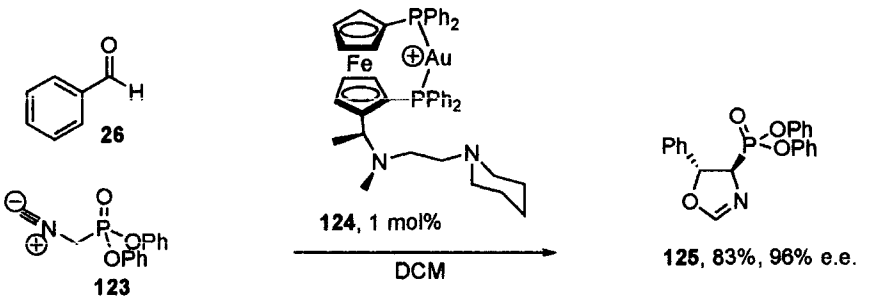

Equation 24: Gold-catalysed asymmetric aldol reaction.

1.2.4.2 Epoxidation

Aggarwal *et al.* had described a successful catalytic sulfur ylide-mediated process for the epoxidation of carbonyls with good yield and very good e.e.s (71%, 93% e.e.).[97] However, the reaction is only successful with relatively high catalyst loading (20 mol%). If loading is reduced, a competing process in which the metal carbene reacts with the diazo compound to form stilbene **128** becomes prominent (Scheme 9).

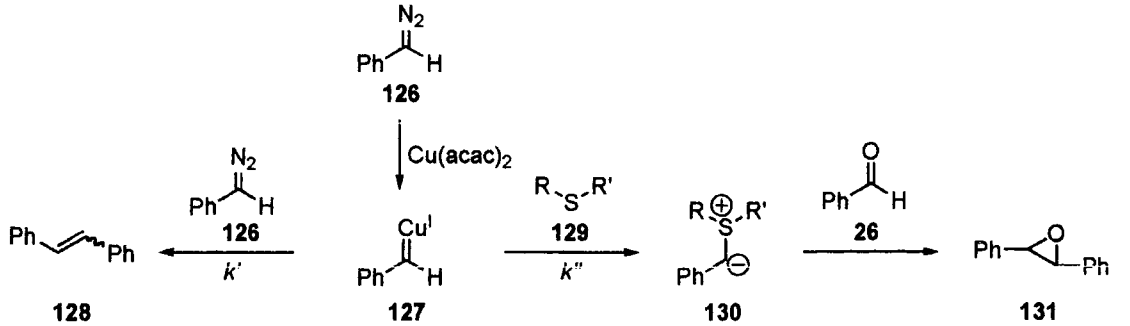

Scheme 9: Sulfur ylide epoxidation of carbonyls.

The bifunctional catalyst **133** (Equation 25) was produced with the expectation that by intramolecularising the reaction between the sulfide and the metal carbene on a modular, catalytic system the reaction could be improved.[98] Catalyst **135** was found to be effective at lower catalyst loadings with increased yields and excellent diastereocontrol but reduced e.e.s. The reduced e.e. is likely to be caused by the relative lack of an asymmetric template around the sulfur compared with Aggarwal's previous system.

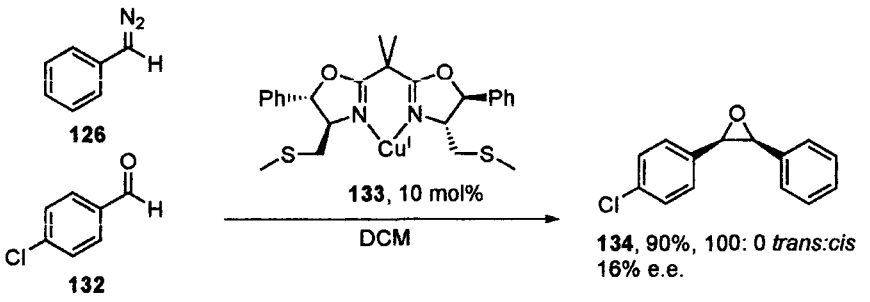

Equation 25: Copper-catalysed asymmetric epoxidation.

The proposed mechanism of the process is illustrated in Scheme 10. The ligated copper **133** reacts to form the metal carbene **135**. The carbene **135** reacts with the side-arm sulfide to form ylide **136**. Ylide attack on the aldehyde followed by cyclisation releases the catalyst and epoxide **137**.

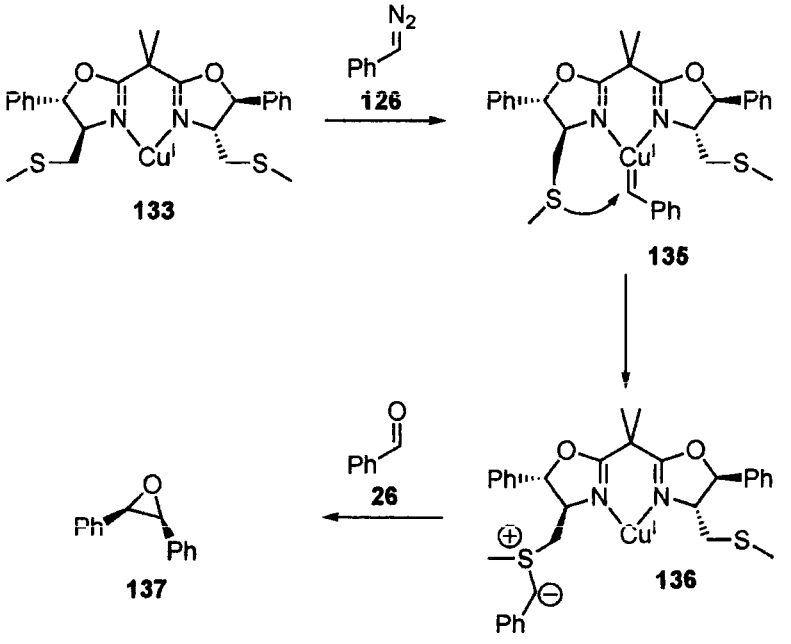

Scheme 10: Mechanism copper-catalysed asymmetric epoxidation.

1.2.5 Nucleophilic Lewis Base - Functional group

The area of organocatalysis has developed strongly in recent years, with enamine catalysis and, in particular, proline-based systems being influential.[6, 99-102] The generalised enamine catalytic cycle is illustrated in Scheme 11.

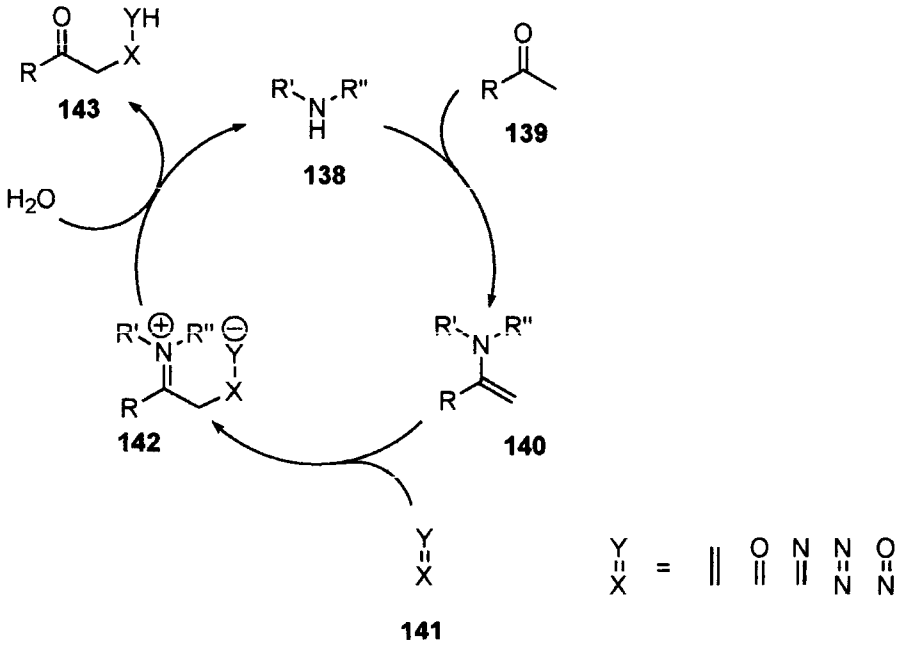

Scheme 11: Generalised enamine catalytic cycle.

1.2.5.1 Proline based enamine catalysis

Proline was first applied to asymmetric enamine catalysis in the 1970's with the Hajos-Parrish-Eder-Sauer-Wiechert reaction, a proline-catalysed intramolecular aldol.[103, 104] Recently List *et al.*,[105] followed by other groups,[106-109] have developed the proline-catalysed enantioselective intermolecular aldol reaction. The mechanism of this process has been investigated and a bifunctional mechanism has been proposed[105] (Scheme 12).

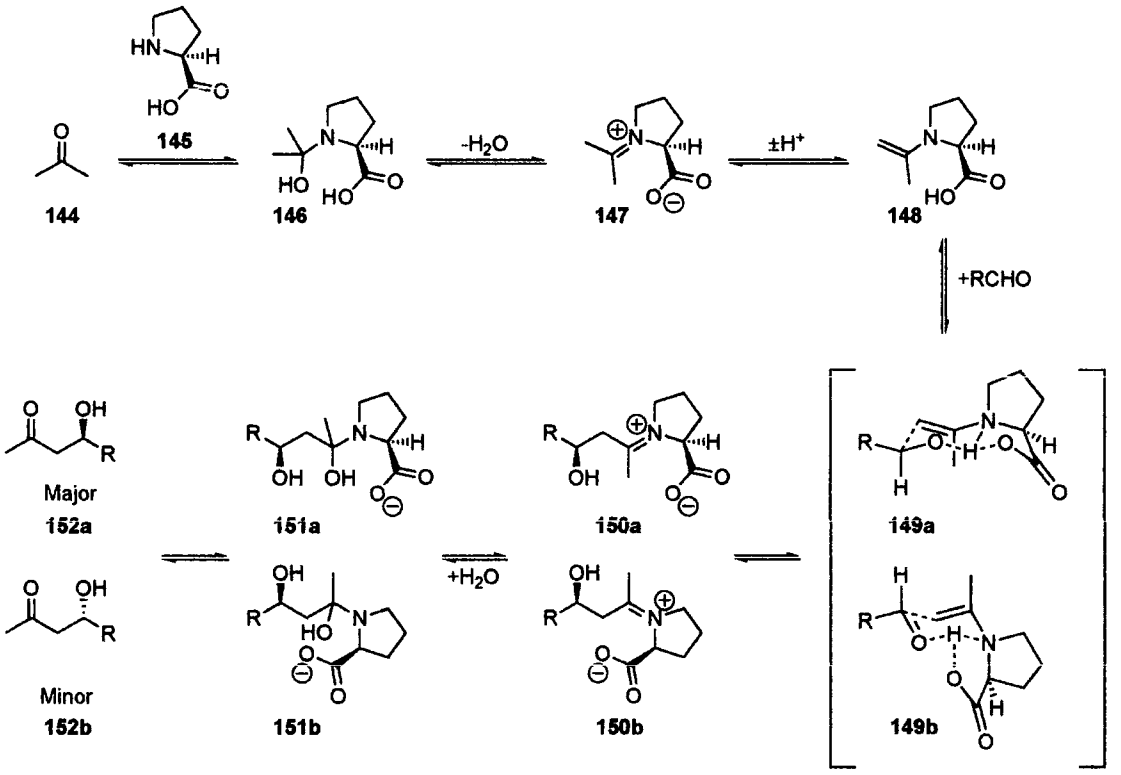

Scheme 12: Postulated reaction mechanism for the proline-catalysed aldol reaction.

The mechanism of the proline-catalysed aldol is thought to be enamine catalysis. The carboxylic acid / carboxylate functionality is thought to be involved in each step of the reaction by assisting proton transfer and by H-bonding in each of the following stages: the nucleophilic attack of the amino group of **145**; the dehydration of the carbinol amine species **146**; the deprotonation of the iminium species **147**; the stabilisation and orientation of the likely transition states **149a** and **149b**; and the hydrolysis via **150a**, **150b** and **151a**, **151b** to the products **152a** and **152b**. The mechanism has been described as a 'micro-aldolase' mechanism.[105]

The critical stereochemistry-determining step of the reaction is the formation of a metal-free Zimmerman-Traxler[110] type transition state. In this model, a tricyclic hydrogen-bonded framework provides enantiofacial selectivity, with *re*-facial attack *via* **149a** being energetically favoured.

The proline and derivatives-based bifunctional enamine catalysis has been developed and optimised for aldol reactions (Equations 26-29).

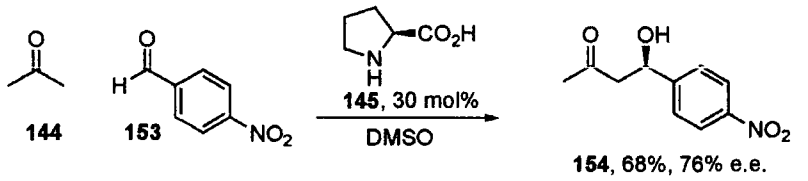

Equation 26: Proline-catalysed aldol.

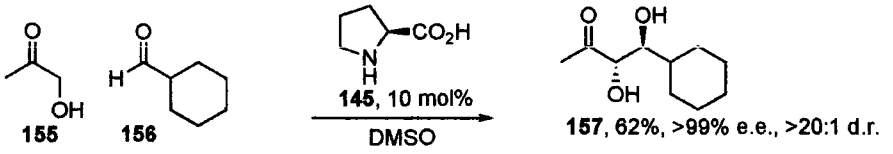

Equation 27: Proline-catalysed aldol.

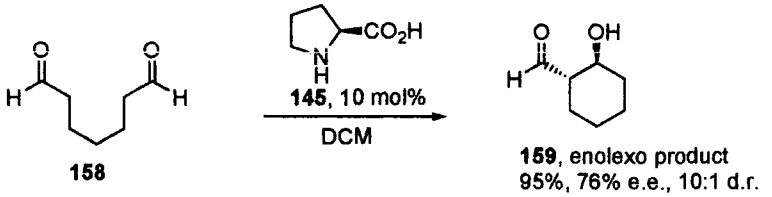

Equation 28: Proline-catalysed aldol.

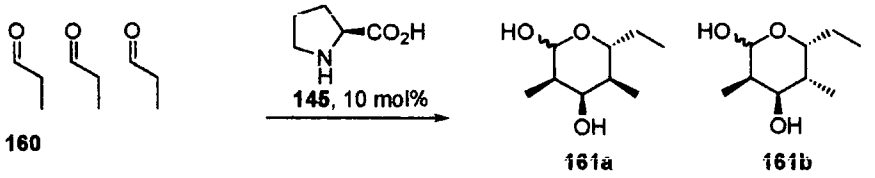

Equation 29: Proline-catalysed aldol.

The first modern example of the asymmetric proline-catalysed aldol was discovered by List *et al.* (Equation 26).[105] The reaction was optimised and the substrate range defined, including highly diastereoselective syntheses of *anti*-1,2-diols (Equation 27).[111] List *et al.* have described the 6-enolexo selectivity of the proline catalyst as contrary to Baldwin's rules (Equation 28).[112] Barbas *et al.* have described enzyme-like asymmetric assembly reactions to synthesise triketides (Equation 29).[113, 114]

Wu *et al.* have developed an alternative to the proline-based systems for the direct aldol reaction (Equation 30). Catalyst **162** is thought to act by a nucleophilic Lewis base - H-bonding mechanism instead of general acid catalysis, as in the proline-based system. Catalyst **162** consistently outperformed proline, producing higher e.e.s and requiring lower catalyst loadings.

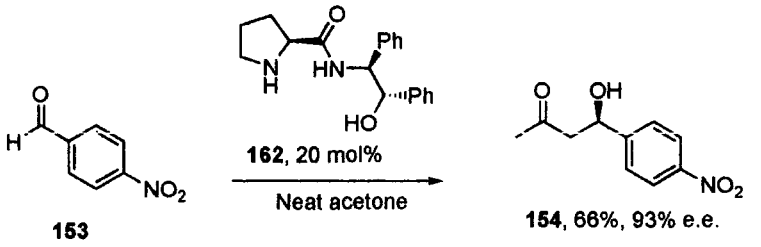

Equation 30: Wu *et al.* proline-derived direct aldol reaction.

The bifunctional enamine strategy has been successfully extended to other highly efficient asymmetric α-functionalisation reactions (Equations 31-34).

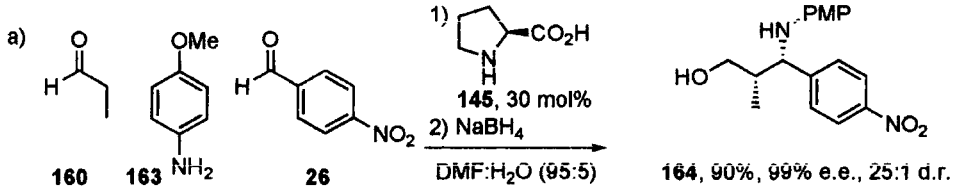

Equation 31: Asymmetric proline-catalysed Mannich reaction.

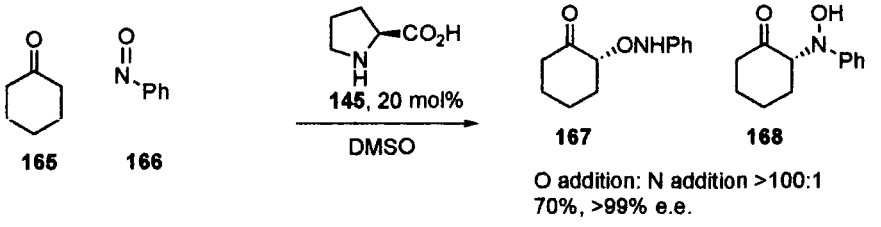

Equation 32: Asymmetric proline-catalysed α-amino-oxylation.

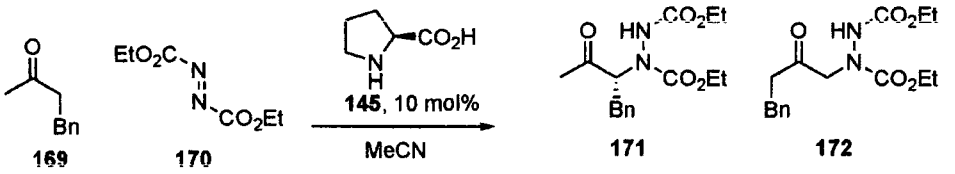

Equation 33: Asymmetric proline-catalysed α-amination.

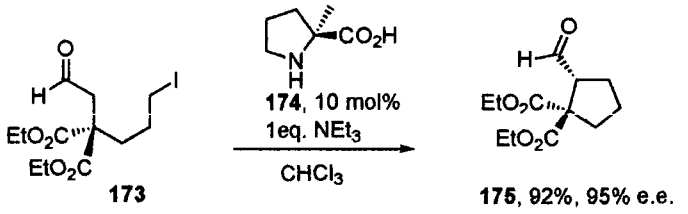

Equation 34: Asymmetric proline-catalysed intra-molecular alkylation.

Asymmetric Mannich reactions, including direct 'one-pot' versions, have been reported with excellent e.e.s (Equation 31).[115-121] The α-amino-oxylation reaction with excellent selectivity for oxygen addition under certain conditions has been reported, providing easy access to α-hydroxyketones and α,α'-hydroxyketones with excellent enantiopurity (Equation 32).[122-127] Asymmetric α-oxidation has also been achieved with iodosobenzene, *N*-sulfonyloxaziridines[128] and molecular oxygen,[129] with reduced e.e.s. With DEAD **170** as the electrophile α-amination occurs with good to excellent e.e.s (Equation 33).[130-132] Enantioselective intra-molecular alkylations have been achieved with a proline derivative **174** (Equation 34).[133] Proline has also been found to catalyse Michael additions with good to excellent e.e. and d.r. and poor to moderate e.e. and d.r.[134, 135]

1.2.5.2 Aza-Bayliss-Hillman

Shi *et al.* have investigated the action of chiral phosphine Lewis base **178** on the aza-Bayliss-Hillman reaction with unprecedented success (Equation 35). Moderate to good e.e.s (49-84% e.e.) were observed for this tricky reaction.[136]

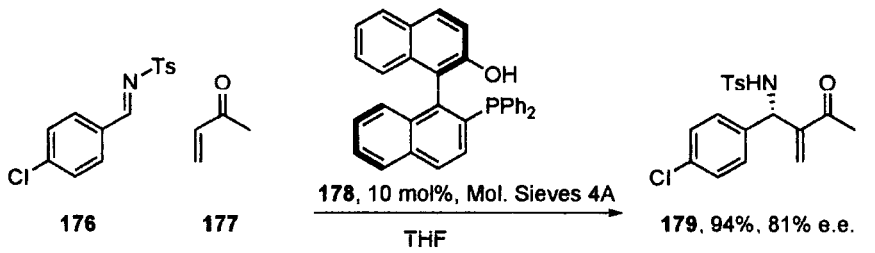

176 177 179, 94%, 81% e.e.

Equation 35: Bifunctional Lewis base-catalysed aza-Bayliss-Hillman.

In the postulated reaction mechanism (Scheme 13) the first step is the nucleophilic attack of the Lewis basic phosphorous of **178** onto the Michael acceptor **177** with the assistance of the phenolic group. The phenol functionality acts as a Lewis acid by H-bonding (Brønsted acid as a Lewis acid) to the formally negatively charged oxygen to form the key stabilised enolate intermediate **180**. Attack of intermediate **180** on the *N*-sulfonated imine **181** can give rise to two relatively stable diastereomeric intermediates **182a** and **182b** in which the phenolic OH stabilises the formally negative nitrogen in conjunction with the sulfonyl group. Intermediate **182a** is energetically favoured due to its having one major steric interaction of the aryl group with the $C(O)CH_3$ group, compared with two major steric interactions in **183b** with both the $C(O)CH_3$ group and the phenyl group attached to the phosphorous. Hence, the reaction proceeds to give **183a** as the major enantiomer.

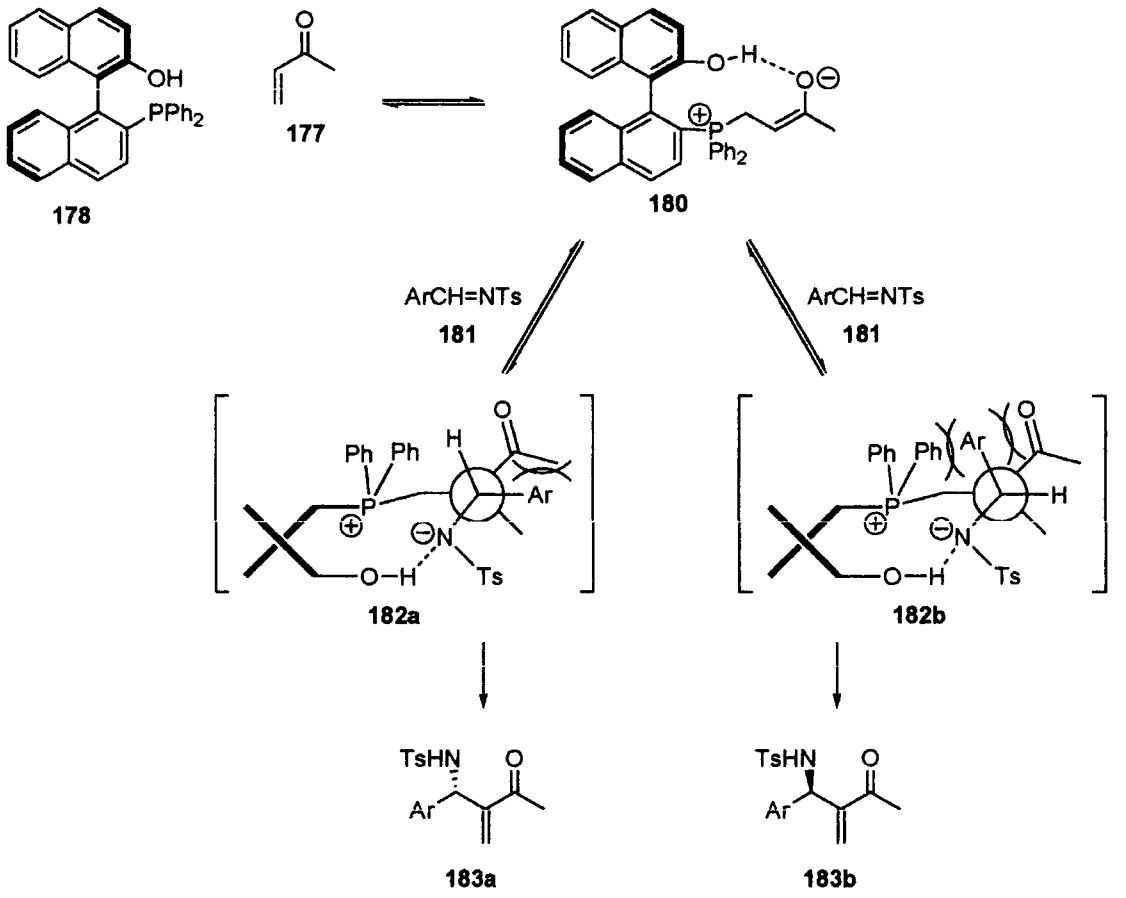

Scheme 13: Postulated reaction mechanism of the bifunctional Lewis base-catalysed aza-Bayliss-Hillman.

In the absence of the phenolic group on **178** the reaction is sluggish and gives the opposite (*R*)-enantiomer in 13% yield with only 20% e.e.

1.3 Conclusions - Introduction

Successful synthetic bifunctional catalysts are relatively new to organic synthesis, with the first effective examples emerging around the mid-eighties with work from Hayashi *et al.* for aldol and allylic alkylations and Corey *et al.* for the extremely effective CBS reaction. This area of catalysis has developed strongly over the last two decades with much excellent work over many groups and as such has become a highly influential catalytic methodology with many synthetically useful outcomes.

2 Results and discussion

2.1 Aims and overview of the project

As detailed in the introduction, Lewis acid – Lewis base bifunctional catalysis has been a successful catalytic strategy. During this project we sought to synthesise and investigate the catalytic properties of a range of compounds based around the general structure in figure 4, containing both a boron Lewis acid and a nitrogen Lewis base. We envisaged that such compounds had the potential to act as Lewis acid - Lewis base type bifunctional catalysts. The aim of this project was to produce a diverse set of organic aminoboron compounds and screen against a wide range of common reactions to identify any catalytic activity.

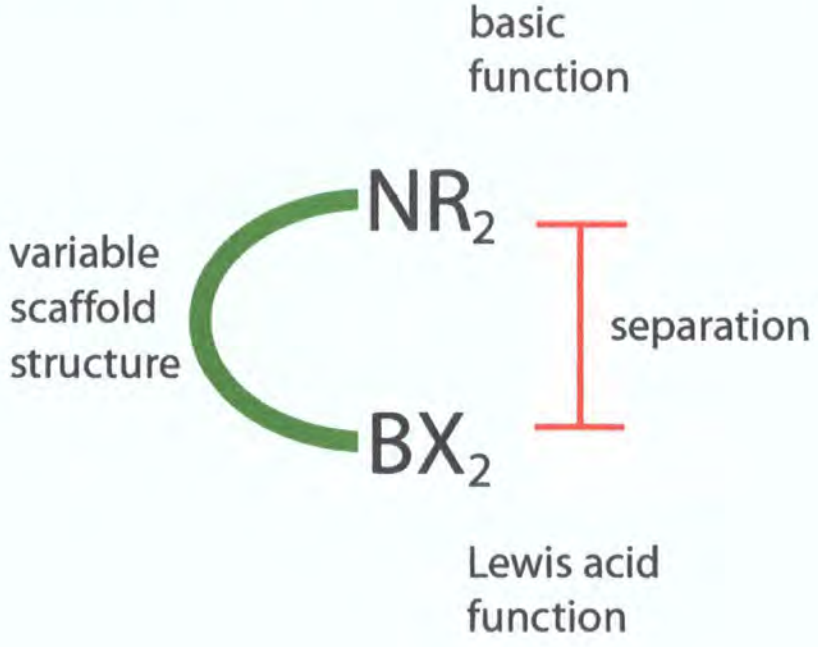

Figure 4: General structure of bifunctional aminoboron compounds targeted.

The first examples of compounds of this type being used as bifunctional catalysts date from 1959. Letsinger *et al.* demonstrated that quinoline-8-boronic acid accelerated the rate of formation of chloride ions from chlorohydrins and was superior to a mixture of quinoline and phenylboronic acid for the same reaction.[137]

2.2 Catalyst design

In the design of the aminoboron compounds (general structure, figure 4), it was noted that the following aspects of the catalysts could be varied: 1) The scaffold structure would determine the flexibility of the molecule, affect the electronic nature of the functional groups, determine the separation of the functional groups and provide an opportunity to introduce chirality; 2) The Lewis acidity of the boron functionality could be tuned, by varying the ligands X, from a weaker Lewis acid such as the boronic acid (X = OH) through to the dibromide. Also, by using a diol as a bidentate ligand it is possible to introduce asymmetry and/or vary steric requirements around the boron centre; 3) The electronic nature and sterics of the nitrogen Lewis basic centre could be varied by using both sp^2 and sp^3 nitrogen centres and altering the nitrogen substituents. The nitrogen centre also offers a good opportunity to introduce asymmetry into the molecule as many chiral amines are commercially available.

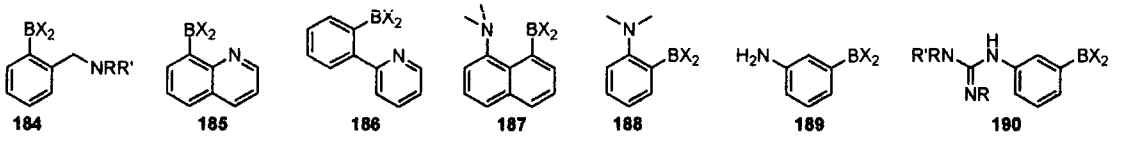

Several series of these compounds were targeted during this project. The benzylamine-2-boronic acid series **184** would allow us to vary the R and R' groups on nitrogen and to study the effect this would have on the intramolecular boron-nitrogen chelation. The quinoline-8-boronic acid series **185** would allow us to study a rigid system where the boron and the nitrogen are in close proximity, but are unable to intramolecularly chelate. The 2-phenylpyridine-2'-boronic acid series **186** is analogous to the quinoline-8-boronic acid series in that an sp^2 nitrogen is proximal to a boron function, but here there is much more flexibility within the molecule and also the possibility of intramolecular chelation. The *N,N*-dimethylaminonaphthylamine-8-boronic acid series **187** positions the boron and nitrogen function in such a way that in order to form the intramolecular chelate they must form a 5-membered ring. The *N,N*-dimethylaniline-2-boronic acid series **188** is analogous to the *N,N*-

dimethylaminonaphthyl-1-amine-8-boronic acid series **187** in that an anilinic nitrogen is proximal the boron, except that the intramolecular chelate would be a 4-membered ring. We were keen to investigate the structure and reactivity of these two similar series. In the aniline-3-boronic acid series **189** the boron and nitrogen functionalities are separated by a larger distance over a rigid framework. Analogous to this is the guanylbenzene-3-boronic acid series **190**, which replaces the aniline functionality with the much more basic guanidine function.

2.3 Catalyst synthesis and structure

The decision was taken at the beginning of the project to target boronic acids in preference to borinic acids or dialkylated arylborons. This was because boronic acids lend themselves most readily to derivatisation, allowing for the tuning of the boron Lewis acid strength.

The aminoboronic acids synthesised in this project generally formed boronic acid anhydrides on dehydration **192**. Protection with diols to produce compounds of type **193** enabled purification by column chromatography, frequently improving elution and preventing deboronation on the column. Fluorination of boron should allow the synthesis of compounds of type **194**, which should be derivatisable to compounds of type **195**, thus giving access to a more Lewis acidic boron functionality (Scheme 14).

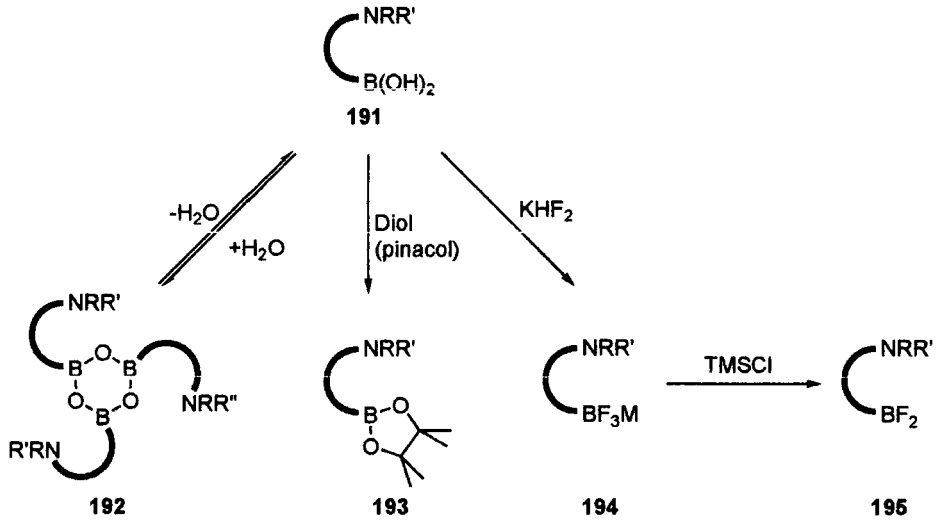

Scheme 14: Derivatisation of boronic acids.

The boronic acids themselves were synthesised by many and varied methods as described below.

2.3.1 *N,N*-dialkylbenzylamine-2-boronic acid series and related structures

A wide range of compounds in the *N,N*-dialkylbenzylamine-2-boronic acid series **184** were studied. We were particularly interested to explore whether amino-boronate systems could be prepared in which the amine and boronate groups are not permanently coordinated to each other. It was believed that by manipulating the steric requirements of the alkyl groups on nitrogen it would be possible to influence the intramolecular B-N chelation. A number of strategies were attempted to synthesise these compounds before a reductive amination route was found to be most successful.

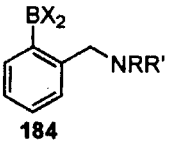

184

2.3.1.1 Directed *o*-lithiation methodology

We first attempted to synthesise *o*-boronated benzylamine **197** by the directed *ortho*-lithiation route. Unfortunately, the reaction was unsuccessful (Equation 36), producing a complex mixture of at least six products, as evidenced by TLC, NMR and mass spectrometry, which were not readily separable by column chromatography. Efforts to synthesise **197** by this route were abandoned.

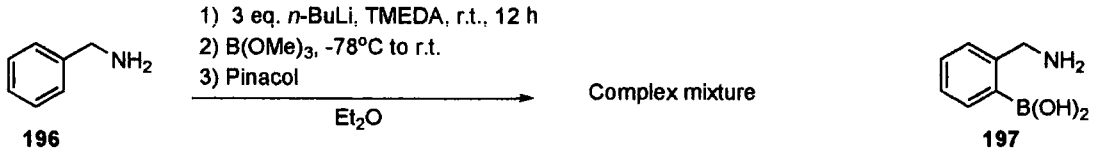

196 **197**

Equation 36: Attempted *o*-lithiation of benzylamine.

It is notable that Lauer *et al.* attempted to synthesise boronic acid **198** by the *ortho*-lithiation route, but instead produced diarylboron compound **199**. In the same publication, Lauer also detailed the synthesis of *N,N*-dimethylbenzylamine-2-boronic acid **200**, which is now available commercially.[138]

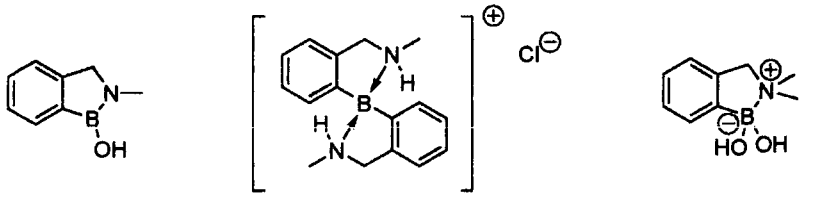

198 **199** **200**

Within the research group, Coghlan synthesised *N,N*-diisopropylbenzylamine-2-boronic acid **206** (Scheme 15). Coghlan's route employed the synthesis of amide **203**, directed *ortho*-lithiation followed by triisopropylborate quench to give *N,N*-diisopropylbenzamideboroxine trimer **204**, which was protected with pinacol **205** and reduced with borane give the desired boronic acid **206**. This could be converted to hydrogen trifluoride salt **207** by treatment with KHF_2 (aq.).[139]

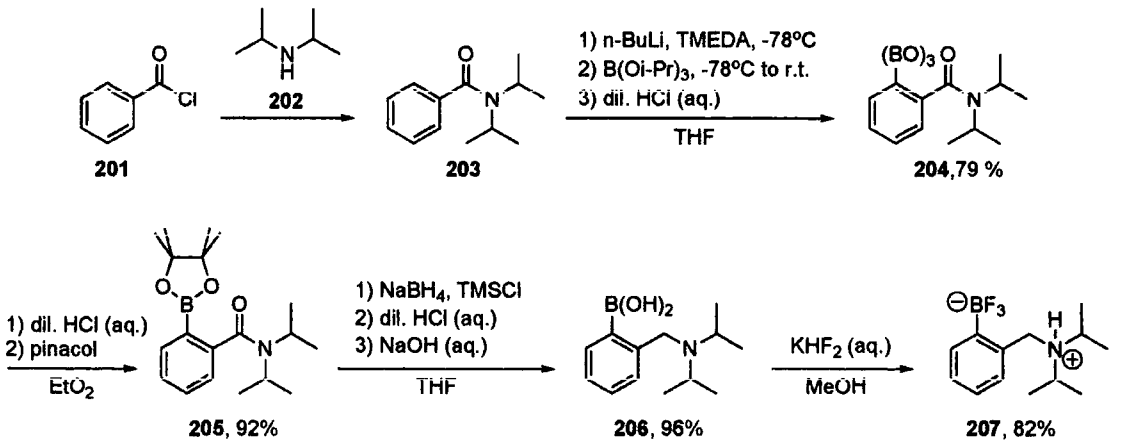

Scheme 15: Coghlan's route to *N,N*-diisopropylbenzylamine-2-boronic acid **206**.

An attempt was made to extend this methodology to the synthesis of the chiral boronic acid (*S,S*)-(-)-bis(α-methylbenzyl)amine-*N*-benzylamine-2-boronic acid **208**, a chiral analogue of **206**.

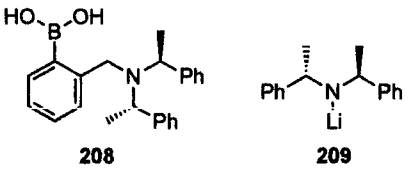

As lithium amide **209** has been shown by Simpkins *et al.* to be effective for stereoselective kinetic deprotonation in the formation of enolates,[140-142] it was hoped that the introduction of this moiety into the catalyst design would give us access to enantioselective catalysis. Synthesis of **208** was thus attempted utilising the directed *o*-metalation methodology (Scheme 16). The parent amine **210** was purchased from Aldrich under the potentially misleading moniker of [*S*-(*R**,*R**)]-(-)-bis(α-methylbenzyl)amine.

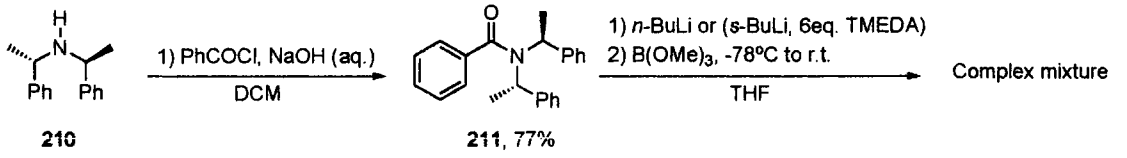

Scheme 16: Attempted *o*-lithiation of **211**.

Schötten-Baumann acylation of amine **210** proceeded smoothly in 77% yield to give chiral amide **211**. Attempts to lithiate **211** with *n*-BuLi at -78°C yielded only recovered starting material after trimethylborate quench and hydrolytic work-up. An alternative procedure utilising *s*-BuLi and TMEDA was investigated. No colour change was observed in the reaction initially at -78°C, but as the reaction was allowed to warm to room temperature the colour changed from colourless to bright red, which was presumed to indicate the formation of the desired *ortho*-lithiated species. The colour persisted as the reaction was cooled to -78°C and disappeared upon quench with trimethylborate. Hydrolytic work-up of the reaction, however, returned a complex mixture of products not readily separable by treatment with pinacol followed by column chromatography. Although this result was initially rather surprising, investigation of the literature in this area showed that Clayden *et al.* had studied the action of alkyl lithium reagents on *N*-benzylbenzamides and related compounds[143-155] and had observed interesting reactivity with compounds similar to **211** (Scheme 17).[153, 154]

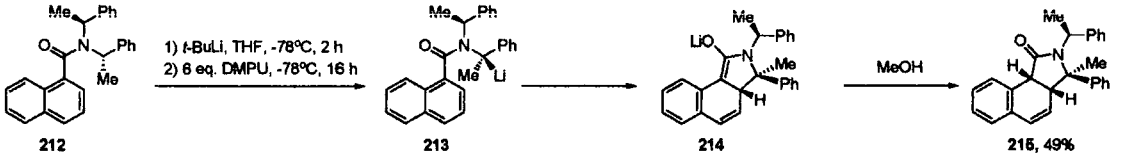

Scheme 17: Clayden *et al.* dearomatising anionic cyclisation of naphthamides.

Clayden *et al.* observed that **212**, the 1-napthalene analogue of **211** preferred a dearomatising anionic cyclisation to the expected *o*-lithiation. In separate studies Clayden *et al.* also observed that the lithiated *N,N*-dibenzylbenzamide **217** ring closed to the enolate **218**, which could attack the electrophile to give **219**, **220** or **221** (Scheme 18).[149, 150, 155]

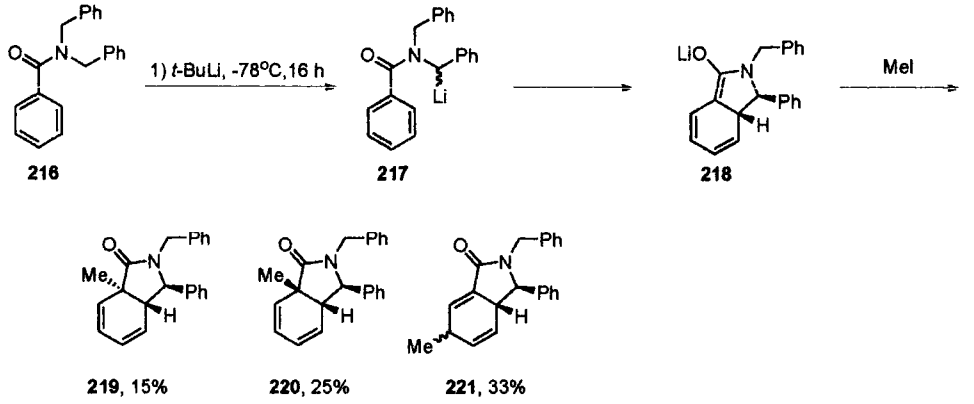

Scheme 18: Dearomatising anionic cyclisation of *N,N*-dibenzylbenzamide.

We would thus expect that the bright red colour observed in the lithiation of **211** (Scheme 16) is due to the formation of the benzyllithium species **222** (Scheme 19), which is characteristic of benzyllithium species.[153] Dearomatising anionic cyclisation would give enolate **223**, which upon quenching we believe would generate a series of diastereomeric forms of the ring-closed product. As our main interest was the synthesis of boronic acid **208**, this methodology was abandoned and alternative routes for this synthesis were sought.

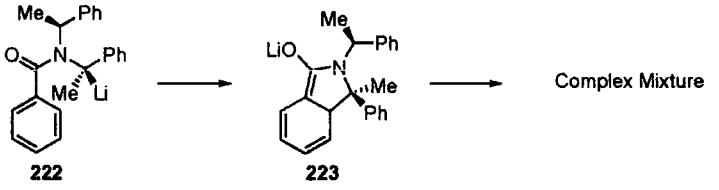

Scheme 19: Proposed path of lithiation reaction.

2.3.1.2 Reductive amination methodology

After these first attempts to synthesise **208** *via* lithiation reactions, it was discovered that 2-formylbenzeneboronic acid **224** was commercially available, initially from Frontier Scientific and later from Lancaster. This allowed us to investigate a reductive amination route to directly access benzylamine-2-boronic acids **226** (Equation 37).

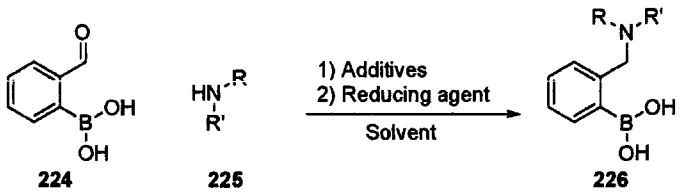

224 **225** **226**

Equation 37: Reductive amination route to benzylamine-2-boronic acids.

We believed it to be necessary to utilise neutral conditions for the reductive amination in order to avoid the risk of proto-deboronating either starting material or product by prolonged exposure to acid.[156]

We initially attempted the reaction using conditions developed by Mattson *et al.* (Equation 38). [157] This pH neutral method uses titanium (IV) isopropoxide as a Lewis acid to promote the formation of the imine (as opposed to the commonly used single equivalent of acetic acid[158]), followed by reduction with sodium cyanoborohydride.

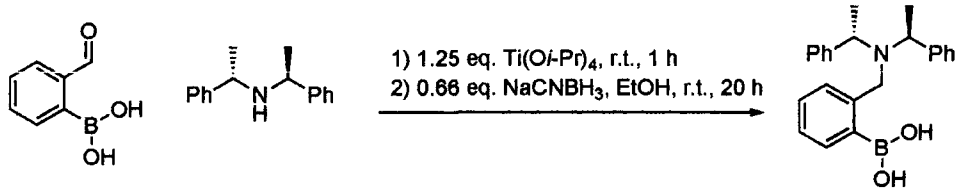

224 **210** **208**, ~ 2% HPLC-MS

Equation 38: Reductive amination Mattson methodology.

Analysis of the crude product mixture by HPLC-UV/MS (ESMS) indicated that the reaction had produced only ~2% of the desired boronic acid, as evidenced by integration of the HPLC-UV peak principally containing an ion with *m/z*

360.15. The only other HPLC-UV peak represented unreacted starting material (*m/z* 226.12). As sodium cyanoborohydride was used, care was taken not to acidify the reaction and produce hydrogen cyanide within the syrupy product, so neutral and basic aqueous work-up were used. Unfortunately this method failed to produce clean product. This was partly due to the low levels of product produced. An alternative higher yielding method was sought.

A modified application of the methodology developed by Abdel-Magrid *et al.*[158] utilising sodium triacetoxyborohydride was then investigated (Scheme 20).

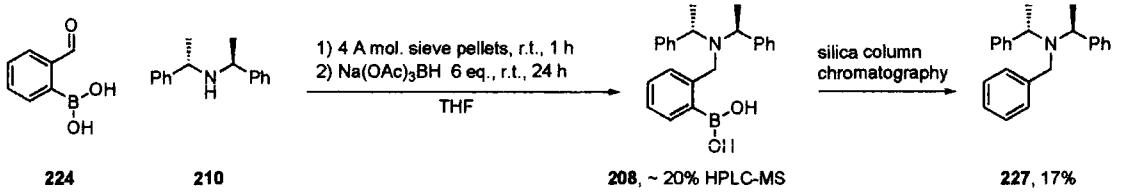

224 **210** **208**, ~ 20% HPLC-MS **227**, 17%

Scheme 20: Reductive amination Abdel-Magrid methodology.

Activated molecular sieves were used as an additive to drive the formation of the iminium ion by removal of water. This was used as an alternative to the equivalent of acetic acid (w.r.t. aldehyde) suggested for aiding the formation of iminium ions with sterically demanding secondary amines by Abdel-Magrid *et al.*[158] The iminium ion formation appeared to occur rapidly, with the reaction taking on a clear yellow appearance within several minutes. After one hour, sodium triacetoxyborohydride was added, forming a rather viscous mixture which nevertheless could still be stirred. After 24 hours the reaction was quenched with water.

Analysis of the crude by HPLC-UV/MS (ESMS) indicated approximately 20% conversion to boronic acid (by HPLC-UV integral of peak containing ion at *m/z* 360.15), with unreacted starting material the only other major component (*m/z* 226.12). However, upon purification by silica column chromatography the deboronated amine **227** was isolated in 17% yield (presumably the product of protodeboronation during chromatography) with none of the desired boronic

acid **208** isolated. The same reaction was also attempted in the absence of molecular sieves with identical purification, resulting in a drop in the yield of amine **227** to 11%.

Although the desired product was not isolated during this reaction, there was good evidence for its formation from the HPLC-MS and proof of the success of the reductive amination from the isolation of amine **227**. This methodology offered several advantages over the Lewis acid mediated route: the yield was slightly higher, although still low, and the starting materials and crude reaction mixture were much less toxic. We decided to investigate if this method could be made synthetically useful.

Method development of the reductive amination route was continued with diisopropylamine, a cost effective, sterically encumbered, model substrate for optimisation studies of the synthesis and isolation of a benzylamine-2-boronic acid, before the methodology was applied to a range of amines.

We investigated the reductive amination of diisopropylamine with benzaldehyde-2-boronic acid **224** under various conditions (Equation 39, Table 1), studying the effect of stirring and the amount of molecular sieves and reducing agent on the yield. Initially the work-up conditions for boronic acid **206** were addition of 5% (w/v) HCl (aq.), filtration, azeotropic removal of THF and neutralisation with saturated $NaHCO_3$ (aq.). Boronic acid **206** crystalised upon standing from this mixture. This method later became unreliable as crystalisation ceased to occur on neutralisation even when seed crystals were added. This coincided with starting a new bottle of aldehyde **224** starting material, which was slightly yellow instead of bright white, although apparently pure by ^1H NMR analysis. When using the lower grade aldehyde **224** starting material, the boronic acid **206** could be obtained in high purity by extraction into DCM (x 4), solvent removal, redissolution into 5% (v/v) aqueous hydrochloric acid, washing with DCM, pH adjustment to 10 and extraction back into DCM. Subsequently within the group, Knowles demonstrated that the latter work-up method returned 99% of starting material when starting from pure **206**.[159] The compound was isolated solely as the

free boronic acid **206** from both methods. However, upon exhaustive drying under vacuum at higher temperature in a drying pistol some anhydride **228** was detected by electrospray mass spectrometry at *m/z* 453 (Equation 40). It is noteworthy that there was no evidence for formation of boroxine, the common anhydride for boronic acids. Evaporative crystallisation of a sample of boronic acid **206** from DCM produced crystals which were suitable for single crystal X-ray analysis (*vide infra*).

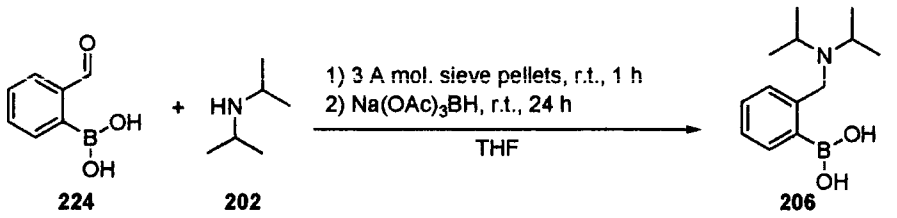

224 **202** **206**

Equation 39: Method development - reductive amination.

Entry	$Na(OAc)_3BH$ eq.	Mol. sieve pellets (g(mmol cpd. **224**)$^{-1}$)	Stirring	Isolated yield **206**
1	2	2.6	Yes	42%
2	6	0	Yes	63%
3	6	0.66	Yes	71%
4	6	1.42	Yes	77%
5	6	1.33	No	36%

Table 1: Reductive amination route to *N,N*-diisopropylbenzylamineamine-2-boronic acid **206**.

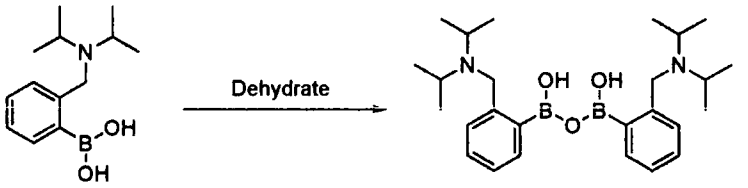

206 **228**

Equation 40: Boronic acid anhydride formation.

Activated molecular sieves were established to have a profound effect on the reaction. It might be expected that water removal would force the equilibrium over towards the formation of the iminium ion prior to reduction and so it seems, with the increase in the quantity of activated molecular sieves from

none to 0.66 gmmol^{-1} to 1.42 gmmol^{-1} (with respect to the aldehyde **224)** so increases the isolated yield from 63% to 71% to 77% (Entries 2, 3 and 4, Table 1). It was also found to be advantageous to use an large excess of the reducing agent, with isolated yields increasing from 42% to 77% with an increase in the number of equivalents of reducing agent from 2 to 6 (Entries 1 and 4, Table 1). Reductive amination using sodium triacetoxyborohydride and molecular sieve pellets produced a somewhat viscous and sticky reaction mixture. If this mixture was not stirred, the isolated yield suffered considerably, decreasing from 77% to 36% (Entries 4 and 5, Table 1). However, if molecular sieve powder was used the reaction was totally unstirrable with a magnetic stirrer. For this reason all reactions presented here used sieves in pellet form. The optimised conditions for the reaction therefore comprised; a large excess of reducing agent, the addition of activated molecular sieve pellets and efficient stirring.

Having developed a methodology giving viable yields, the synthesis of a range of benzylamine-2-boronic acids was attempted. Parent amines included a primary amine and three secondary amines of increasing steric bulk (Scheme 21, Table 2).

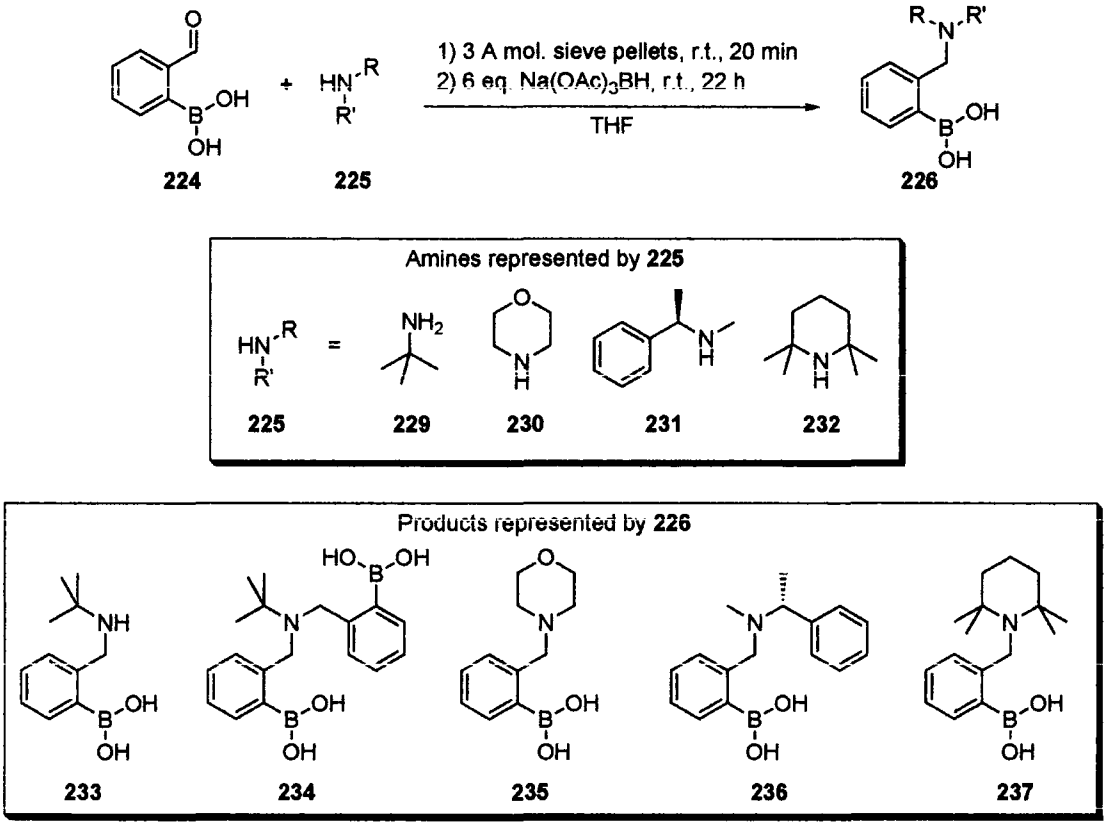

Scheme 21: Reductive amination route to series of *N,N*-benzylamine-2-boronic acids.

Entry	Parent amine	Isolated yield	Notes
1	**229**	0%	Complex mixture
2	**230**	61%	
3	**231**	62%	
4	**232**	0%	No product in crude by ^{1}H NMR

Table 2: Yields - benzylamine-2-boronic acids.

The reaction of *t*-butylamine **229**, where one might have expected a large degree of double amination at the nitrogen to give product **234**, produced a crude material with an exceptionally complex TLC and ^{1}H NMR spectum. It was not possible to isolate any pure material from this reaction by solid phase extraction using a Varian mega-bond elut SCX™ (a prepacked silica bonded C-18 benzene-*p*-toluenesulfonic acid column) or pH based aqueous work-up, as sucessfully applied to **226** (Entry 1, Table 2)

Morpholinobenzylamine-2-boronic acid **235** was successfully synthesised. As expected, **235** was soluble in both organic and polar solvents, including water at high and low pH. Hence pH based aqueous work-up as applied to **226** was less successful. The compound was also not readily isolable by silica column chromatography and instead was purified by solid phase extraction on a Varian Mega-bond elut SCX™ column. The product was heavily contaminated with unreacted morpholine after elution, but this was removed by extended application of high vacuum (Entry 2, Table 2). The chiral bifunctional boronic acid **236** was also isolated using the Varian Mega-bond elut column with a similar yield to **235**, despite **231** being a more bulky substrate (Entry 3, Table 2). In order to generate a structure with a high degree of steric hindrance around the nitrogen, the reductive amination of 2,2,6,6-tetramethylpiperidine **232** was attempted (Entry 4, Table 2). Although bulky amines **231** and **202** had both proved fruitful substrates, it appears that the steric bulk around the nitogen in 2,2,6,6-tetramethylpiperidine **232** was enough to prevent iminium ion formation and thus reductive amination, resulting in full recovery of the starting material by solid phase extraction on Varian mega-bond elut SCX™.

2.3.1.3 Spectroscopy of *N,N*-dialkylbenzylamine-2-boronic acids

At this stage we had in hand four benzylamine-2-boronic acids with steric bulk around nitrogen increasing in the order **200** < **235** < **236** < **206**. We sought to determine the structure and properties of this series in order to investigate the effect of steric hindrance around nitrogen on intramolecular chelation and the corresponding ability of the compounds to act as bifunctional catalysts.

Boronic acid **200** is supplied as a mixture of the intramolecular 'ate' complex and its anhydride boroxine trimer **238** in 70:30 ratio (as evidenced by ^{11}B NMR integration of peaks at δ 19.3 and 9.7 ppm respectively) (Entry 1, Table 3). This is due to the low levels of steric hindrance imposed by the two methyl groups to the formation of the intramolecular chelate. However, all *N,N*-dialkylbenzylamine-2-boronic acids **226** produced in this project appear to

possess a 'free' boronic acid functionality in solution, indicated by structures **226a** and **226b**, (structural assignment based on ^{11}B shifts of between δ 30.1 and 28.9 ppm) (Entries 2-4, Table 3).

We had expected that by increasing the steric bulk on compounds of type **226** that we would be able to prevent B-N coordination. What is perhaps surprising is the small increase in steric bulk required to affect this changeover. Morpholinobenzylamine-2-boronic acid **235** exhibits hardly any extra steric demand in comparison to **200**, but appears to exist as the 'free' boronic acid in solution (Entry 2, Table 3). It follows that boronic acid **236** with its relatively bulky α-methyl benzyl group also appears to exist as the free boronic acid **226a** in equilibrium with **226b** (Entry 3, Table 3).

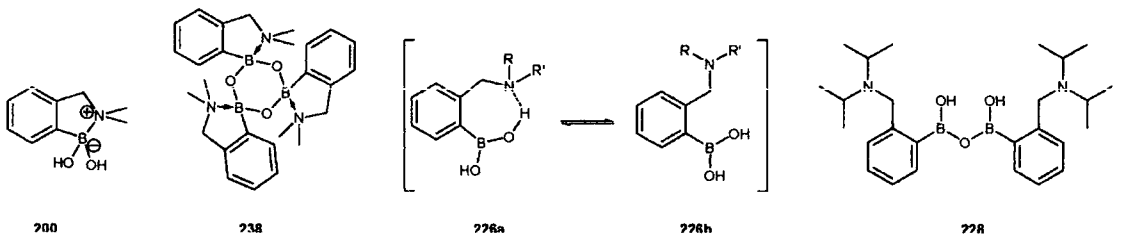

Entry	Benzylamine-2-boronic acid	^{11}B NMR δ	Solvent	Notes
1	**200**	19.3 and 9.8 ppm	$CDCl_3$	Boroxine trimer and intramolecular 'ate' complex approx. 70:30 by ^{11}B NMR integration
2	**235**	29.9 ppm	$CDCl_3$	'Free' boronic acid
3	**236**	30.1 ppm	$CDCl_3$	'Free' boronic acid
4	**206**	29.1 ppm	$CDCl_3$	'Free' boronic acid

Table 3: ^{11}B NMR shifts *N,N*-dialkylbenzylamine-2-boronic acids.

Single crystal structure analysis of **206** (Figure 5) shows that it exists as the free boronic acid in the solid state, with intramolecular hydrogen bonding of the nitrogen to a boron hydroxyl group. Another interesting aspect of the solid-state structure is that boronic acid **206** retains the boronate-to-phenyl-ring conjugation, as evidenced by the coplanarity of the two functions in the crystal structure. As mentioned previously, **206** forms a seven-membered ring with a relatively linear and extremely short hydrogen bond to the diisopropylamine

nitrogen (2.637 Å (O1-H1-N1), compared to a median value from the Cambridge Structural Database of 2.861 Å[160]).

Dehydration of **206** has been shown to yield dimer **228** (Equation 40) an atypical boronic acid anhydride in which hydrogen bonding would still be able to occur, twice over!

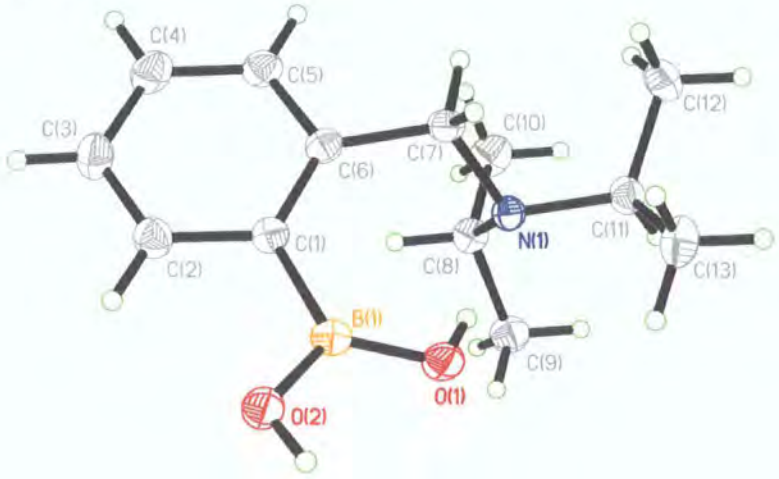

Figure 5: ORTEP X-ray crystal structure of boronic acid **206**, projected to show N-H-O-B H-bonding, showing 50% probability ellipsoids.

2.3.1.4 Fluorinated derivatives

In the pursuit of a more Lewis acidic aryldifluoroboron derivative of the catalyst, a co-worker, S. Coghlan, had previously synthesised hydrogen trifluoroborate salt **207**. The procedure was reproduced with minor modifications to generate material for the study of the difluoroborate **239** (Scheme 22). The reaction of **206** with potassium hydrogendifluoride provides the HF salt **207**, rather than the potassium salt,[161] or the neutral difluorborane **239** which can result when there is a basic function proximal to the boron centre, as in the N,N-dimethylnaphthyl-1-amine-8-boronic acid system **240** (*vide infra*). In this case, both the basicity of the amino group and the appearance of a hydrogen bond between a fluorine atom and the N-H seem to work together to give preference for formation of the HF salt **207** (Figure 6) (X-ray structure reproduced with permission from Coghlan *et al.*).[139]

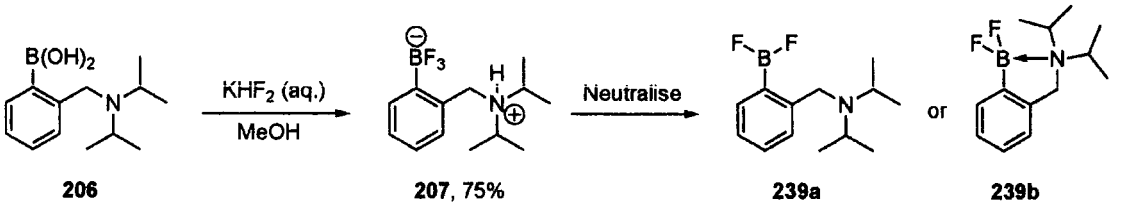

Scheme 22: Fluorinated *N,N*-diisopropylbenzylamine-2-boronic acid derivatives

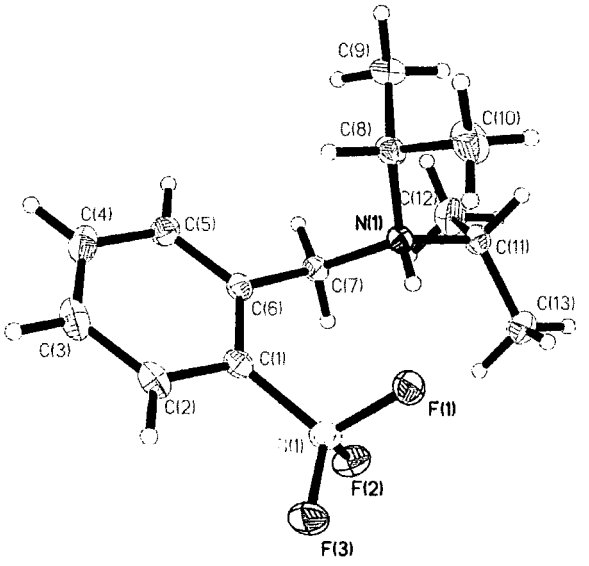

Figure 6: ORTEP X-ray crystal structure of trifluoroborate **207**, showing 50% probability ellipsoids.[139]

It was expected that formation of the difluoroborane **239** would be possible by direct neutralisation of the HF salt. Several attempts to achieve this were made using, for example, sodium carbonate, sodium methoxide, sodium hydride, calcium hydride, *n*-butyllithium or *t*-butyllithium. However, the difluoroborane could not be isolated as a pure, stable compound from any of these attempts. It was, however, possible to gather some evidence for formation of the intramolecular chelate **239b** in solution (acetonitrile), especially with calcium hydride, by ^{11}B NMR, which showed a clear, sharp triplet at δ 3.68 (*J* 56.3 Hz). This is diagnostic of both the difluoroborane function and the fact that there is strong B-N chelation, with the low chemical shift suggesting **239** exists as **239b** rather than **239a**. However, this product was observed to rapidly decompose within minutes of synthesis to a complex

mixture. This instability of the aryldifluoroboron product was frustrating as it meant that **239** was unsuitable for study as a bifunctional catalyst.

2.3.1.5 Bromo-(*S,S*)-(-)-bis(α-methylbenzyl)amine]-*N*-benzamides – Miyaura methodology

An alternative three-step route to boronic acids **206** and **246** was also briefly explored around the same time as the reductive aminations, but was abandoned in favour of the one-step reductive amination procedure (*vide supra*). Acylation, palladium catalysed cross-coupling with a diboron reagent, followed by reduction to simultaneously reduce the amide and deprotect the boron, was expected to give boronic acids **206** and **246** (Scheme 23).

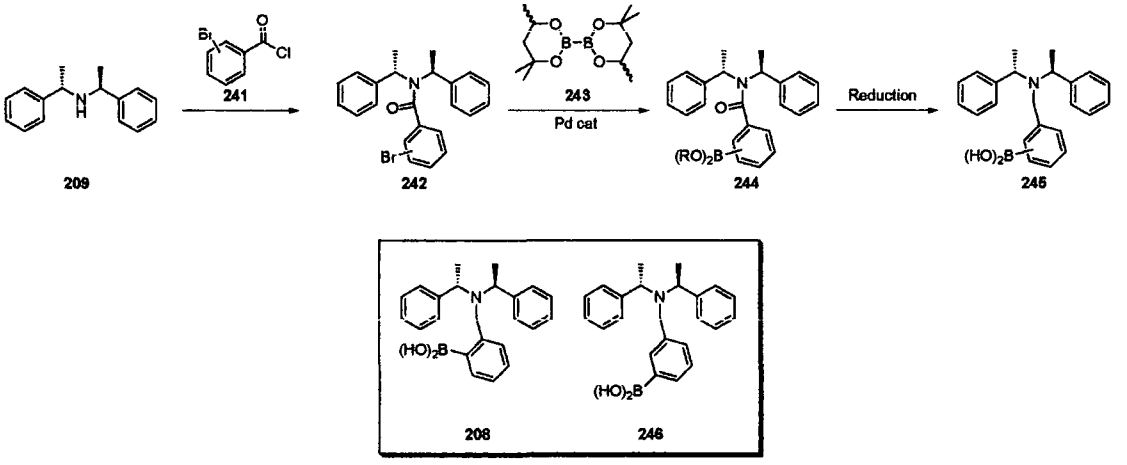

Scheme 23: Acylation-transmetalation-reduction route to benzyamine-2-boronic acids.

Acylation was achieved by drop-wise addition of acyl chlorides **247** or **249** to amine **209** dissolved in diethyl ether or DCM in biphasic mixture with aqueous sodium hydroxide (5% w/v), in good yields of 72% and 85% respectively (Equations 41 and 42). Samples of **248** and **250** suitable for single crystal X-ray structural determination were obtained (*vide infra*).

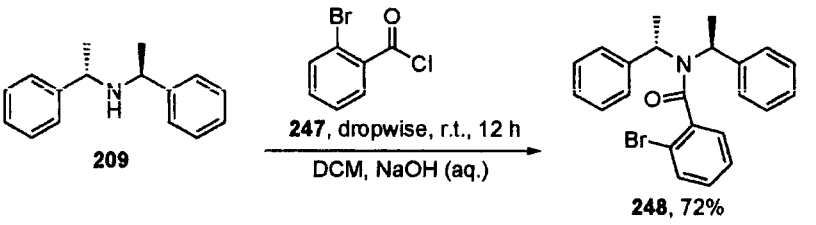

Equation 41: Acylation of (*S,S*)-(-)-bis(α-methylbenzyl)amine.

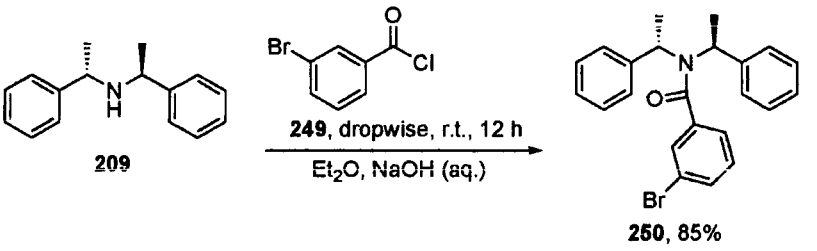

Equation 42: Acylation of (*S,S*)-(-)-bis(α-methylbenzyl)amine.

Amide **248** existed as two rotamers in a 60:40 ratio on an ^{1}H NMR timescale in $CDCl_3$ and D_6-DMSO, as evidenced by peak integration. ^{1}H NMR spectra were acquired in D_6-DMSO at 24, 60, 70, 80, 90, 100, 110, 120 and 130°C (Figure 8). As the temperature of the sample increased, the spectrum simplified significantly. At room temperature peaks corresponding to benzyl hydrogens H_b and H_c (Figure 7) appeared at δ 4.82 and 4.64: δ 4.72 and 4.60, 60: 40, with appropriately coupled methyl peaks due to H_a and H_d δ 1.88 and 1.77: δ 1.83 and 1.62, 60: 40. These peaks gradually coalesced as the temperature was increased and at 130°C the spectrum showed broad singlets at δ 4.75 corresponding to H_a and H_d, and at δ 1.80, corresponding to H_b and H_c. It was not possible however to determine the timescale of rotation τ using equation 43[162], as coupling constants between (H_a and H_b) and (H_b and H_c) appear identical in the 2 rotameric forms (at J = 6.74). This prevents us from distinguishing the value δν. HPLC-UV and TLC analysis of **250,** however, showed only one compound, indicating that the two rotameric forms were inter-converting on the analysis timescale in solution at room temperature.

The comparison between **248** and **211** is striking. Both of these compounds, neither of which possesses an *ortho* substituent on the C(=O)Ar ring, exhibit free rotation on the NMR timescale, as evidenced by broad singlet signals for

all benzyl protons (at δ 4.80 for **250** and 4.80 for **211**) and all methyl protons (at δ 1.75 for **250** and 1.69 for **211**) at room temperature.

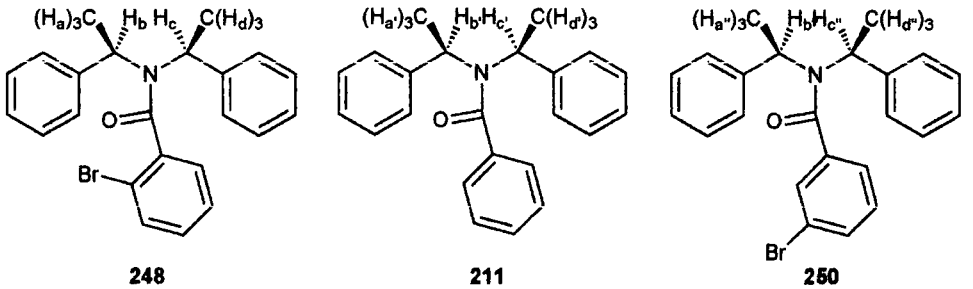

248 **211** **250**

Figure 7: Proton labelling in (S,S)-(-)-bis(α-methylbenzyl)amine]-*N*-benzylamine series.

$$\tau \approx (1/2\pi)/\delta\nu$$

Equation 43: Rotation timescale.

In the solid state **248** succeeds in minimising its energy by placing the two phenyl rings on the opposite side of the amide bond junction to the bromine (Figures 9 and 10). In the solid state structure of **250**, although the two phenyl rings still crystallise on the same side of the amide bond junction, the bromine is placed either on the same or the opposite side to the phenyl rings, with both forms found in a 1:1 ratio in a single crystal! (Figure 11).

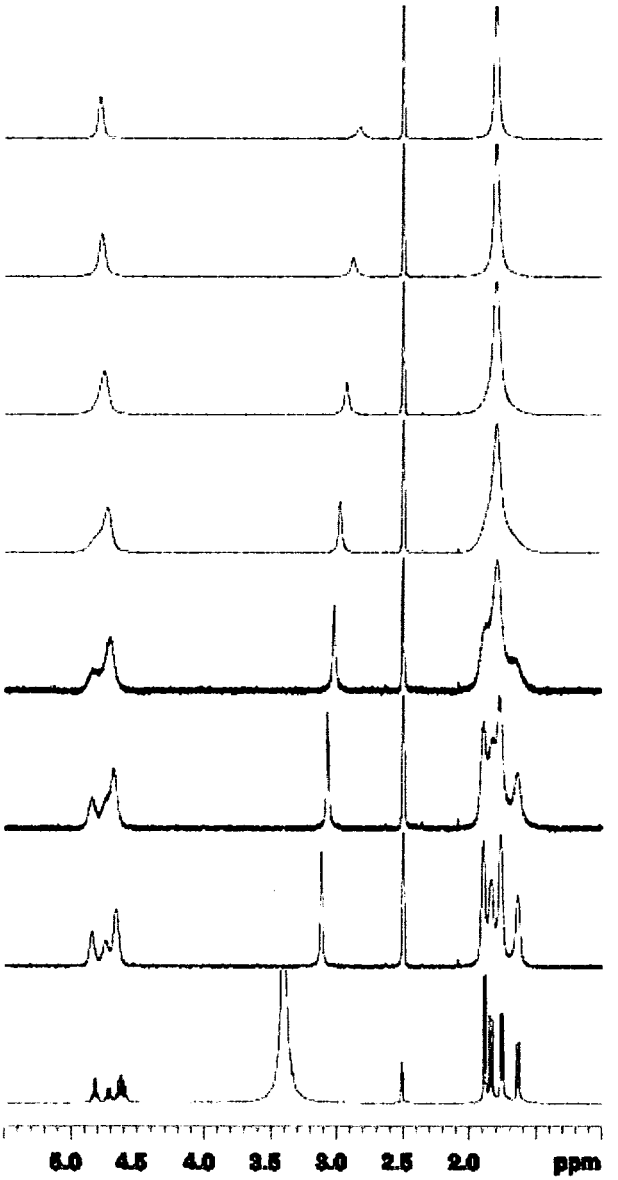

Figure 8: Coalescence of benzyl and methyl ^{1}H NMR peaks (δ 4.8-4.5 and 1.95-1.55 ppm) with graduated heating in D_6-DMSO, from 24, 70, 80, 90, 100, 110, 120, 130°C respectively (ascending).

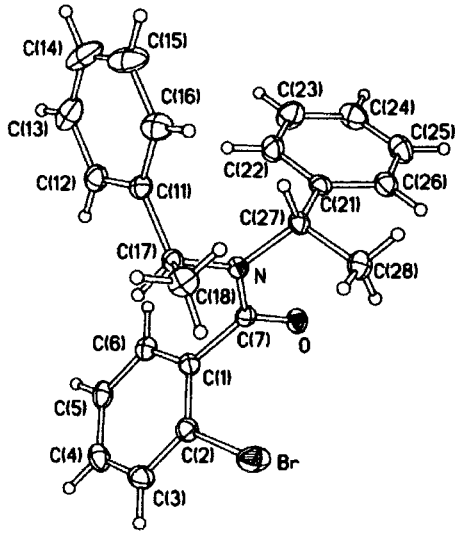

Figure 9: ORTEP X-ray crystal structure of bromide **248**, showing 50% probability ellipsoids.

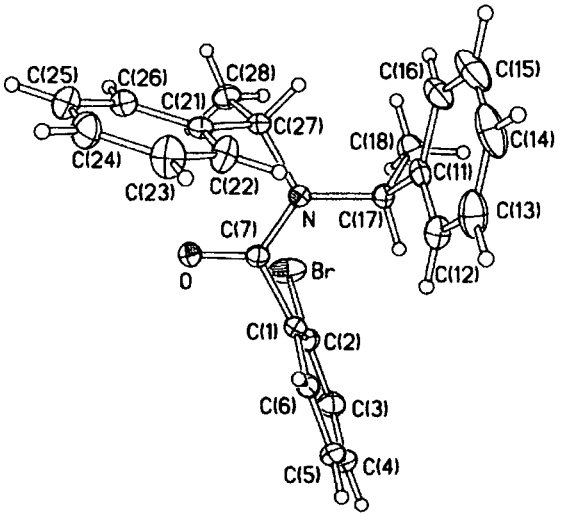

Figure 10: ORTEP X-ray crystal structure of bromide **248**, showing 50% probability ellipsoids, alternative view.

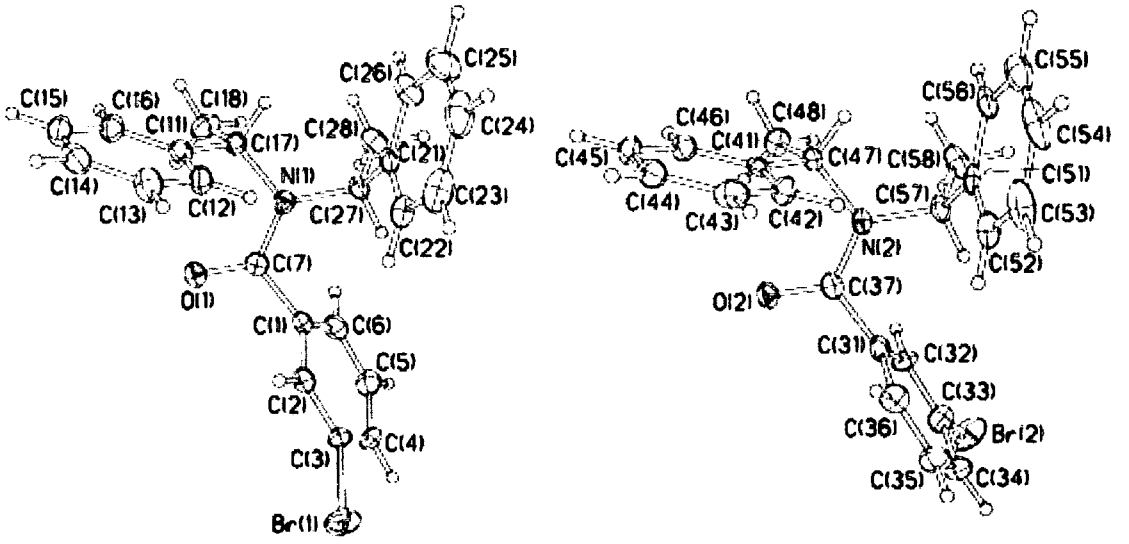

Figure 11: ORTEP X-ray crystal structure of bromide **250**, showing 50% probability ellipsoids.

Palladium-catalysed coupling with diboron reagent **243** utilising the methodology developed by Miyaura *et al.*[163] failed to produce the desired product (Equation 44). HPLC-UV/MS$^+$ analysis indicated almost total recovery of the amide starting material (*m/z* 408.1) with some evidence for a very small amount (~ 1% UV peak area by HPLC-UV-MS) of dimer **251** (*m/z* 657.9) in the crude mixture. It was not possible to isolate this product on this scale (1 mmol). However, this does suggest that the Miyaura boronation reaction was taking place to some degree. It is likely that under these conditions the Miyaura coupling is slowly generating the arylboron, which then reacts with the excess arylbromide in the mixture by a Suzuki-type cross-coupling reaction[164] to give the dimer. The fact that the dimer is observed in very low conversion with none of the arylboron observed suggests that the Suzuki reaction takes place much more rapidly than the Miyaura reaction.

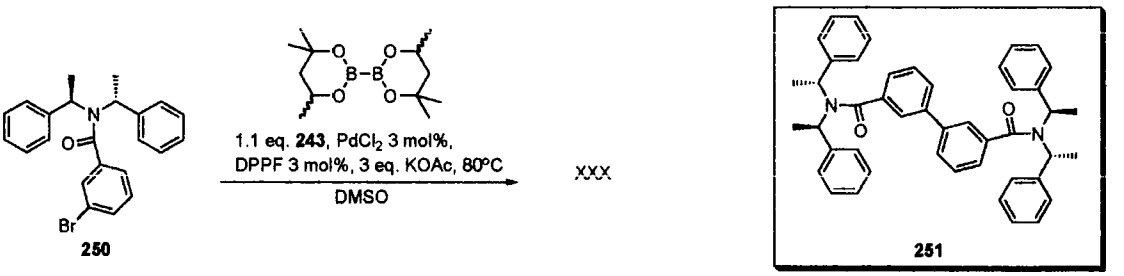

Equation 44: Failed Miyaura-type Palladium-catalysed cross-coupling reaction.

2.3.1.6 Summary – *N,N*-dialkylbenzylamine-2-boronic acid series

In summary, reductive amination of secondary amines was found to be a generally applicable route to compounds in the *N,N*-dialkylbenzylamine-2-boronic acid series, except where the steric bulk on the parent amine is prohibitively large. Structures have been synthesised with increasing steric bulk. Surprisingly, relatively little steric demand on the nitrogen is required to prevent intramolecular B-N chelation. A chiral example has been produced. A trifluoroborate salt has been synthesised and converted to the difluoroborate, which proved to be a very short-lived species. With the exception of difluoroborate **239** all compounds synthesised in the *N,N*-dialkylbenzylamine-2-boronic acid series were found to be stable and could be conveniently handled in air. All boronic acids synthesised in this series were soluble in most organic solvents at room temperature, except for very non-polar solvents, and were soluble in water at high and low pH.

2.3.2 Quinoline-8-boronic acid series

In the quinoline-8-boronic acid series **185** the boron and the nitrogen are in close proximity, but are unable to intramolecularly chelate due to the structural rigidity provided by the fused rings.

Synthesis of quinoline-8-boronic acid **253** was originally accomplished following the method described by Letsinger *et al.* (Scheme 24).[137] All spectroscopic and analytical details were identical to those reported in the literature.[165, 166] This compound was later acquired from Lancaster Synthesis.

In order to synthesise the fluorinated derivative, a methanolic solution of **253** was treated with aqueous KHF_2 producing hydrogen trifluoroborate salt **254** as hygroscopic crystals (Scheme 24). The solubility of **254** was very poor in organic solvents and in water. Maximum solubility was observed in D_6-DMSO and in D_3-MeCN. Although all other analysis was possible, ^{13}C NMR analysis is inconclusive, with peaks insufficiently distinct from the inherent noise, even with 12 hours of NMR data collection. It was not possible to generate difluoroborane **255** by the action of TMSCl using the method described by Vedejs *et al.*[161]

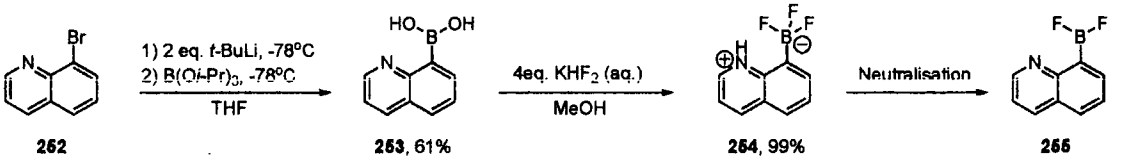

252 **253**, 61% **254**, 99% **255**

Scheme 24: Synthesis quinoline-8-boronic acid series.

Synthesis of boronic acid **257** was attempted using a Heck coupling of a vinyl boronate **256** to arylbromide **252**, using a methodology developed within the group (Equation 45).[167]

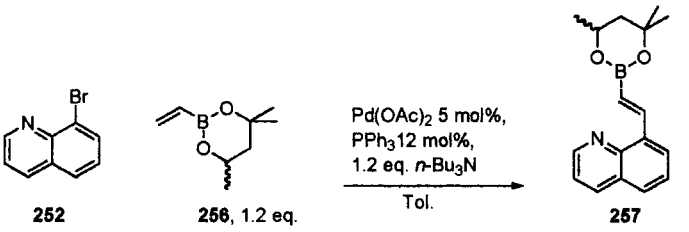

Equation 45: Attempted Heck coupling.

No reactivity was observed when the reaction was heated for 20 hours at reflux or when the reaction was irradiated for seven minutes in a microwave reactor. A literature search revealed that pyridine-type compounds make poor substrates for the Heck reaction with no successful examples thus far published.

In summary, boronic acid **253** is an interesting rigid aminoboronic acid, with no possibility for intramolecular chelation between its sp^2 nitrogen centre and its boron centre. It is very sparingly soluble in non-polar organic solvents and exhibits increased solubility as solvent polarity increases, with maximum solubility observed in acetonitrile and methanol (in the former of which it would be expected to be converted to the dimethylborate). The neutral difluoroborate **255** was not readily generated from its HF salt **254**.

2.3.3 2-Phenylpyridine-2'-boronic acid series

The 2-phenyl-2'-boronic acid series **186** is analogous to the quinoline-8-boronic acid series **185** in that both compounds contain a sp^2 nitrogen. However, there exists the possibility of B-N coordination due the fact that we would expect shorter B-N separation, greater scaffold flexibility and free rotation about the single bond between the rings.

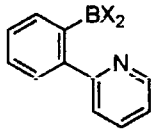

186

Zoltewicz *et al.* demonstrated that 2-phenylpyridine is capable of inter-ring lithiation to give **259**, as evidenced by the product of electrophilic quench (Scheme 25).[168] The synthesis of boronic acids and derivatives of type **186** was attempted by this methodology (Scheme 26).

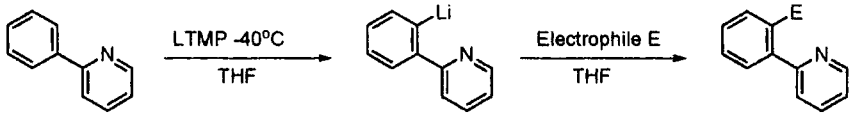

258 **259** **260**

Scheme 25: Zoltewicz *et al.* directed inter-ring *o*-lithiation with electrophilic quench.

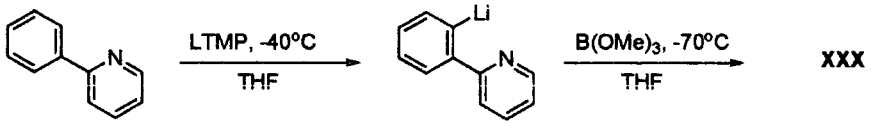

258 **259**

Scheme 26: Direct inter-ring *o*-lithiation with trimethylborate quench.

The reaction was repeated several times with different work-up methods used each time. Attempts to isolate the products of the reaction by direct Kugelröhr distillation of the crude, as had been successful on the naphthyl-1-amine-8-boronic acid series **187** (*vide infra*), led to tar formation. TLC of the crude after quench with NH_4Cl (aq.) showed no separation of the components. When the

crude product was treated with pinacol and subjected to silica column chromatography a high number of products was apparent (7 components, 8 including the pinacol), making purification of individual components impossible. Hence a series of mixtures was obtained. It is worth noting that not one of the mixtures eluted appeared to contain the desired pinacol-protected boronic acid, or in fact the unprotected boronic acid, as evidenced by ^{11}B NMR and ^{1}H NMR.

From within the department, Beeby *et al.* were able to supply a quantity of 2'-bromo-2-phenylpyridine **261**,[169-171] which was subjected to lithium-halogen exchange[172, 173] followed by boronation (Equation 46).

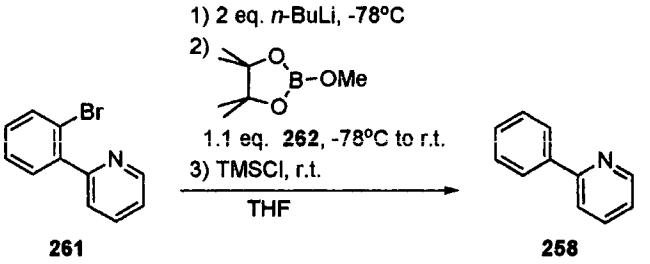

Equation 46: Attempted lithium-halogen exchange route to 2-phenylpyridine-2'-boronic acid series.

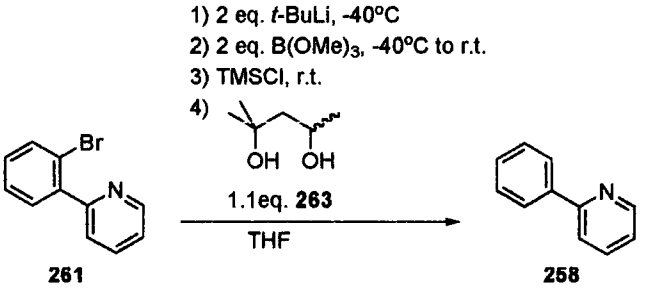

Equation 47: Modified lithium-halogen exchange route to 2-phenylpyridine-2'-boronic acid series.

Initially, *n*-BuLi was used for the exchange reaction, with boronation from mixed borate species **262**, which would be expected to quench directly to give pinacol-protected 2-phenylpyridine-2'-boron species **264**. However, the reaction proceeded to give 2-phenylpyridine **258** in 87% yield. (All spectroscopic and analytical details were identical to those described in the

literature[174, 175]). Alternative conditions utilising *t*-BuLi at a slightly higher temperature with a more reactive boron electrophile followed by work-up with TMSCl and finally addition of diol **263** were attempted (Equation 47). Diol **263** had been found, within the group, to produce boronic acid esters which were more stable towards deboronation during silica column chromatography.[167] However, 2-phenylpyridine **258** was again recovered in almost quantitative yield, alongside unreacted starting material. Production of 2-phenylpyridine suggests that the lithium halogen exchange was successful. The fact that no silicon-quenched product **265** was observed suggests that boron quench was complete and that the TMSCl treatment was working as intended to give TMSOMe and LiCl. It seems likely then that in the presence of a proton, either provided by diol **263** or more likely the acidic surface of the silica gel, the boron of the boronated product **264** was rapidly replaced by hydrogen.

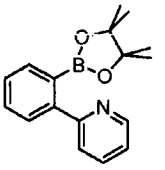

264

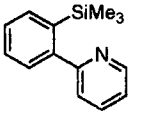

265

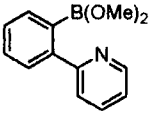

266

2.3.4 *N,N*-Dimethylnaphthyl-1-amine-8-boronic acid series

Compounds in the *N,N*-dimethylnaphthyl-1-amine-8-boronic acid series **187** were studied to investigate the effect on catalysis of intramolecular B-N coordination relative to the analogous *N,N*-dimethylaniline-2-boronic acid series **188** where intramolecular B-N coordination is less likely.

2.3.4.1 Directed *o*-lithiation methodology

Boron was introduced into *N,N*-dimethylnaphthyl-1-amine **267** by reaction with *n*-BuLi, which results in the thermodynamically favoured lithiation at the '8' position, **268**, followed by quenching with either trimethylborate or triisopropylborate to yield the dialkylborate **269**, which in the latter case was readily isolable by distillation. Hydrolysis of **269** results in the formation of the boroxine trimer **270** (Scheme 27).

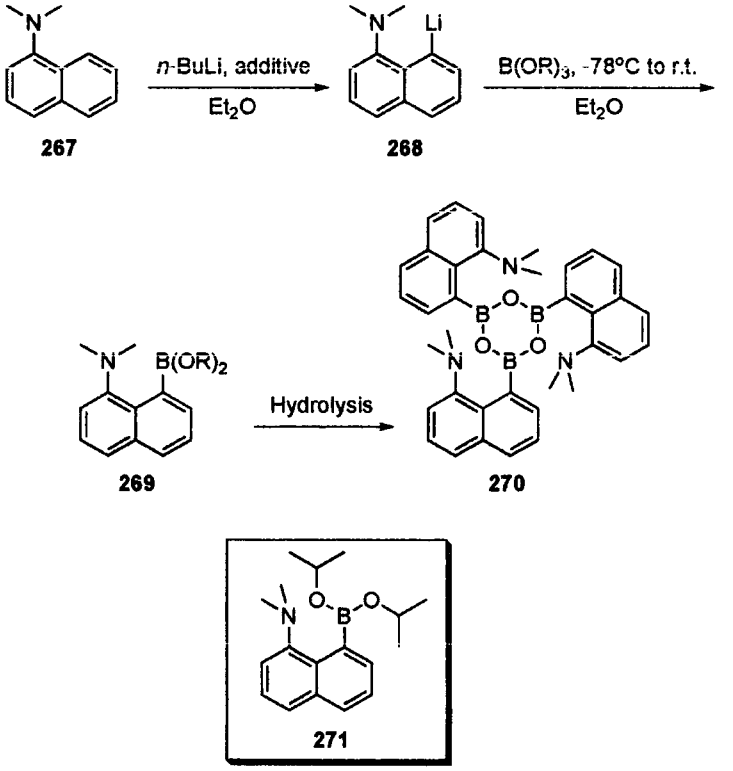

Scheme 27: Synthesis of *N,N*-dimethylnaphthyl-1-amine-8-boroxime trimer **270**.

Two methods were investigated for the generation of naphthyllithium **268** (Table 4). The first method, developed by van Koten *et al.*, used TMEDA as an additive.[176] The second method was developed by Corriu *et al.* and used no additives. [177] (Both of these studies were made *en-route* to non-boronated targets). We also varied the work-up procedures.

Entry	Additive	Electrophile	Conditions	Work-up method	Yield (**271**), **270**	Notes
1	TMEDA	$B(O\textit{i}\text{-}Pr)_3$	Reflux, 4h	Direct quench	60%	
2	TMEDA	$B(O\textit{i}\text{-}Pr)_3$	Reflux, 4h	Distillation then quench	N/A	Unsuitable for distillation
3	None	$B(OMe)_3$	r.t., 125 h	Direct quench	69%	
4	None	$B(O\textit{i}\text{-}Pr)_3$	r.t., 120 h	Distillation then quench	(48%) 43%	

Table 4: Synthesis of **269** and **270** with and without TMEDA additive.

With TMEDA as an additive the generation of the naphthyllithium **268** proceeded quickly and after direct quench (*i.e.* one-pot boronation and hydrolysis) gave the crystalline product **270** with 60% yield (Entry 1, Table 4). However, the presence of TMEDA seems to make the isolation of the isopropylborate ester **271** by distillation difficult. This reaction produced a crude product with a waxy consistency poorly suited to Kugelröhr distillation (Entry 2, Table 4). In the absence of additive the lithiation took considerably longer to complete, but the isolated yield of 69% of the boroxine trimer **270** was greater for the direct quench reaction (Entry 3, Table 4) and distillation of the isopropylborate ester **271** was viable (Entry 4, Table 4). It was possible to produce crystals of boroxine trimer **270** suitable for single crystal X-ray structure analysis from this material by placing a diethylether solution of **271** over a layer of water. This resulted in a 90% yield of **270** with respect to the isopropylborate ester (43% overall yield). The material produced by this method was otherwise spectroscopically identical in all respects to that produced by direct quench of the boronated product (Entry 3, Table 4) and to the material produced from the TMEDA-mediated reaction (Entry 1, Table 4).

Due to the moisture sensitivity of the isopropylborate ester **271**, a more stable pinacol ester was prepared in order to aid structural studies of this class of aminoboronic acids. Boroxine trimer **270** was resistant to pinacol protection of the boron in ethyl acetate and also in a biphasic water/ethyl acetate solvent system. Esterification was eventually achieved in 60% yield by treating boroxine **270** with pinacol in a biphasic water-ethyl acetate solvent system with *para*-toluenesulfonic acid catalysis to produce the stable, crystalline (*vide infra*) pinacol ester **272** (Equation 48).

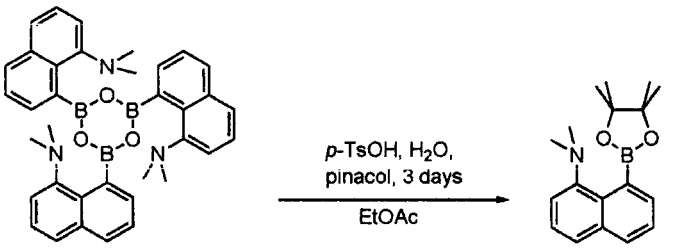

270 **272**, 60%

Equation 48: Pinacol protection of boroxine trimer.

2.3.4.2 Fluorinated derivative

In order to prepare the corresponding difluoroborane compound **273** from boroxine **270**, it is usually necessary to make the corresponding potassium trifluoroborate salt (*i.e.* of type $ArBF_3K$), which may then be converted to difluoroborane ($ArBF_2$) by treatment with chlorotrimethylsilane or boron trifluoride.[161, 178-182] However, in the case of boroxine **270**, upon treatment with aqueous KHF_2 in refluxing THF (in order to provide complete dissolution of the substrate), the air-stable difluoroborane **273** was produced directly (Equation 49). THF was found to be an effective solvent for this reaction after methanolic reactions failed to give any product. Reactions entailing pre-treatment of boroxine **270** with methanol followed by addition of aqueous KHF_2, and treatment of **270** with a mixture of methanol and aqueous KHF_2, both resulted in all starting material being recovered.

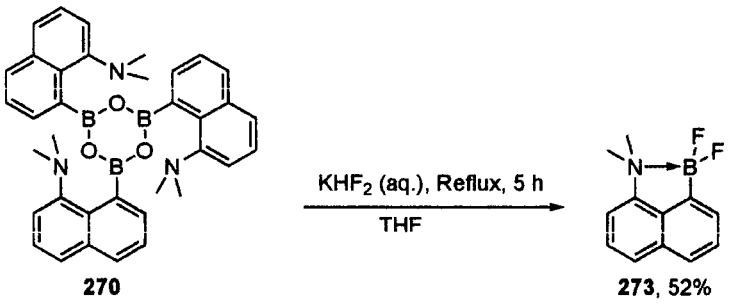

270 **273**, 52%

Equation 49: Fluorination of boroxine trimer.

2.3.4.3 Spectroscopy

Having isolated the boroxine **270**, the boronate ester derivatives **271** and **272** and the difluoroborane **273**, it is interesting to note that all the structures show clear evidence for formation of an intramolecular "ate"-complex in solution by ^{11}B NMR, as shown by chemical shifts of δ 19, 18, 22 and 10 ppm respectively. In each case, the proximal 1,8-relationship of the dimethylamino function to the boron centre ensures approximate tetrahedral geometry at boron. This is further reinforced by X-ray structure analysis of single crystals of boroxine **270** (Figures 12 and 13) and pinacol ester **272** (Figure 14). In each case the effect of the B-N interaction can be seen, despite the geometric compression required for B-N interaction and the relatively low basicity of the aryl amine group. Indeed, the fact that the boroxine trimer **270** shows any sign of B-N interaction is particularly interesting since boroxine trimer systems, being moderately aromatic,[183-187] are usually planar. This system is crystallographically unique as far as we are aware, despite several reports of intramolecular boroxine-benzylamine systems,[188-190] since it clearly shows deformation of the boroxine ring away from planarity, as shown by a small O-B-O-B torsion of 0.6° and much larger B-O-B-O torsion of 10.3°. Hence, in this case, the proximal placement of the nitrogen function forces intramolecular B-N interaction to occur, providing partial quaternisation at the boron centre and puckering of the boroxine ring. Clearly, despite the boron atoms being in a boroxine ring, they are still sufficiently Lewis acidic to interact with the neighbouring nitrogen atom. The weak nature of the B-N interaction in the boroxine system **270** is evidenced by a C-B-N bond angle of 92°, a

C-N-B bond angle of 103° and a relatively long N-B bond length of 1.97 Å. There is also bending of the amino and boron groups towards each other, causing angle compression from the usual 120° to 114° and 112° for the C(Ar)-C(Ar)-N and C(Ar)-C(Ar)-B angles respectively. In contrast, the pinacol ester **272** is capable of greater B-N chelation, with a C-B-N bond angle of 95°, a C-N-B bond angle of 113°, a shorter B-N bond length of 1.89 Å and slightly more severe angle compression from the usual 120° to 113° for both the C(Ar)-C(Ar)-N and C(Ar)-C(Ar)-B angles. The fact that the ^{11}B shift is 22 ppm for pinacol ester **272**, versus 18 ppm in the diisopropyl ester **271**, can be explained by the reported[191] effect of ring strain imposed by the pinacol ester versus the acyclic ester.

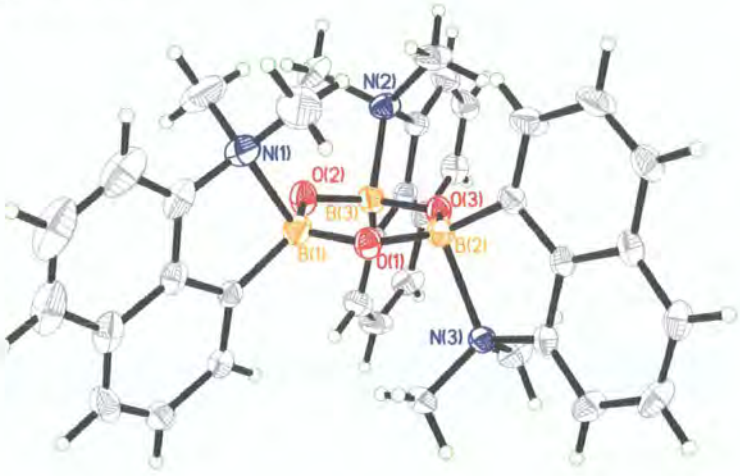

Figure 12: ORTEP X-ray crystal structure of boroxime trimer **270**, showing 50% probability ellipsoids.

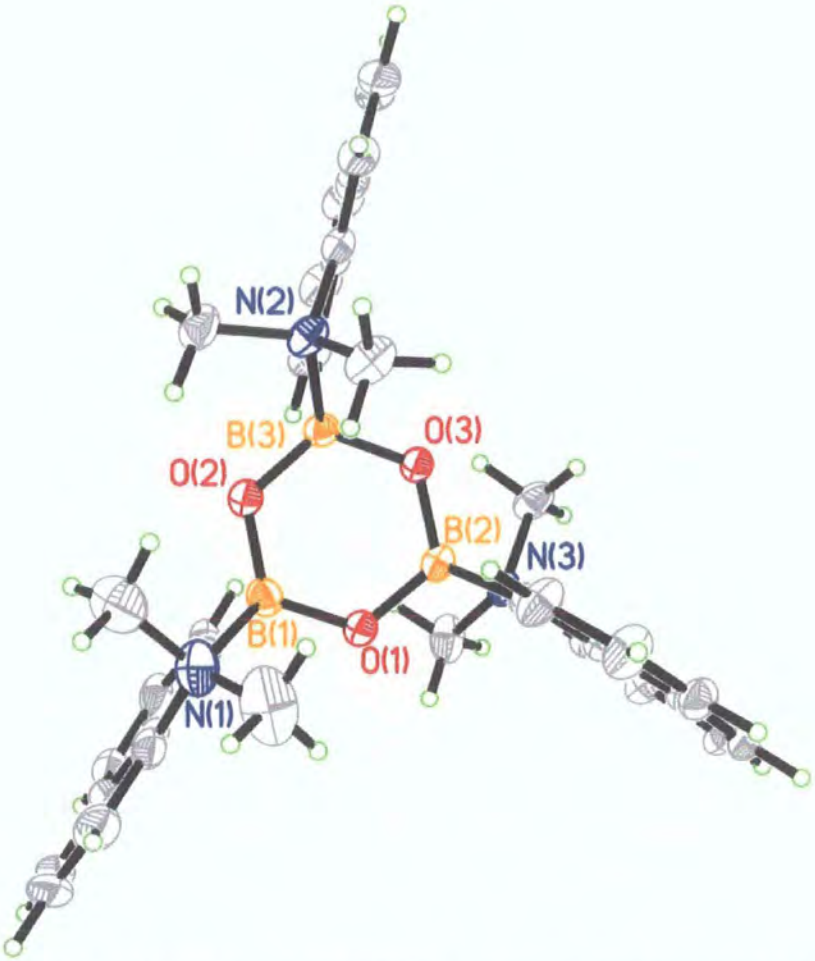

Figure 13: ORTEP X-ray crystal structure of boroxime trimer **270**, projected onto the boroxine ring, showing 50% probability ellipsoids.

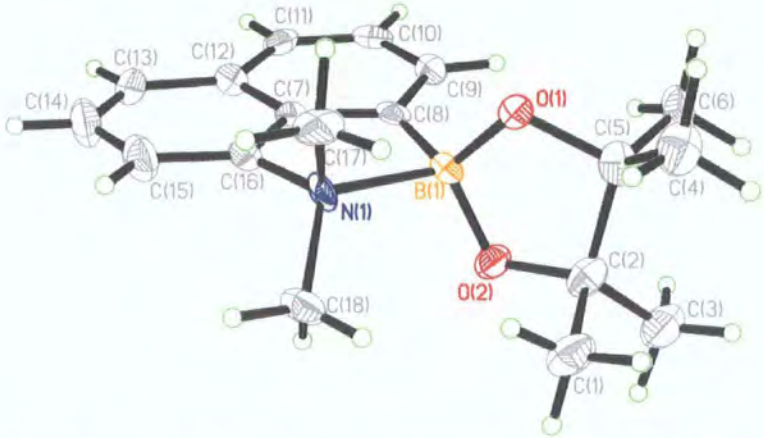

Figure 14: ORTEP X-ray crystal structure of pinacol ester **272**, showing 50% probability ellipsoids.

Although the difluoroborane system **273** has yet to yield crystals suitable for single crystal structure analysis, this compound also shows clear signs of B-N chelation, as evidenced by a ^{11}B NMR shift of approximately 10 ppm and ^{11}B-^{19}F coupling of 58 Hz, producing a broad triplet (Figure 15). As anticipated,[192] the ^{19}F NMR spectrum is diagnostic of fluorine attached to an asymmetric (boron) quadrupole, resulting in a broad, unsymmetric quartet signal (Figure 16). Thus, the effect of the two fluorine atoms on boron is to enhance the Lewis acidic nature of the boron centre, resulting in a strong B-N interaction, producing an approximately tetrahedral boron and thus, an entirely predictable ^{11}B NMR chemical shift, in complete agreement with such a structural analysis.[161]

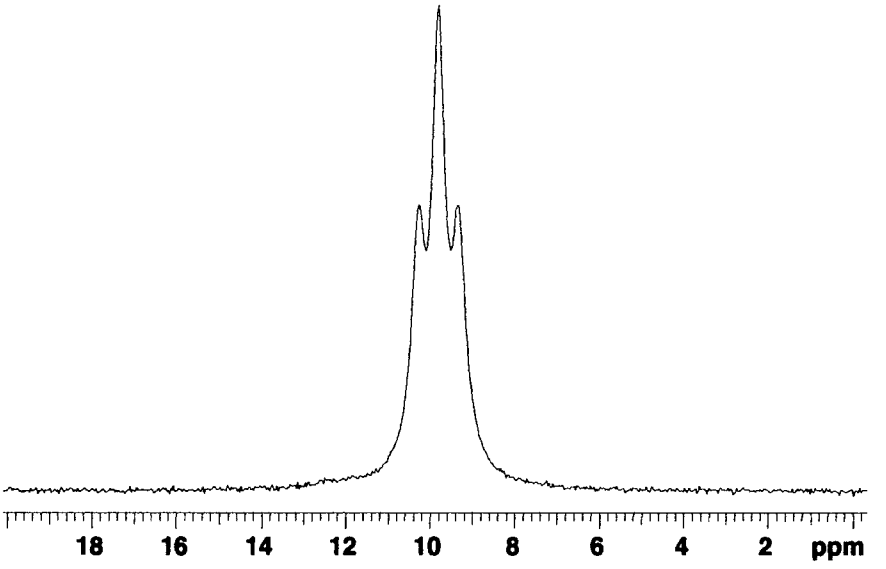

Figure 15: ^{11}B NMR spectrum of difluoroborane **273**, showing ^{19}F coupling.

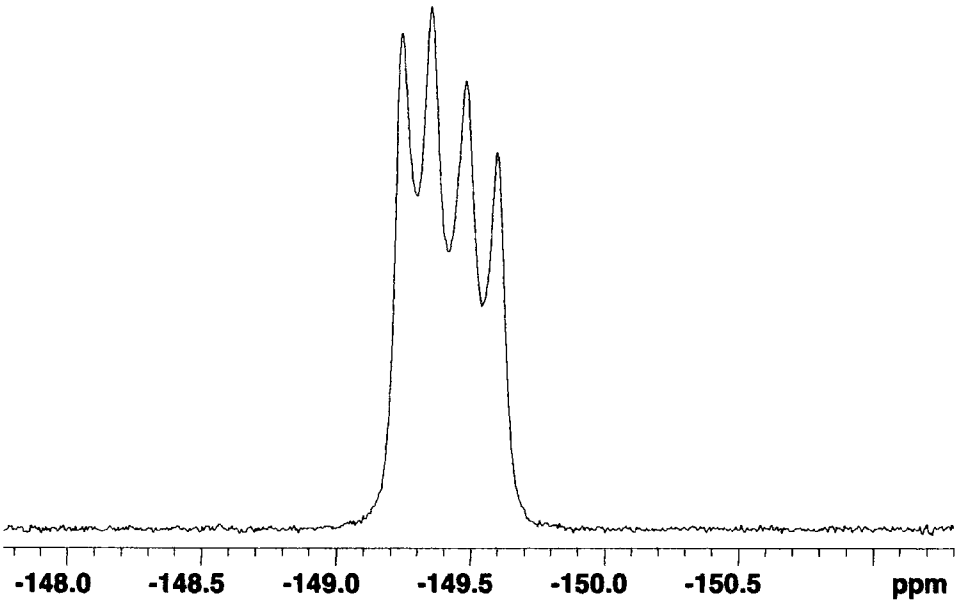

Figure 16: ^{19}F NMR spectrum of difluoroborane **273**, showing the effect of the asymmetric boron quadrupole.

2.3.4.4 Summary – *N,N*-Dimethylnaphthyl-1-amine-8-boronic acid series

All compounds synthesised in the *N,N*-dimethylnaphthyl-1-amine-8-boronic acid series can be handled conveniently. It is clear that the nitrogen and boron functions interact, despite the relatively low nitrogen basicity, even in the novel boroxine system **270**. Boroxine **270** exhibits exceptional resistance to hydrolysis and hence fluorination and diol protection. All compounds produced were soluble in the full polarity range of organic solvents at room temperature, with the exception of **270**, which was only soluble in moderately polar organic solvents such as acetonitrile and chloroform.

2.3.5 *N,N*-Dimethylaniline-2-boronic acid series

N,N-Dimethylaniline-2-boronic acid **277** was originally synthesised by Lauer *et al.*[138] However, attempts to reproduce this route proved unfruitful (Scheme 28). The product was observed to rapidly decompose to a brown oily complex mixture during work-up, using the published conditions. Due to the unstable nature of the series, such compounds were deemed unsuitable for study as bifunctional catalysts and the synthesis of this class of compounds was abandoned. It should, however, be noted that the pinacol ester **278** can be obtained commercially from Frontier Scientific.

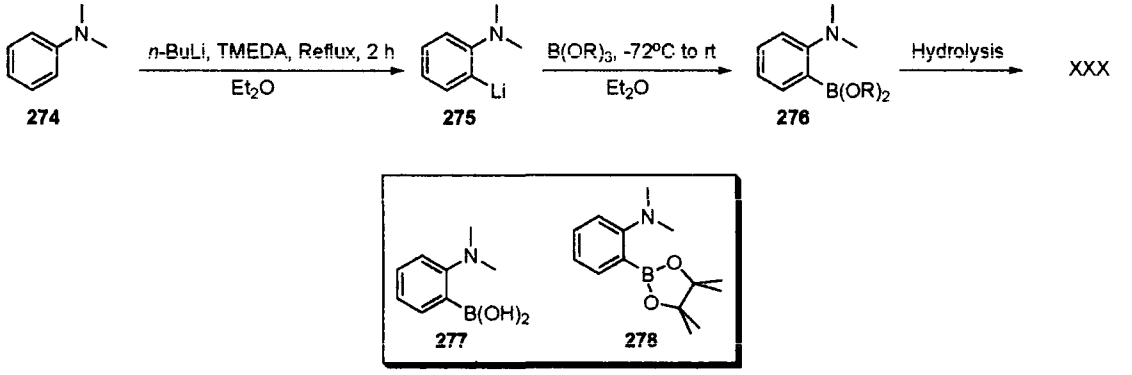

Scheme 28: Boronation of *N,N*-dimethylaniline.

The spectroscopic properties of *N,N*-dimethylaniline-2-boronic acid **277** were published in the original paper.[138] The compound exhibits an ^{11}B shift of 27.9 ppm indicative of a free aryl boronic acid. The apparent lack of intramolecular coordination in this system is likely due to the considerable strain that would be applied to the molecule in forming a 4-membered ring. The contrast with the analogous 1-*N,N*-dimethylamino-8-bononaphthalene series, in which all four compounds (**269**, **270**, **271** and **272**) forming intramolecular 'ate' complexes, is stark.

2.3.6 Aniline-3-boronic acid series

The 3-aminobenzeneboronic acid series **189** is analogous to both the *N,N*-dimethylaniline-2-boronic acid series **188** and the *N,N*-dimethylnaphthyl-1-amine-8-boronic acid series **187** in that it has an anilinic nitrogen. There is, however, no possibility of intramolecular B-N coordination due to the large separation between the boron and nitrogen moieties.

The monohydrate of boronic acid **279** was commercially available from Lancaster. Pinacol protection and column chromatography allowed the isolation of **280** in 93% yield (Scheme 29) with crystals suitable for single crystal X-ray structure analysis (Figure 17). Treatment of **279** with KHF_2 provided the hydrogen trifluoroborate salt **281** (Scheme 29).

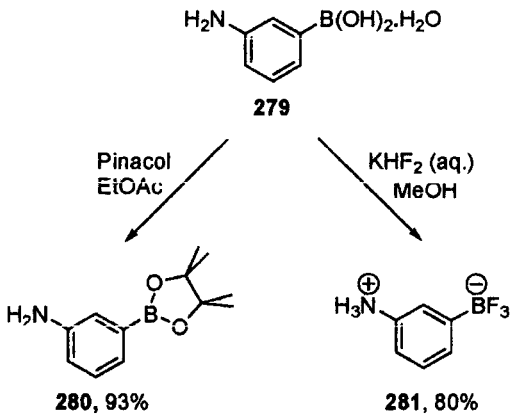

Scheme 29: Derivatisations of 3-aminobenzeneboronic acid.

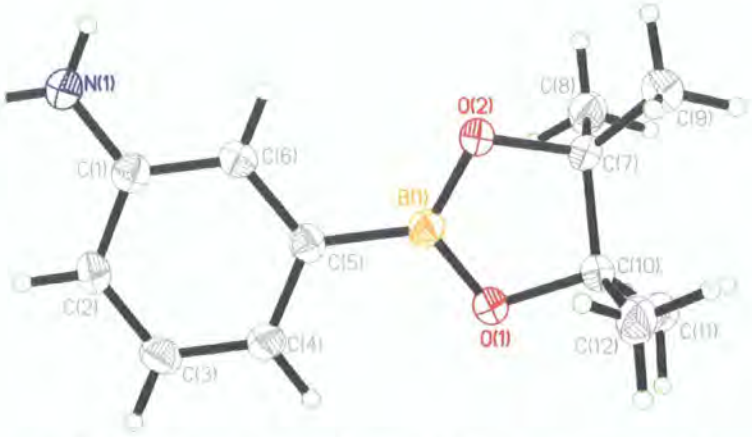

Figure 17: ORTEP X-ray crystal structure of boronate ester **280**, showing 50% probability ellipsoids.

As expected, both the boronic acid **279** and the pinacol ester **280** exhibit non-complexed neutral boron centres at neutral pH, as evidenced by ^{11}B NMR shifts of δ 29.2 (s) in D_2O[193] and of 31.0 (s) in $CDCl_3$, respectively. The boron of the pinacol ester appears to retain the boronate-to-phenyl ring conjugation, as evidenced by the coplanarity of the two functions in the crystal structure. Pinacol ester **280** was soluble in both polar and non-polar organic solvents, but only sparingly soluble in water. The trifluoroborate functionality of **281** can be recognised from characteristic ^{11}B NMR shift of δ 3.2 ppm indicating a boron 'ate' complex and from coupling to boron in the ^{19}F spectra δ -142.6 (q, J = 81.9) in MeCN.

2.3.7 Guanidinobenzene-3-boronic acid series

Attempts were made to guanidinate the pinacol ester **278** in order to generate the analogous guanylbenzene-3-boronic acid series **190**, which would offer a much more basic amine functionality. Initially guanidination was attempted with *O*-methylisourea (Equation 50), utilising a primary amine guanidination methodology developed for derivatisation of primary amines in peptides.[194] This method utilised *O*-methylisourea as the guanidinating agent with aqueous sodium hydroxide. Unfortunately, in this case chromatographic

isolation of products of the reaction on silica failed due to streaking of guanidine derivatives on the column with all conditions attempted. Changing to an organic base with solely organic solvent failed to alter the poor chromatographic performance of the products. Hence guanidination with the more lipophilic *N,N*-di-*iso*-propylisourea **283** was also attempted (Equation 51). It was hoped that this reaction would generate a guanidinated product with better chromatographic performance. This proved not to be the case.

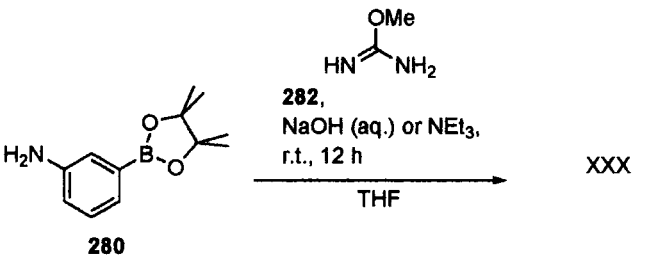

Equation 50: Attempted guanidination of 3-aminobenzeneboronic acid with O-methylisourea.

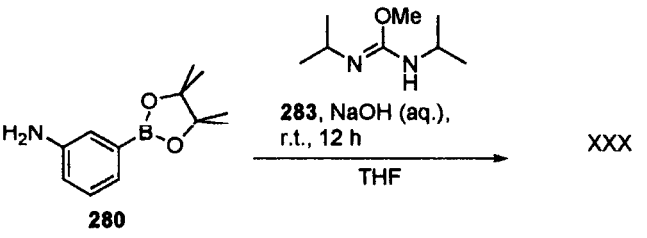

Equation 51: Attempted guanidination of 3-aminobenzeneboronic acid with lipophilic guanidine derivative.

2.3.8 Conclusions - Synthesis

Several interesting aminoboronate systems have been synthesised and their properties investigated during this work.

A one stage, generally applicable, high yielding method for the synthesis of compounds in the *N,N*-dialkylbenzylamine-2-boronic acid series from secondary amines has been produced, replacing the four stage low yielding lithium base route. It has been demonstrated that by fine-tuning the steric requirements on the alkyl groups that intramolecular B-N chelation can be prevented. A homologous series of amides with interesting spectroscopic properties was also synthesised as part of this work. Possible extensions of this series exist, notably the possibility of the formation of compounds of type **285** from boronic acid **284**, which is commercially available (Equation 52). An interesting synthesis described by Hawkins *et al.* indicates that boroxine **286** is reacted to simultaneously produce both secondary amine and double boronated analogues of general structure **184** (Equation 53).[195]

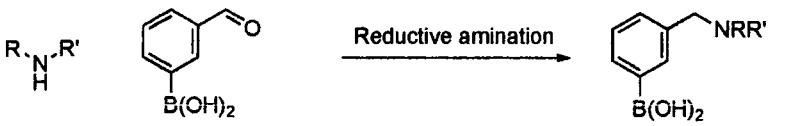

225 **284** **285**

Equation 52: Route to *N,N*-dialkylbenzylamine-3-boronic acid series.

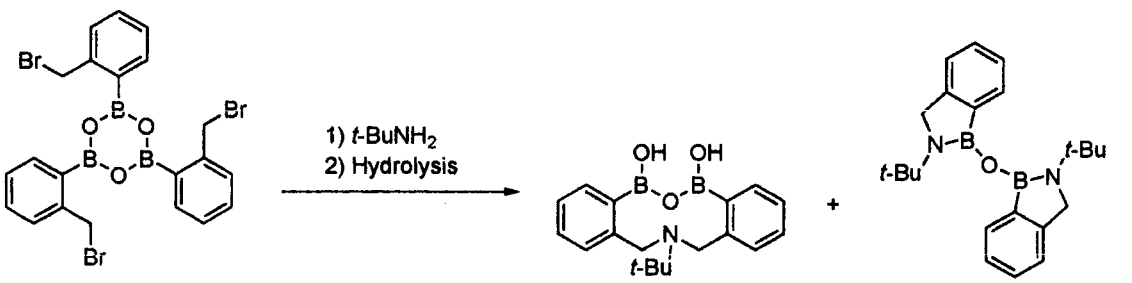

286 **287** **288**

Equation 53: Route to *N,N*-dialkylbenzylamine-2-boronic acids and trifunctional derivatrive.

Studies into the *N,N*-dimethylnaphthylamine-8-boronic acid series produced several readily handlable catalyst candidates with intramolecular B-N coordination, including the only truly stable aminoarylboron difluoride produced during this project. The analogous *N,N*-dimethylaniline-2-boronic acid proved to rapidly decompose. This exceptionally short shelf life made it a poor candidate for catalyst screening. However, the final analogous series of aniline compounds, the aniline-3-boronic acid series, proved readily handlable and suitable for screening. Elaboration of **280** to more basic guanyl derivatives failed due to very poor chromatographic performance of crude products derived from the guanidination reaction.

Of the series containing sp^2 nitrogen centres only the synthesis of quinoline-8-boronic acid series proved fruitful, with 2-phenylpyridine-2'-boronic acid appearing to rapidly decompose on work-up and Heck-type coupling of vinyl boronate **256** to quinoline-8-bromide unsuccessful.

In summary, a range of aminoboronates was produced for catalyst screening both within this project and other projects within the group.

2.4 Complexation studies of arylboron difluorides

We were originally interested in bifunctional aminoarylboron difluorides such as **239** as potential catalysts, as arylboron difluoride compounds have been established to be effective as strong Lewis acidic catalysts, offering alternatives to boron trifluoride.[178] A study was planned with a series of model boron difluorides being combined with a range of common Lewis acid substrates to better understand arylboron difluoride complexation.

Towards this end, potassium phenyltrifluoroborate and potassium *o*-nitrobenzenetrifluoroborate were synthesised using the methodology developed by Vedejs *et al.*[161, 182] The latter reaction proceeded in quantitative yield to give crystals suitable for single crystal X-ray analysis (*vide infra*) (Equation 54).

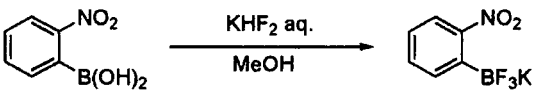

289 **290**, 100%

Equation 54: Synthesis of potassium trifluoroborate salt **290**.

In the solid state structure of **290** (Figure 18) the nitro functionality appears to retain its phenyl ring conjugation, as evidenced by the coplanarity of the two functions in the crystal structure, an orientation which would allow the functionality to effectively accept electron density. The boron is in the expected tetrahedral geometry and forms the potassium salt in preference to the HF salts which are generally observed with aminoboronates.

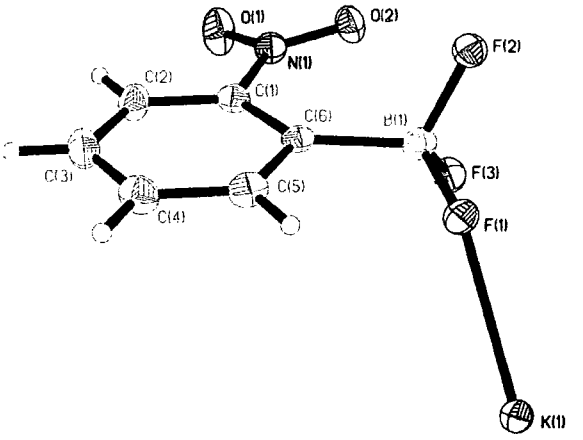

Figure 18: ORTEP X-ray crystal structure of potassium borontrifluoride **290**, showing 50% probability ellipsoids.

Phenylboron difluoride and *o*-nitrobenzeneboron difluoride were generated *in situ* utilising the Vedejs *et al.* methodology and were not isolated prior to use because arylboron difluorides are typically volatile and prone to decomposition when handled on a small scale (Equation 55).[161, 178] Elution of potassium phenyltrifluoroborate and **290** through dried silica gel with dry methanol was briefly investigated as an alternative procedure for the generation of the aryldifluoroborons **297** and **298**. It was hoped that the high affinity of silica for fluorine would result in partial defluorination. This proved not to be the case and the starting material was recovered in its entirety.

$$ArBF_3K + TMSCl \longrightarrow ArBF_2 + TMSF\ (g)$$

Equation 55: *In situ* generation of arylboron difluorides.

The NMR-scale complexation study of a range of boron fluorides with common reagents was undertaken (Equation 56, Table 5). The model compounds chosen for investigation were phenyldifluoroboron **298** and *o*-nitrobenzene difluoroboron **297**, which were tested alongside boron trifluoride-THF complex. Stock solutions of Lewis acids BF_3.THF, **297** and **298** in dry D_3-MeCN were combined in equimolar ratio with substrates **160**, **291**, **26**, **292**, **293**, **294**, **295** or **296**, mixed and analysed by ^{11}B NMR and ^{1}H NMR.

We would expect borontrifluoride to be the most Lewis acidic of these compounds, followed by *o*-nitrobenzeneboron difluoride, whose *ortho*-nitro substituent should make it more Lewis acidic than phenylboron difluoride.

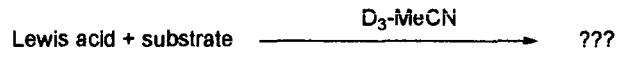

Equation 56: Arylboron difluoride complexation studies.

Substrate / Lewis Acid	 **160**	 **291**	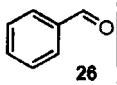 **26**	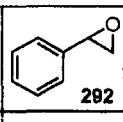 **292**	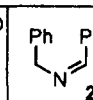 **293**	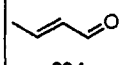 **294**	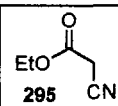 **295**	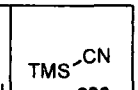 **296**
$BF_3.OEt_2$								
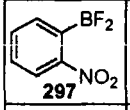 **297**								
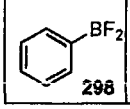 **298**								

Table 5: Arylboron difluoride complexation studies.

Generally speaking, the study did not give good results. What was observed for all systems was an equilibrium between complexation of the solvent and the substrates, as evidenced by ^{11}B NMR shifts in the region δ -0.45 for BF_3 to δ 3.5 for the less electron-deficient **298** (Scheme 30). The small differences of Δδ in ^{11}B signals between the solvated and complexed boron atoms were often insufficiently distinct from the inherent error due to the broadness of ^{11}B NMR peaks and so it was not possible to definitively assign the differences between the Lewis acids, or in some cases to determine whether complexation was taking place. Also the Lewis acids were often partially destroyed by residual water in the reagents. Typically arylboron difluorides **297** and **298** suffered ~5-20% hydrolysis to the corresponding boronic acids, as evidenced by ^{11}B NMR shifts in the δ 30 ppm region.

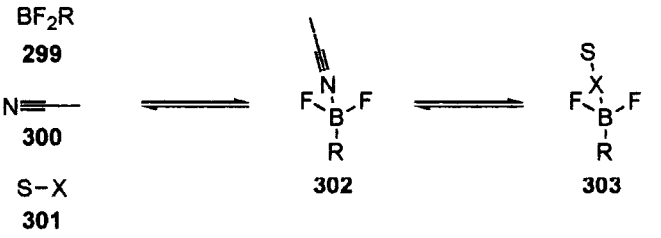

Scheme 30: Complexation equilibrium

Perhaps the most significant results came with the aldehyde acrolein **291**, where the effect of boron-oxygen complexation of the aldehyde C=O could be observed on the aldehyde proton H^1 (Table 6). Complexation reduces shielding and lowers the ^1H shift of the proton, and the effect is more pronounced for the complexation of the most electronegative boron centre, dropping off as the electron withdrawing power decreases in the order fluorine to *o*-nitrophenyl to phenyl (Entries 1, 2 and 3, Table 6).

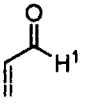

291

Entry	Lewis acid	Acrolein H^1 Δδ
1	$BF_3.OEt_2$	-0.3
2	**289**	-0.25
3	**298**	-0.2

Table 6: ^1H NMR Δδ with Lewis acids BF_3.THF, **297** and **298**.

In conclusion, the initial intention of the project was to investigate bifunctional aminoarylboron difluorides as catalysts. However, we were only able to isolate **273** as a stable aminoarylboron difluoride, with other investigations delivering highly unstable aminoarylboron difluorides such as **239**. This, coupled with the realisation that for our planned screening reaction molarities (1-20%) we could expect to see considerable hydrolysis unless extra care was taken to make all reactions anhydrous, led us to screen only the air-stable bifunctional compounds such as the boronic acids and pinacol esters.

2.5 Catalyst *vs.* Reaction screening

Catalysts synthesised early in this project were screened against a wide variety of different reactions. The aim of this investigation was the identification of reactions where the bifunctional amino-boron compound out-performs the uncatalysed reaction, the modular amine-catalysed reaction, the modular boronic acid-catalysed reaction and finally the reaction in the presence of both modular amine and modular boronic acid. If the latter point is true, bifunctionality is implicated as a plausible mechanism. As we had little idea of what kind of catalytic reactivity to expect from these novel amino-boron compounds, we decided to test the compounds against a large and diverse set of reactions.

2.5.1 Automated methods - Liquid Handling workstation

Due to a collaboration with GlaxoSmithKline, Tonbridge, it was possible to utilise a Gilson SK-233 Microdart liquid handling workstation for the screening of a selection of catalysts synthesised up to that point in the project. The details of this type of apparatus are described below.

The Gilson SW215 liquid handling workstation is pictured in figures 19, 20 and 21. The apparatus consists of a computer-controlled robotic arm, **A**, capable of delivering a septa-piercing needle, **B**, to any position within the tray space, **C**. The needle is connected to a syringe pump, **D**, allowing the machine to aspirate and dispense liquids to any position within the tray space, **C**. Reagents and solvents are delivered from the reagent vial rack, **E**, to the temperature-controlled reactor rack, **F**. Samples are removed from the reactors and dispensed to the analytical vial rack, **G**, where the sample is quenched, mixed and diluted down sequentially into neighbouring vials in the analytical vial rack to a concentration suitable for HPLC analysis. An HPLC-UV system is connected online to the Gilson SW-215 apparatus and an injection port, **H**, allows the apparatus to deliver the sample to the HPLC system. The HPLC sample is then delivered from the analytical vial rack to the

HPLC injection port, **H**. Figure 21 shows the injection port being addressed by the needle. In this way it is possible to monitor reactions by HPLC-UV over time. In order to prevent cross-contamination between vials, after each time the apparatus makes a transfer it washes the needle in the system solvent at the wash station, **I**, and also washes the injection port after each address. Positive sense pipetting (a slight excess is taken for each transfer and is wasted after dispensing) prevents the system solvent from mixing with the sample being transferred.

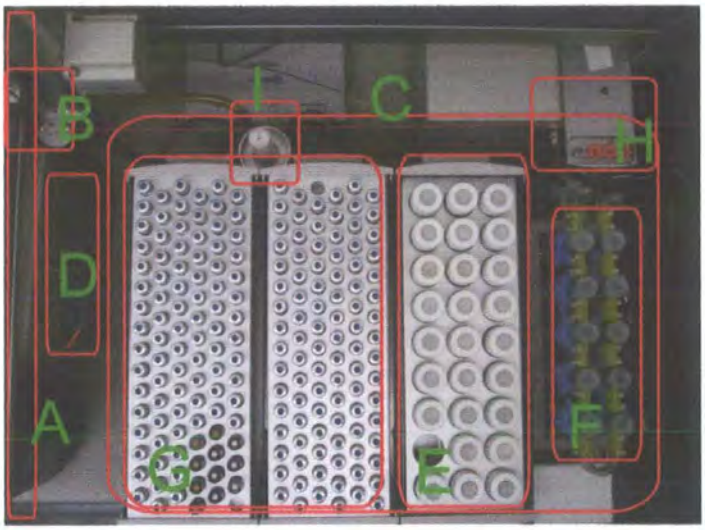

Figure 19: Overhead view of Gilson SW-215 liquid handing apparatus.

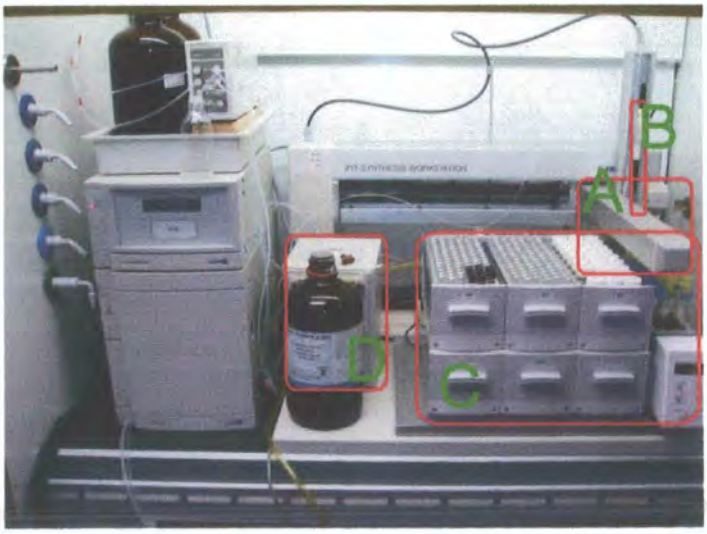

Figure 20: Front view of Gilson SW-215 liquid handling apparatus.

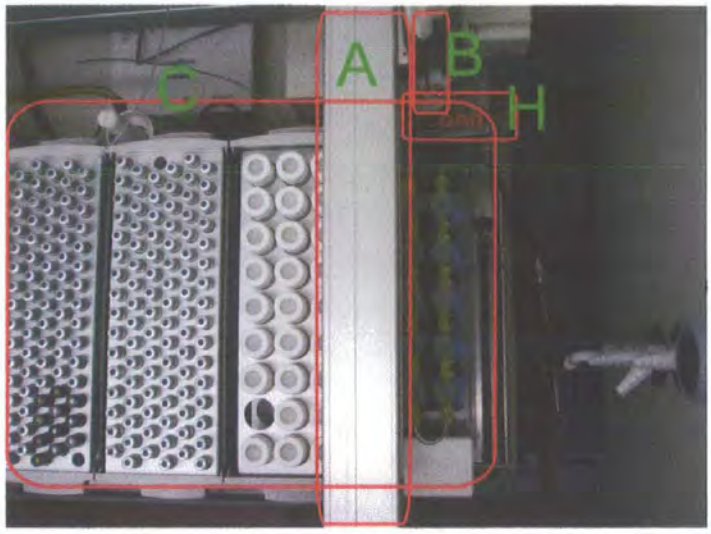

Figure 21: Overhead view of Gilson SW-215 liquid handling apparatus with needle addressing HPLC port.

2.5.2 Multi-reaction screening

The SK-233 system used for the multi-reaction screening experiment is a similar but slightly larger version of the SW-215 (*vide supra*). In place of the ten-place heating block to the right of the machine (Figures 19, 20 and 21) is positioned a block containing 96 separate reactor positions with temperature control and magnetic stirring. Each position is capable of holding a standard 1.5 ml HPLC vial (Figure 22).

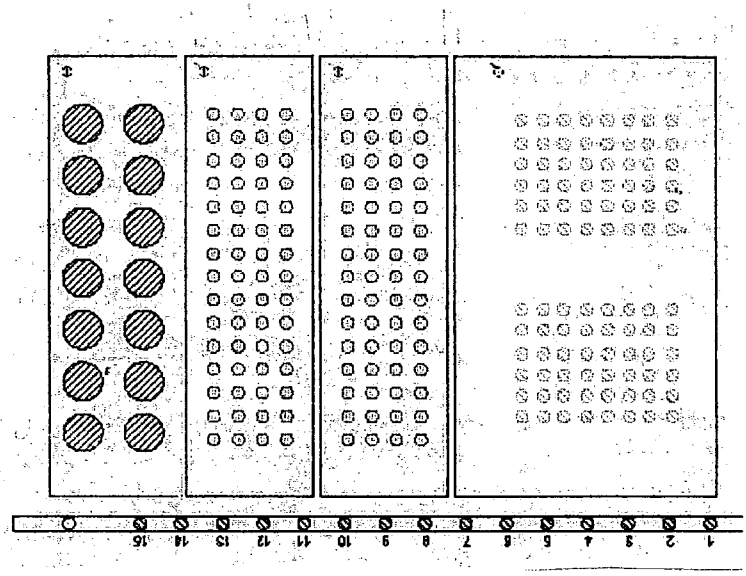

Figure 22: Plan view of SK-233 Microdart layout.

On this scale 24 separate reactions were run in parallel (Equation 57, Table 7). The individual reactions consist of a nucleophile (**38**, **304**, **295**, **305**, **160** or **306**), an electrophile (**160**, **26**, **293** or **307**) and either one of the then available catalyst candidates (**270**, **279** or **253**) or modular amine and/or boronic acid standards (**308**, **309**, **310**, (**308** and **309**) or uncatalysed) at 10 mol% (or 3.33 mol% for boroxine trimer **270**). Selected reaction sets were repeated with THF: H_2O, 80: 20 (Table 8). After 1 hour and 12 hours a sample was taken from each of the reactions and serially diluted (by transfer of a aliquot of sample from one vial to neighbouring empty vial followed by addition of diluent and mixing, two times) with acetonitrile to concentration suitable for HPLC-UV analysis. The diluted samples were then analysed by HPLC-UV.

Nucleophile **38**, **304**, **295**, **305**, **160** or **306**

and

Electrophile **160**, **26**, **293** or **307**

Catalyst candidate 10 mol% (w.r.t. B) or standard(s) or blank
Sampling at 1 h and 12 h

THF or (THF: H_2O, 80: 20)

???

Equation 57: Multi-reaction screening.

Electrophiles \ Nucleophiles	**38**	**304**	**295**	**305**	**160**	**306**
160						
26						
293						
307						

Standards

308 **309** **310** **308** and **309** Blank

Catalyst candidates

270 **279** **253**

Table 7: Multi-reaction screening.

		Screening performed with	
Entry	Catalyst candidate	0 Mol% water added	20% (v/v) water added
1	Uncatalysed	No	Yes
2	**308**	Yes	No
3	**309**	Yes	No
4	**308** and **309**	Yes	Yes
5	**270**	Yes	Yes
6	**253**	Yes	Yes
7	**279**	Yes	No

Table 8: Inclusion of water in multi-reaction screening.

The aim of the investigation was the identification of reagent combinations where the bifunctional catalysts (Entries 5, 6 and 7, Table 8) outperformed the standards (Entries 2, 3 and 4, Table 8) and the uncatalysed reactions (Entry 1, Table 8) to produce either a new clean product or significantly more product.

Firstly, generally effective HPLC-UV conditions were established for all of the starting materials and the catalysts, an optimal detection wavelength range of 211-212 nm was determined, as were all retention times of reagents and catalysts. With the exception of propionaldehyde all compounds under investigation were readily detectable at 211-212 nm due to their possession of a UV-chromaphore. Any products that might be formed would also be expected to retain these UV-chromaphores and thus be detectable by HPLC-UV provided their elution times differed from the starting materials and the catalysts. The exception to this would be a self-condensation and some other reactions of propionaldehyde, which may well not be detected by these methods. As the starting materials and the products of the reactions would not be expected to have the same molar extinction coefficient ε as each other over the detection wavelength range (211-212 nm), this analytical method does not give a percentage conversion, but instead is more qualitative than quantitative, akin to TLC analysis.

As expected, the HPLC analysis generated a very large quantity of data. This data was enumerated by the automated peak recognition software, exported to spreadsheet as peak time and peak area and analysed manually as the automated HPLC analysis program was unable to process such a diverse data set.

The results of this screening are detailed in Chart 1 for catalysts **270** (with or without added water), **253** (with or without added water) and **279** (used as acquired from Lancaster as the monohydrate). In the five reaction matrices, colour-coded squares represent the result for each reagent combination:

Positive results: reaction with bifunctional catalyst candidate appears to be forming a single new compound over 12 hours more successfully than standards (green); reaction with bifunctional catalyst candidate appears to be forming two products or one product at a rate slightly superior to standards (yellow).

Negative results: complex mixture formation (light grey); no product formation/product formation at same rate as standards (dark grey); product formation from non-bifunctional system superior (black); no HPLC-UV detection (white).

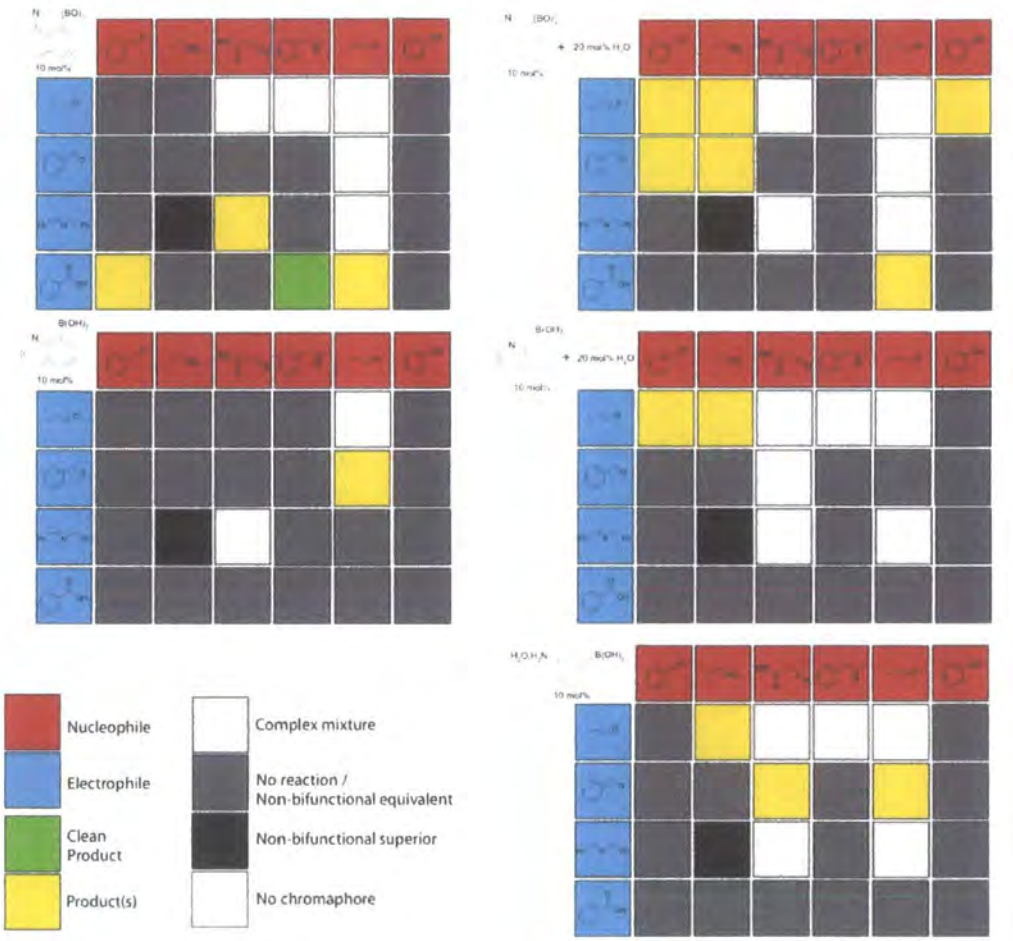

Chart 1: Catalyst screening results.

The 'hit' reactions are further detailed in table 9. The combination of phenyl acetylene, aldehyde catalysts **270** or **253** and water produced a thixotropic mixture (Entries 1 and 2, Table 9). A possible nitro-aldol reaction is observed with wet **270** and **253** (Entries 3 and 4, Table 9). Possible enolate attack onto a carbonyl is observed with dry **270** and **279** (Entries 5 and 6, Table 9). A polar, fast eluting compound is formed with *N*-benzylmethylamine and benzoic acid with dry **270** (Entry 7, Table 9). Possible aldol is observed with **279** (Entry 8, Table 9). Two further combinations gave responses that are less easily explained (Entries 9 and 10, Table 9).

Entry	Reagents		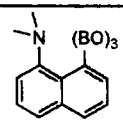 270		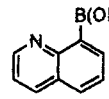 253		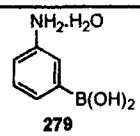 279
	Nucleophile	Electrophile	THF: H_2O 80:20	No H_2O	THF: H_2O 80:20	No H_2O	
1	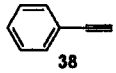 38	 160	+		+		
2	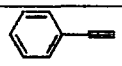 38	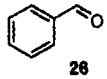 26	+				
3	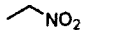 304	 160	+		+		
4	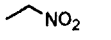 304	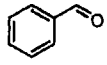 26	+				
5	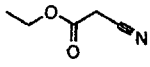 295	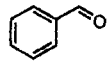 26					+
6	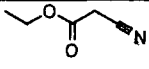 295	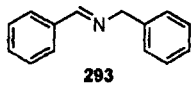 293		+			
7	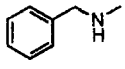 305	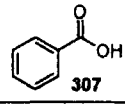 307		+			
8	 160	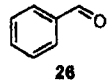 26					+
9	 160	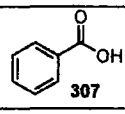 307	+	+			
10	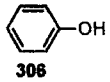 306	 160	+				

Table 9: 'Hit' reactions from multi-reaction screening.

Selected 'hit' reactions from the multi-reaction screening were scaled-up and further investigated as detailed below. Interesting reactivity was observed in the reaction of carboxylic acids and amines. This work is discussed in the following chapter.

2.5.3 Phenylacetylene and benzaldehyde

The scaled-up reaction of phenylacetylene and benzaldehyde in toluene and in THF again produced a thixotropic mixture (Equation 58). Consumption of phenylacetylene could be evidenced by the disappearance of the acetylinic proton peak from the ^1H spectrum at δ 3.0 ppm, whilst the integration of the aldehyde proton of benzaldehyde at δ 10.0 ppm remains roughly constant over the course of the reaction. The result appears to be a mixture of polymerised phenylacetylene products rather than a propargylalcohol which could have resulted from an acetylene coupling reaction,[39] as evidenced by the appearance of five broad signals in the region δ 3.4 to 0.7 ppm of the ^1H NMR spectrum. It is not clear what the role of the aldehyde was in this reaction, but it is clear from the screening that it is a necessary component, otherwise no reaction of phenylacetylene is observed (Chart 1). However, as this reaction is not synthetically useful it was not investigated further.

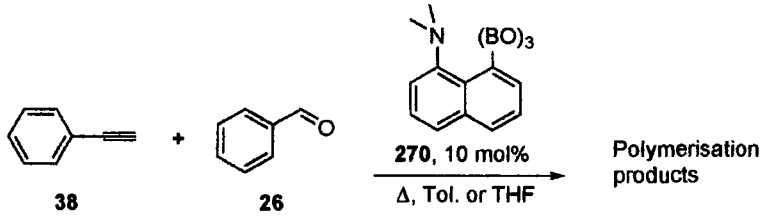

Equation 58: Possible polymerisation of phenyl acetylene.

2.5.4 Nitro-aldol and aldol reactions

The follow-up of the possible positive results for the nitro-aldol and aldol reactions was delegated to a co-worker who had been focusing on these reactions with alternative bifunctional systems. The work resulted in unspectacular catalysis of the nitro-aldol reaction with catalyst **206** (41% conversion of benzaldehyde and nitromethane to the corresponding nitro-alcohol over 60 hours), with all other bifunctional catalysts synthesised in this project producing less nitroaldol product. Aldol reactivity in the reaction of

acetone with benzaldehyde was nonexistent for all bifunctional compounds synthesised in this project.

2.5.5 Conclusions – Catalyst *vs.* Reaction screening

This diversity-orientated approach of screening many reactions against a range of catalyst systems allowed us to cover many reactions, including many reagent combinations we may well not otherwise have studied. The screen provided useful leads, such as the aldol and nitro-aldol reactions, as well as amide bond formation (*vide infra*). Unfortunately, the method suffered from certain inherent disadvantages: 1) very large quantities of complex data were produced which it was not possible to make compatible with current automated analysis software, leading to long manual data analysis times; 2) no immediate means of identification of products was available (e.g. HPLC-MS), leading to false positive results; 3) it was not possible to differentiate co-eluted compounds. The method therefore did not necessarily identify less spectacular catalysis which could nevertheless still represent a useful result after development. In the continuation of this project it is likely that when using this technology the screening of individual reactions simultaneously with a range of catalysts will represent the most efficient usage of time. Prior determination of absorption coefficients and retention times of reagents and all expected products would lead to quantitative results and allow the use of HPLC data analysis software. This would reduce the analysis time considerably.

2.6 Direct amide bond formation

2.6.1 Introduction – Direct amide bond formation

Amide bond formation is an important step in the synthesis of many pharmaceutical entities, natural products, fine chemicals and bulk chemicals. The most common methods used in modern chemistry are the formation of an isolable carboxylic acid derivative such as an acyl chloride, anhydride, mixed anhydride or active ester, which are then reacted with the amine to form the amide in two steps. Although acyl transfer reagents such as DMAP can be added to increase the reactivity of such systems, these methods offer very poor atom and energy economy. Coupling reagents such as diimide reagents can solve the problem of requiring two steps to complete the transformation but they are often toxic and expensive and fail to solve the problem of poor atom economy.[196]

Direct condensation between a carboxylic acid and an amine in equimolar quantities would represent the ideal situation. Direct combination of carboxylic acid and amine produces the carboxylate-ammonium salt. Amide formation by solvent-free heating of the salt has been known since 1923 when Coleman *et al.* showed that acetamide could be produced from ammonium acetate at ~200°C (Equation 59).[197] Benzanilide can be produced by heating of benzoic acid with excess aniline at temperatures up to 225°C with water removal by distillation (Equation 60).[198] More recently the synthesis of amides include pyrolysis of a mixture of a high boiling aliphatic amine and aliphatic acid (Equation 61)[199] and amide formation by azeotropic water removal in non-polar solvent (Equation 62).[200]

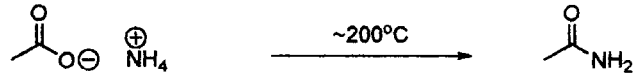

311 **312**, 87%

Equation 59: Pyrolysis of ammonium acetate.

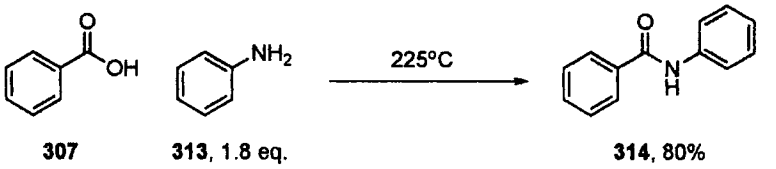

307 **313**, 1.8 eq. **314**, 80%

Equation 60: Pyrolysis of anilinium benzoate.

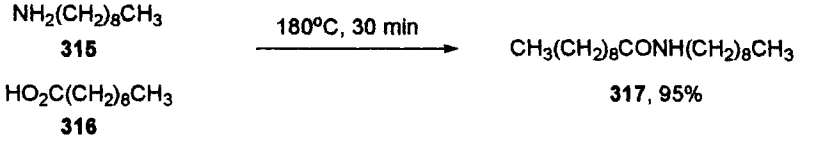

Equation 61: Pyrolysis of aliphatic amine – acid combination.

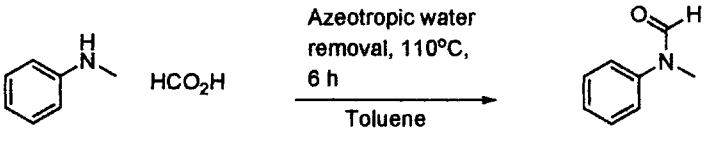

305 **318** **319**, 93%

Equation 62: Thermolysis of *N*-methylanilinium formate.

Considering the importance of the amide bond forming reaction relatively few catalytic routes exist. Helquist *et al.* reported that Ti(O*i*-Pr)$_4$ at 50 Mol% mediated the lactamisation of primary and secondary ω-amino acids.[201] Yamamoto *et al.* demonstrated the utility of Sb(OEt)$_3$ in refluxing toluene for templated macrolactamisation of a 17-membered ring with 90% yield, a reaction in which B(NMe$_2$)$_3$ catalysis yielded 74% (*c.f.* 0% for the uncatalysed reaction).[202] Antimony is also reported to be effective in a synergistic Ph$_3$SbO/P$_4$S$_{10}$ system with aliphatic acids and amines at remarkably low temperatures, typically 40-80°C, with catalyst loadings of 5 and 15 Mol% respectively.[203]

Perhaps the most notable success in this area has been with boron-catalysed amide bond formation. Yamamoto *et al.* first described the reaction with electron-deficient aryl boronic acids in 1996 with catalyst **323** being shown to be effective for amide bond formation at around 110°C with aliphatic acids and nucleophilic amines. Notably, the yield dropped to 11% using catalyst **324**, which possessed an *ortho*-substituent, and to >2% for the uncatalysed reaction (Scheme 31).[204-206] Catalyst **323** was also effective with less

nucleophilic amines under more forcing conditions (Equation 63). Yamamoto *et al.* also developed a fluorous-phase soluble catalyst which was shown to be effective when used in a mixed solvent system of perfluorodecalin/(*o*-xylene or toluene). Though miscible at higher temperatures, this system forms a room temperature biphase which allowed catalyst **325** to be recycled by decantation without any isolation of the catalyst (Equation 63).[207] Wang *et al.* demonstrated that pyridine-3-boronic acid **328** and pyridinium derivative **329** were effective amide bond forming catalysts and have developed a solid-supported version **330** (Scheme 32).[208] Tang has recently demonstrated that boric acid is an effective catalyst for the amide bond forming reaction, a result which rivals the vastly more expensive boronic acid catalysts in toluene (Equation 64) and with heptane as solvent is superior to catalyst **323**.[209]

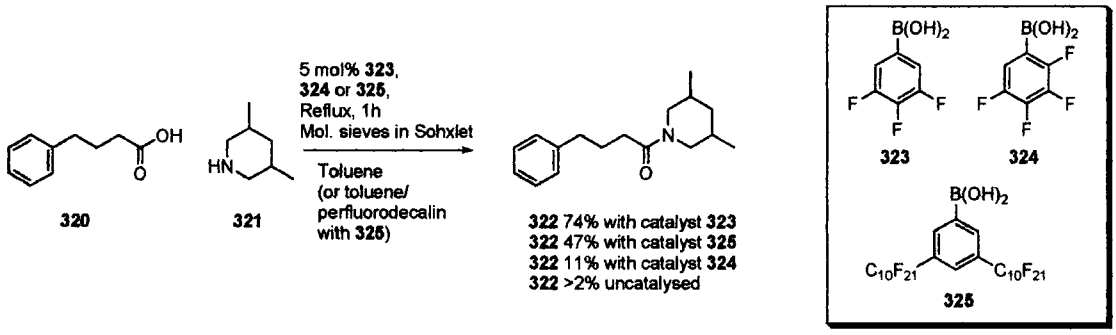

Scheme 31: Yamamoto *et al*, electron deficient boronic acid-catalysed amide bond formation.

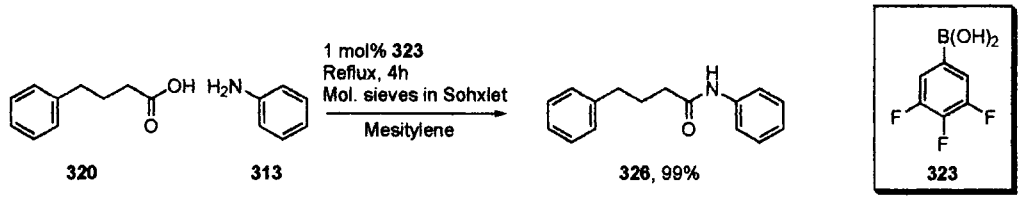

Equation 63: Yamamoto *et al.*, electron deficient boronic acid-catalysed amide bond formation.

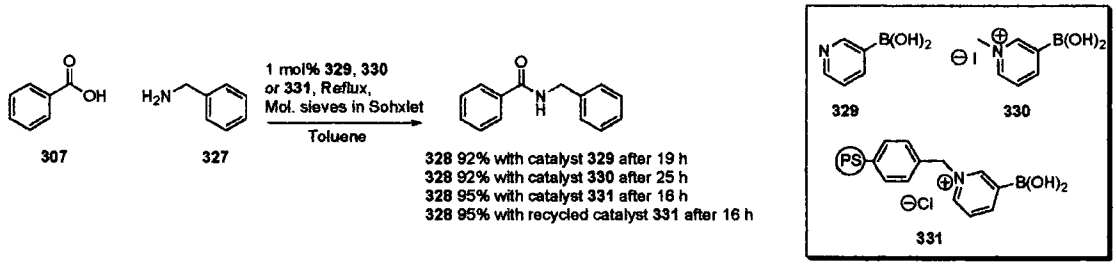

Scheme 32: Wang *et al.*, pyridine-2-boronic acid-catalysed amide bond formation.

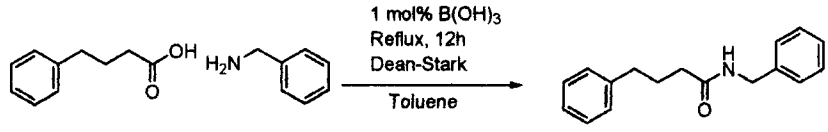

Equation 64: Tang *et al.*, boric acid catalysed amide bond formation.

2.6.2 Identification of catalysts

The initial 'hit' reaction from the screening was the reaction of *N*-methylbenzylamine with benzoic acid in the presence of 10 mol% **270** (w.r.t. boron). This reaction, as well as the uncatalysed reaction, was then investigated at room temperature with 10 mol% of bifunctional boronic acids **270** and **206** in THF, toluene and DCM (Scheme 33, Entries 1-9, Table 10). The reaction was then investigated at higher temperature with dehydration in the presence of 10 mol% **270** (w.r.t. boron) (Scheme 33, Entry 10, Table 10). All of the reactions, including the uncatalysed reaction, produced only the carboxylate-ammonium salt **333**. Assay was by ^{1}H NMR integration of the RNH_2^+ peak at δ 9.30 ppm. A sample of salt **333** was synthesised separately in order to make this comparison. It is not clear what was detected on the HPLC trace which had given the initial 'hit' but these results indicate that it was a false positive result. It is likely that the result represented the detection of a HPLC-stable species with a high molar extinction coefficient which was not apparent by ^{1}H NMR in the crude product of the test reaction.

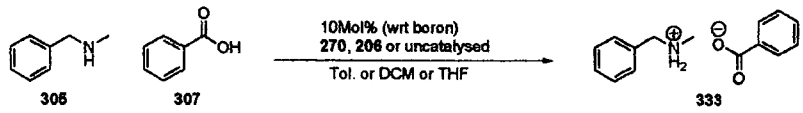

Scheme 33: Follow-up on amide bond forming 'hit' reaction from multi-reaction screening.

Entry	Solvent	Catalyst	Temp.	Dehydration	Product	Time	Conversion
1	THF	None	r.t.	None	Salt	72h	100%
2	Toluene	None	r.t.	None	Salt	72h	100%
3	DCM	None	r.t.	None	Salt	72h	100%
4	THF	**270**	r.t.	None	Salt	72h	100%
5	Toluene	**270**	r.t.	None	Salt	72h	100%
6	DCM	**270**	r.t.	None	Salt	72h	100%
7	THF	**206**	r.t.	None	Salt	72h	100%
8	Toluene	**206**	r.t.	None	Salt	72h	100%
9	DCM	**206**	r.t.	None	Salt	72h	100%
10	Toluene	**270**	Reflux	CaH_2 Sox.	Salt	72h	100%

Table 10: Follow-up on amide bond forming 'hit' reaction from multi-reaction screening.

After consideration of the conditions employed in Yamamoto's work,[206] further investigations into this reaction were made. In the reactions where electron-deficient aryl boronic acid catalyst **323** had been successfully utilised, more forcing conditions had been necessary. In these examples amide formation had been at high temperature with azeotropic water removal. Bifunctional boronic acids **206**, **235**, **200**, **253** and **270** were investigated alongside monofunctional analogue **334**. The condensation of 4-phenylbutyric acid with benzylamine was chosen as the test reaction as this was the rechecked example reaction in the Organic Synthesis papers for boron catalysed amide bond formation with electron-deficient boronic acid **323**, the then leading competitor compound.[206, 209] Hence this reaction was a useful yardstick to compare the performance of the bifunctional boronic acids. The reaction conditions were, toluene as solvent and a slight excess of carboxylic acid (1.1 eq.), as in the work by Yamamoto *et al.* (Scheme 34, Table 11).

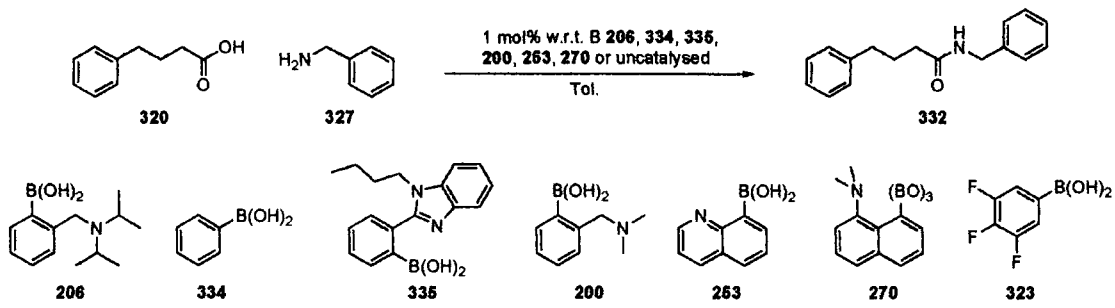

Scheme 34: Conditions, boronic acid-catalysed amide bond formation.

Entry	Solvent	Catalyst	Temp.	Dehydration	Product	Time (h)	NMR Conversion	Isolated Yield
1	Toluene	None	Reflux	None	Amide	20		57%
2	Toluene	**206**	Reflux	None	Amide	20		98%
3	Toluene	**334**	Reflux	None	Amide	20		79%
4	Toluene	**335**	Reflux	None	Amide	20		54%
5	Toluene	**200**	Reflux	None	Amide	20		63%
6	Toluene	**253**	Reflux	CaH_2 Sox.	Amide	20	~30%[a]	
7	Toluene	**270**	Reflux	CaH_2 Sox.	Amide	20	~10%[a]	
8	Toluene	**323**	Reflux	CaH_2 Sox.	Amide	20		98%[206]

Table 11: Boronic acid-catalysed amide bond formation, catalyst screening. [a]Conversion measured by ^1H NMR integration of amide NH peak relative to 1/3 of the salt RNH_3^+ signal.

Of the bifunctional catalysts, **206** produced the most impressive result with a 98% yield in 20 hours in the absence of external dehydration (Entry 2, Table 11). Other bifunctional boronic acids **335** and **200** produced results comparable to (Entries 4 and 5, Table 11) and significantly worse than (Entries 6 and 7, Table 11) the uncatalysed reaction. Some activity was also observed for phenylboronic acid with 79% isolated yield (Entry 3, Table 11). The fact that the reaction proceeded to a significant degree in the absence of boronic acid catalyst was, at the time, an unexpected observation (Entry 1, Table 11), as this result had not been mentioned in papers relating to either the boric acid-catalysed or the electron-deficient boronic acid-catalysed amide bond formation publications.[204, 206, 209] This suspicious result was successfully reproduced several times, including with the use of new glassware and with glassware which had been thoroughly washed twice in 5% (w/v) aqueous hydrochloric acid and twice in 5% (w/v) aqueous sodium hydroxide on top of

usual washing conditions (soapy water, acetone), in order to ensure that no residual catalyst could remain on the glassware. Having identified **206** as an effective amide bond forming catalyst and uncovered the interesting thermal reaction, the conditions of the reaction were more comprehensively investigated. The practice of washing glassware in aqueous acid and base was repeated through all work described in this chapter to minimise the possibility of carry over of catalyst on the glassware from one reaction to the next.

2.6.3 Substrate range

At this early stage in the investigations amide bond formation was attempted for a representative range of substrates with **206** as the catalyst (Equation 65, Table 12). Benzoic acid, unhindered aliphatic acid **320** and hindered aliphatic acid **338** were tested for amide bond formation with benzylamine, aniline, *t*-butylamine, diisopropylamine and morpholine. The reactions of benzylamine and morpholine with **320**, benzoic acid and pivoic acid all produced amide, otherwise no amide was isolated. Of the three acids tested, the aliphatic unhindered acid **320** was the most reactive. In the case of the reaction with benzylamine it produced an impressive 98% yield, compared to 17% with benzoic acid and 15% with pivalic acid. Yields were reduced but in the same order with the secondary amine morpholine. No reaction was observed with secondary hindered amine **202**, primary hindered amine **229** or primary aromatic amine **313** for any carboxylic acid. The decision was taken at this point to optimise the reaction conditions before carrying out a more detailed study incorporating the uncatalysed reaction and competitor compounds.

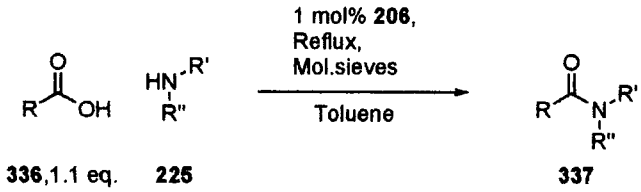

Equation 65: Conditions, substrate range study.

Amines \ Acids	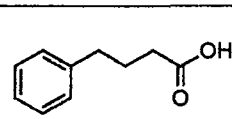 320	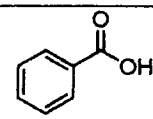 307	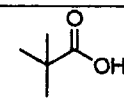 338
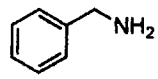 327	98%	17%	15%
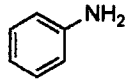 313	0%	0%	0%
 229	0%	0%	0%
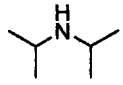 202	0%	0%	0%
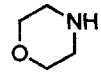 230	28%	-	6%

Table 12: Isolated yields, substrate specificity of catalyst **206**.

2.6.4 Optimisation of conditions

The condensation of 4-phenylbutyric acid and benzylamine was chosen as a model reaction for the optimisation of the conditions for the amide bond forming reactions. Variables studied were solvent, reaction molarity of amine with respect to carboxylic acid and dehydration method.

2.6.4.1 Solvent

A range of solvents was investigated for amide bond formation, varying from water through polar aprotic solvents through to non-polar aprotic solvents. The reactions were performed with 1 mol% catalyst **206** using a slight excess of carboxylic acid **320** to benzylamine (Scheme 35, Table 13).

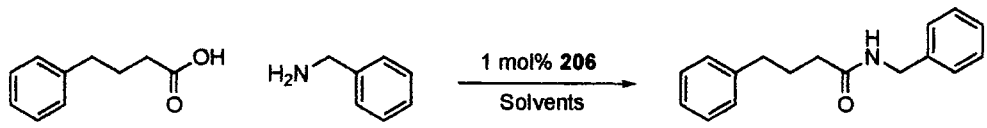

320, 1 eq. **327**, 0.9 eq. **332**

Scheme 35: Conditions, solvent screening.

Entry	Catalyst	Solvent	Solvent B.p.	Temp.	Dehydration	Time (h)	Isolated Yield Amide
1	**206**	1,4-dioxane	100-102	Reflux	None	20	29%
2	**206**	THF	70	Reflux	None	20	11%
3	**206**	1,2-dimethoxyethane	85	Reflux	None	20	17%
4	**206**	Toluene	111	Reflux	None	20	98%
5	**206**	DMSO	189	110	None	20	0%
6	**206**	Xylene	138	110	None	20	74%
7	**206**	Water	100	Reflux	None	20	0%

Table 13: Isolated yields, solvent screening.

Non-polar aromatic solvents toluene and xylene (Entries 4 and 6, Table 13) significantly out-performed all other solvents investigated, with isolated yields of 98% and 74% respectively. The fact that toluene outperforms xylene could be attributed to the fact that at 110°C toluene was gently refluxing, thus was more efficient at driving water out of the reaction and into the vapour phase, forcing the equilibrium more successfully over towards the amide. After post reaction cooling the reactions with toluene and xylene as solvents contained droplets of water attributable to the water eliminated during the condensation. Ether solvents gave less impressive results. The lower boiling ethers, THF and 1,2-dimethoxyethane (Entries 1 and 2, Table 13), gave the poorest yields of 11% and 17% respectively. The higher boiling ether 1,4-dioxane boils at 100-102°C, which is comparable to toluene (B.p. 110°C) but still gave only 29% yield (Entry 3, Table 13). There appears to be a definite correlation in the

ether solvents between the temperature of the reaction and the isolated yield, with a significant increase in yield as the reflux temperature of the solvent increased, but the results were still not as impressive as with the non-polar aromatic solvents. DMSO was investigated as a very polar aprotic solvent (Entry 5, Table 13). No amide bond formation was observed. Finally, and perhaps over-optimistically, water was investigated (Entry 7, Table 13) in the hope that the equilibrium might be so far towards the amide that condensation might occur. This proved not to be the case.

2.6.4.2 Reaction molarities

The effect of reagent molarities on the reaction of carboxylic acid **320** and benzylamine was studied in parallel using the following conditions: With and without 1 mol% of catalyst **206**, with a slight excess of acid, a slight deficiency of acid and with equimolar acid and amine, all without a dehydrating agent (Scheme 36, Table 14).

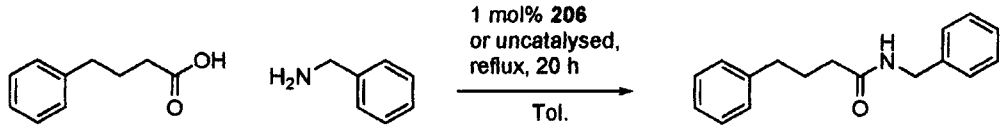

320 **327**, 0.9 eq.or 1.0 eq.or 1.1 eq. **332**

Scheme 36: Conditions, effect of reaction molarity on amide bond formation.

Entry	Solvent	Catalyst	Temp.	Dehydration	Acid/Amine (mmol)	Product	Time (h)	Isolated Yield
1	Toluene	**206**	Reflux	None	10/9	Amide	20	98%
2	Toluene	**206**	Reflux	None	10/10	Amide	20	91%
3	Toluene	**206**	Reflux	None	10/11	Amide	20	85%
4	Toluene	None	Reflux	None	10/9	Amide	20	68%
5	Toluene	None	Reflux	None	10/10	Amide	20	59%
6	Toluene	None	Reflux	None	10/11	Amide	20	66%

Table 14: Isolated yields, effect of reaction molarity on amide bond formation.

With catalyst **206**, the yield was highest when a slight excess of acid **320** was used. The yield dropped off for the equimolar reaction and the lowest yield was observed with a deficiency of acid **320** (Entries 1, 2 and 3, Table 14). In the uncatalysed reaction the highest yield came when the reaction had either an excess of carboxylic acid **320** or an excess of benzylamine (Entries 4, 5 and 6, Table 14). It is notable that in literature examples of boron-catalysed amide bond formation, the presence of an slight excess of acid is ubiquitous.[206, 208, 209]

2.6.4.3 Dehydration method

Various dehydration methods were tested in parallel in order to determine if water removal, either from the reaction mixture or from the reflux condensate above the reaction, improved the reaction performance (Scheme 37, Table 15).

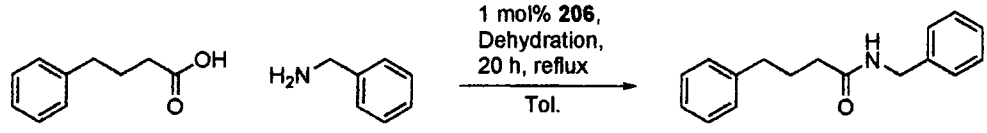

320, 1 eq. **327**, 0.9 eq. **332**

Scheme 37: Conditions, dehydration method screening.

Entry	Solvent	Catalyst	Temp.	Dehydration	Product	Time (h)	Isolated Yield
1	Toluene	**206**	Reflux	None	Amide	20	95%
2	Toluene	**206**	Reflux	$MgSO_4$	Amide	20	11%
3	Toluene	**206**	Reflux	Mol. Sieves 3Å pellets	Amide	20	80%
4	Toluene	**206**	Reflux	CaH_2 Sox.	Amide	20	98%

Table 15: Isolated yields, dehydration method screening.

In this experiment the yield for the reaction in the absence of dehydrating agent was 95% (Entry 1, Table 15). This is lower than, but within experimental error of, two previous repetitions of this experiment in which the yield was 98% (Entry 4, Table 15 and Entry 1, Table 15), making an average yield of

97%. This compares well with the reaction where a Soxhlet apparatus containing a thimble filled with CaH_2 was used as a means of dehydrating the reflux condensate (Entry 4, Table 15), in which the reaction proceeded with 98% yield, suggesting that on this scale of reaction (10 mmol **320** and 9 mmol **327**) there is little need to dehydrate the reaction. Inclusion of magnesium sulfate in the reaction mixture saw significant diminuation of the yield (Entry 2, Table 15). Probably due to basic magnesium sulfate reacting with the carboxylic acid **320** and boronic acid **206**, reducing the amount of free acid **320** available for reaction. In this reaction the mixture became a gel-like mass. A decrease in yield was also observed when activated 3Å molecular sieve pellets were added to the reaction (Entry 3, Table 15), possibly explained by adsorption of the reagents on to the surface of the sieves.

2.6.4.4 Summary – Optimisation of conditions

The optimised conditions for the amide bond forming reaction are non-polar aprotic solvent at high temperature with a slight excess of acid and with dehydration of the condensate stream (provided in this case by calcium hydride in a Soxhlet apparatus), although the reaction is still effective in the absence of additional dehydration on small scale.

2.6.5 Effect of molecular sieves

The question of whether the activated 3Å molecular sieves themselves could catalyse the dehydration reaction when added directly to the reaction mixture was briefly investigated (Scheme 38, Table 16). Such a reaction could possibly compete with the boron-catalysed route, so it was necessary to establish if the sieves themselves had any effect.

The reaction in the absence of the sieves (Entry 1, Table 16) gave a slightly better yield then when the sieves were added (Entry 2, Table 16). The difference, however, is small and could well be within experimental error.

Thus this result indicates no improvement in reactivity in the presence of sieves.

Cossy *et al.* have reported activated 4Å molecular sieves as an effective catalyst for the amide bond forming reaction with various aliphatic acids.[210] In this report, however, there is no comparison of the molecular sieve-catalysed reaction with the uncatalysed reaction. The conditions of the reported reactions are very similar to the solvent-free pyrolysis route with temperatures in the range 140-180°C, in which reactivity would be expected in the uncatalysed reaction,[199] hence it is likely that the amide bond formation observed is not due to the sieves.

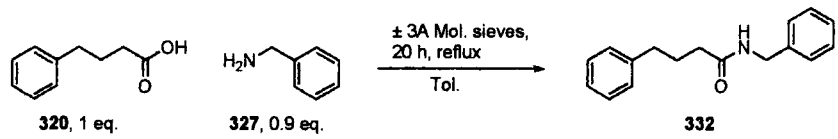

320, 1 eq. **327**, 0.9 eq. **332**

Scheme 38: Conditions, effect of activated molecular sieves on the amide bond forming reaction.

Entry	Solvent	Temp.	Dehydration	Product	Time (h)	Isolated Yield
1	Toluene	Reflux	None	Amide	20	63%
2	Toluene	Reflux	Sieves	Amide	20	60%

Table 16: Isolated yields, effect of molecular sieves on amide bond forming reaction.

2.6.6 Rate determination

2.6.6.1 Methodology

A representative set of six amide bond forming reactions was studied with catalysts **206**, **334**, **339** and **323**, as well as the uncatalysed reaction (Scheme 39, Table 17). Benzoic acid (aromatic) and 4-phenylbutyric acid (aliphatic) were reacted with benzylamine (primary benzylic amine), morpholine (secondary aliphatic amine) and 4-phenylbutylamine (primary aliphatic amine). The aim of the investigation was determine the relative efficacy of the different boron acids and to provide mechanistic insight. The formation of the amides was followed by HPLC-UV. Raw HPLC data was treated to give results as concentration values and percentage conversion. Alongside bifunctional catalyst **206**, the main competitor compound, electron-deficient boronic acid **323**, was included.[204, 206] Tang's publication of boric acid-catalysed amide bond formation,[209] which occurred during these studies, prompted us to include boric acid for study. Phenylboronic acid **334** was included as a reference boronic acid for comparison with bifunctional catalyst **206** and electron-deficient catalyst **323**.

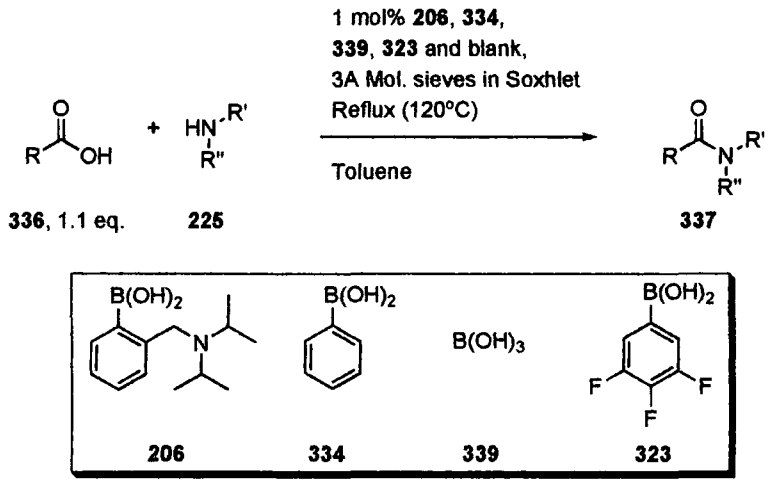

Scheme 39: Conditions, amide bond forming kinetics experiments.

	Acid	Amine	Amide
1	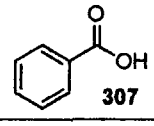 307	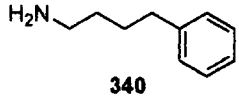 340	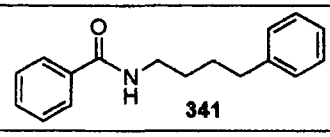 341
2	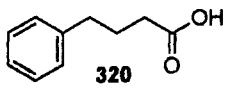 320	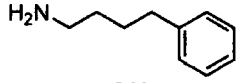 340	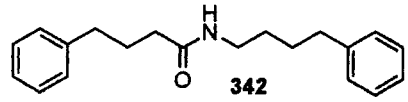 342
3	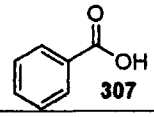 307	 230	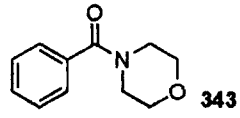 343
4	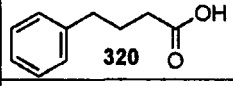 320	 230	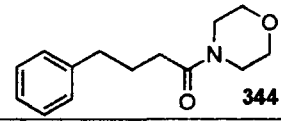 344
5	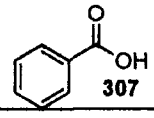 307	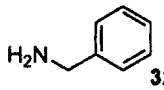 327	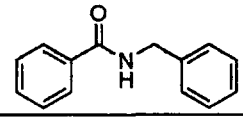 328
6	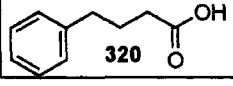 320	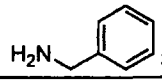 327	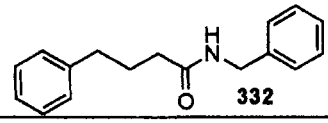 332

Table 17: Amide bond formation kinetics experiments.

The reaction of aniline with acids **320** and **307** was also investigated, but poor quality results were obtained due to some tar formation, resulting in multiple products on HPLC-UV. It is likely that the mediocre spectroscopic purity of the aniline '99% purity' used was partly to blame. The material could be evidenced to contain an unidentified contaminant by HPLC-UV. It was not possible to commercially obtain aniline of sufficient quality for studies of this kind, which rely on very good UV spectroscopic purity of starting materials and products.

2.6.6.2 Experimental set-up

The study was run on a Gilson SW215 synthesis workstation with online HPLC-UV analysis and 10 place heating block (*vide supra*). We developed a glassware system especially for the amide bond formation reaction on the

Gilson SW215 apparatus (Figures 19, 20 and 21). The new glassware system is a 'micro dehydration' apparatus, which incorporates overhead inert gas supply and a cup to allow the suspension of a dehydrating agent in the condensate stream of the reflux system (Figure 23). In contrast to the standard reflux condenser glassware system (Figure 24), this allowed for the continuous removal of water from the reaction.

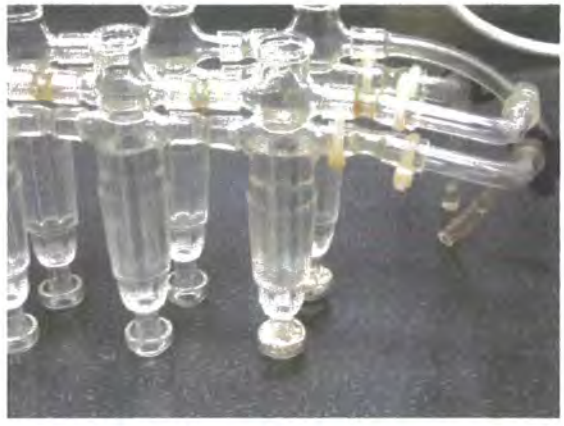

Figure 23: Micro dehydration heads loaded with molecular sieve pellets (the two cups to the right).

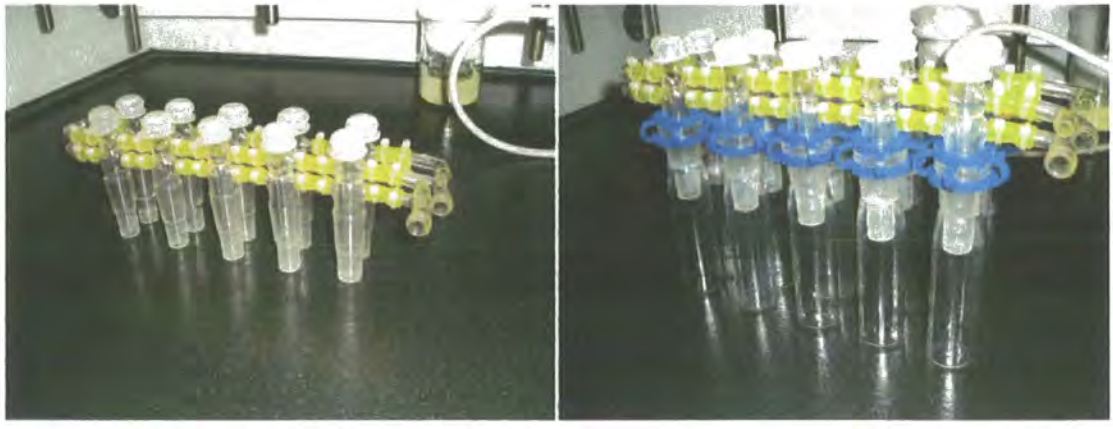

Figure 24: Standard Gilson SW215 reflux heads.

Calcium hydride was originally tested as the dehydrating agent, but was found to be inadequate as it tended to react too violently with the water produced, sending the dehydrating agent into the reaction mixture during reaction as well as making the apparatus difficult to assemble without spilling the powder

into the reaction flask. Activated 3Å molecular sieve pellets were found to be the ideal dehydrating agent for the study as they made the apparatus easier to assemble and did not carry over into the reaction.

A larger volume traditional Soxhlet type apparatus was also designed and built for the Gilson SW215 apparatus, but this system gave very poor results as the septum (needle sampling point) was, necessarily, in the flow of the condensate and the seal was rapidly damaged by the refluxing toluene. This alternative apparatus was not used to obtain any results presented in this thesis.

2.6.6.3 Results – Rate determination

In all amide formations the reactions catalysed by the four boron acids and the uncatalysed reaction were run in parallel, using the optimised conditions of a slight excess of acid in toluene with condensate dehydration (Scheme 39, Table 17). The heating block was set to 120°C to ensure a steady flow of the azeotrope over the dehydrating agent. On the ten-place heating block reaction tubes were laid out in a zigzag pattern (*i.e.* no reaction had another reaction in a laterally or longitudinally neighbouring vessel) to ensure all positions were heated evenly. The heating block position of each catalyst and the uncatalysed reaction was randomised by drawing of lots for each amide formation, in order that it would be possible to identify if an individual position was constantly producing superior results. This was demonstrated not to be the case. Samples were taken every 2 hours from 0 h to 22 h, quenched by immediate 1000-fold dilution in MeCN (reaction rate is shown to be negligible at room temperature, *vide infra*), and immediately analysed. At this concentration samples fall within the linear section of the UV-absorbance curve, simplifying HPLC-UV calibration. The effective molar extinction coefficients ε_{acid} and ε_{amide}) as well as the ratios ($\varepsilon_{acid}/\varepsilon_{amide}$) were determined at the analysis wavelength. This was achieved by HPLC-UV acquisition of an external calibration 'curve' over the concentration range of the experiment using analytically and spectroscopically pure samples of each compound.

HPLC data was also obtained for the salt **345** which had been synthesised by Kenny Arnold, another member of the project team. As expected, elution of the salt in the very low pH elution system used throughout these studies (gradient elution from 100% water/TFA 0.05% (v/v) to 100% MeCN/TFA 0.05% (v/v) on C18 column) caused the rapid conversion of the carboxylate salt to carboxylic acid and amine.TFA salt. Hence salt **345** produced peaks identical in area and retention time to samples of **320** and **327** of the same concentration when analysed by HPLC-UV under the same elution conditions (Equation 66). Also, none of the other carboxylate salts produced in these studies were HPLC stable (under low pH conditions), and all amine.TFA salts were eluted on the solvent front.

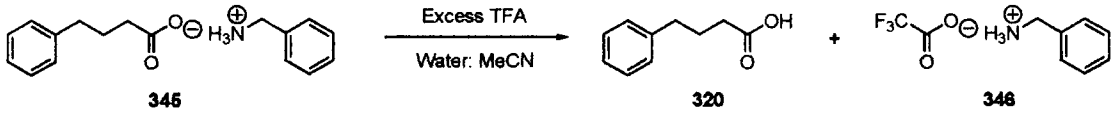

345 320 348

Equation 66: Conversion of carboxylate salt to TFA salt and free acid.

Raw HPLC areas were transformed to concentration data and to percentage conversion (see appendix B for Excel spreadsheet containing all calculations). Graphs and data are presented below (Charts 2, 3, 4, 5, 6 and 7, Tables 18, 19, 20, 21, 22 and 23).

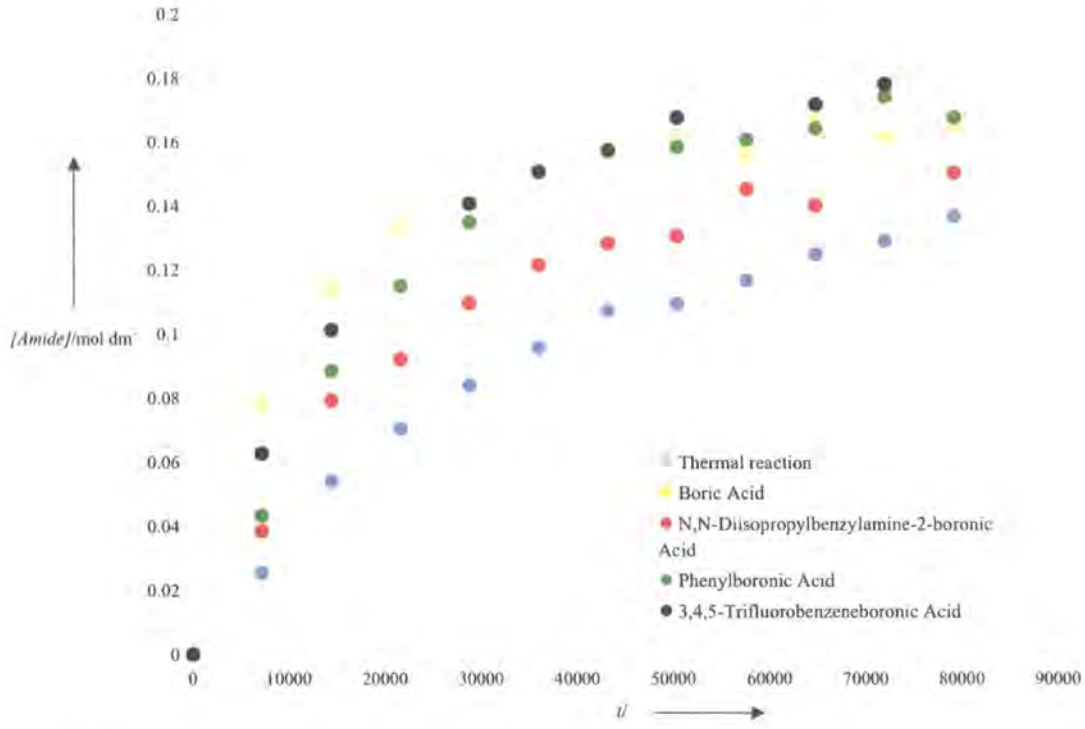

Chart 2: Formation of *N*-benzyl-4-phenylbutyramide

Benzylamine + Phenylbutyric acid	Rate constant k_{obs} (s^{-1})	Conversion 22 h
Thermal reaction	$(2.91 \pm 0.2) \times 10^{-5}$	64%
Boric acid	$(8.18 \pm 0.47) \times 10^{-5}$	77%
N,*N*-Diisopropylbenzylamine-2-boronic acid	$(4.49 \pm 0.35) \times 10^{-5}$	71%
Phenylboronic acid	$(4.97 \pm 0.31) \times 10^{-5}$	79%
3,4,5-Trifluorobenzeneboronic acid	$(5.60 \pm 0.31) \times 10^{-5}$	89%

Table 18: Rate constants, formation of *N*-benzyl-4-phenylbutyramide.

The reaction of **320** with **327** (Chart 2, Table 18) shows the highest level of uncatalysed thermal reaction, resulting in surprisingly high *ca.* 60% conversion to **332** after 22 hours. In comparison and even more surprisingly, all the catalysed reactions are only incrementally better than the thermal reaction, with little difference seen between results from boric acid, **323** and **334**. These results immediately raised the question as to whether much of the catalytic activity observed, albeit only 20% of the conversion (*i.e.* over the thermal reaction), was due to the to the formation of boric acid by proto-deboronation under the forcing and acidic reaction conditions.

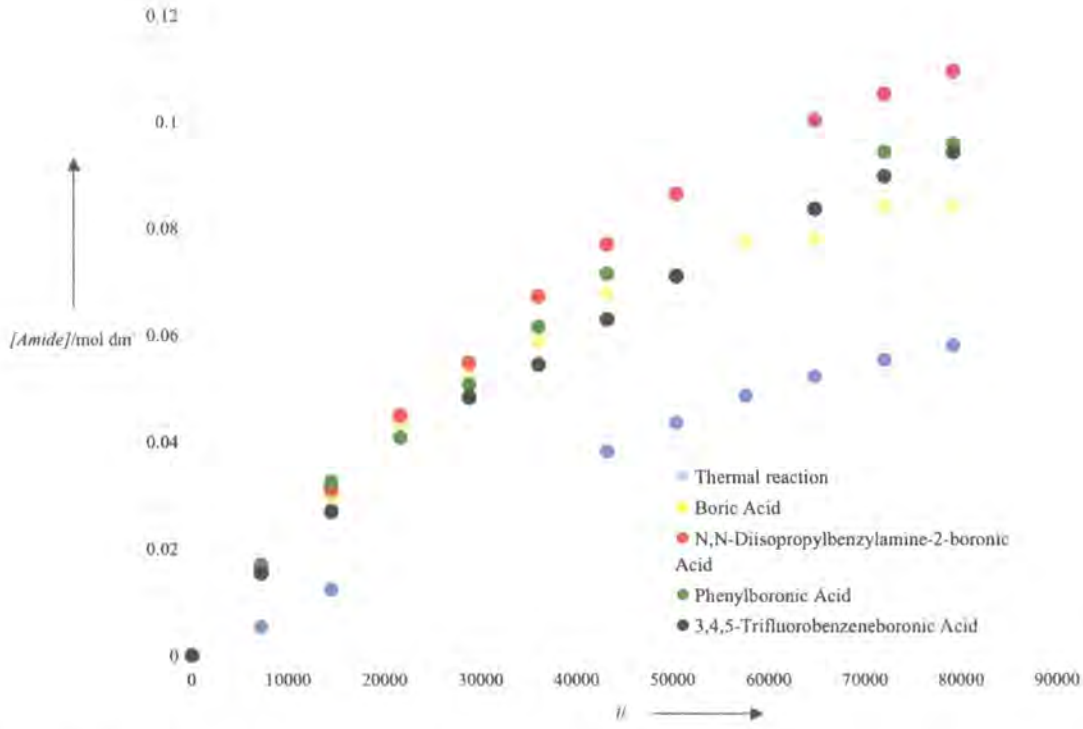

Chart 3: Formation of *N*-morpholino-4-phenylbutyramide.

Morpholine + Phenylbutyric acid	Rate constant k_{obs} (s^{-1})	Conversion 22 h
Thermal reaction	$(1.46 \pm 0.14) \times 10^{-5}$	26%
Boric acid	$(2.73 \pm 0.15) \times 10^{-5}$	38%
N,*N*-Diisopropylbenzylamine-2-boronic acid	$(1.59 \pm 0.08) \times 10^{-5}$	49%
Phenylboronic acid	$(1.87 \pm 0.17) \times 10^{-5}$	43%
3,4,5-Trifluorobenzeneboronic acid	$(1.36 \pm 0.10) \times 10^{-5}$	42%

Table 19: Rate constants, formation of *N*-morpholino-4-phenylbutyramide.

For the formation of *N*-morpholino-4-phenylbutyramide (Chart 3, Table 19) the catalytic effect of the boron acids was more pronounced. In this case the bifunctional catalyst **206** the showed the most impressive result, producing *ca.* twice the quantity of amide as the uncatalysed reaction. However it must once again be noted that the performance of the boronic acids investigated is strikingly similar to the performance of boric acid. This once again raises the question of deboronation under these conditions.

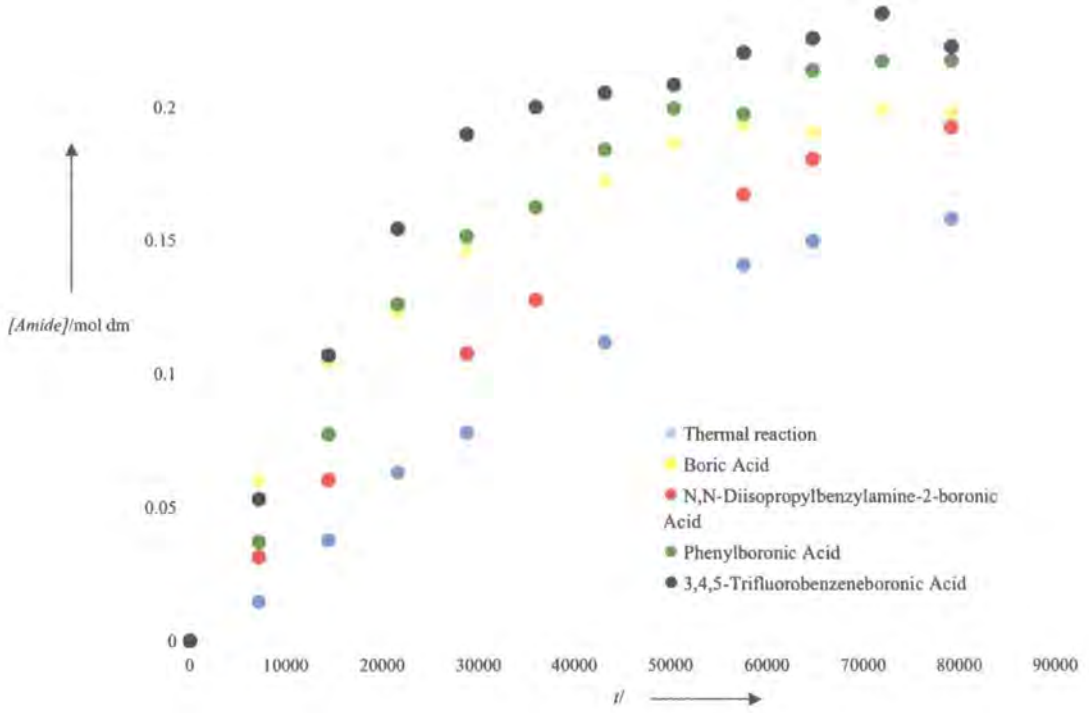

Chart 4: Formation of *N*-4-phenylbutyl-4-phenylbutyramide.

4-Phenylbutylamine + Phenylbutyric acid	Rate constant k_{obs} (s^{-1})	Conversion 22 h
Thermal reaction	$(1.98 \pm 0.27) \times 10^{-5}$	72%
Boric acid	$(4.42 \pm 0.23) \times 10^{-5}$	90%
N,*N*-Diisopropylbenzylamine-2-boronic acid	$(2.08 \pm 0.97) \times 10^{-5}$	88%
Phenylboronic acid	$(3.35 \pm 0.30) \times 10^{-5}$	99%
3,4,5-Trifluorobenzeneboronic acid	$(4.88 \pm 0.43) \times 10^{-5}$	102%

Table 20: Rate constants, formation of *N*-4-phenylbutyl-4-phenylbutyramide.

For the formation of *N*-4-phenylbutyl-4-phenylbutyramide (Chart 4, Table 20) the thermal reaction once again produced reasonable quantities of amide, *ca.* 72% conversion after 22 hours. Once again all of the boron acids investigated increased the rate and the conversion to amide over the 22 hour timescale. The fastest initial rate of reaction was observed for the electron withdrawn boronic acid **323** at *ca.* 2.5 times the rate of the thermal reaction, in a reaction that produced quantitative conversion. Of the other boron acids, boric acid and phenyl boronic acid **334** produced similar results, with bifunctional boronic acid **206** producing the least impressive performance.

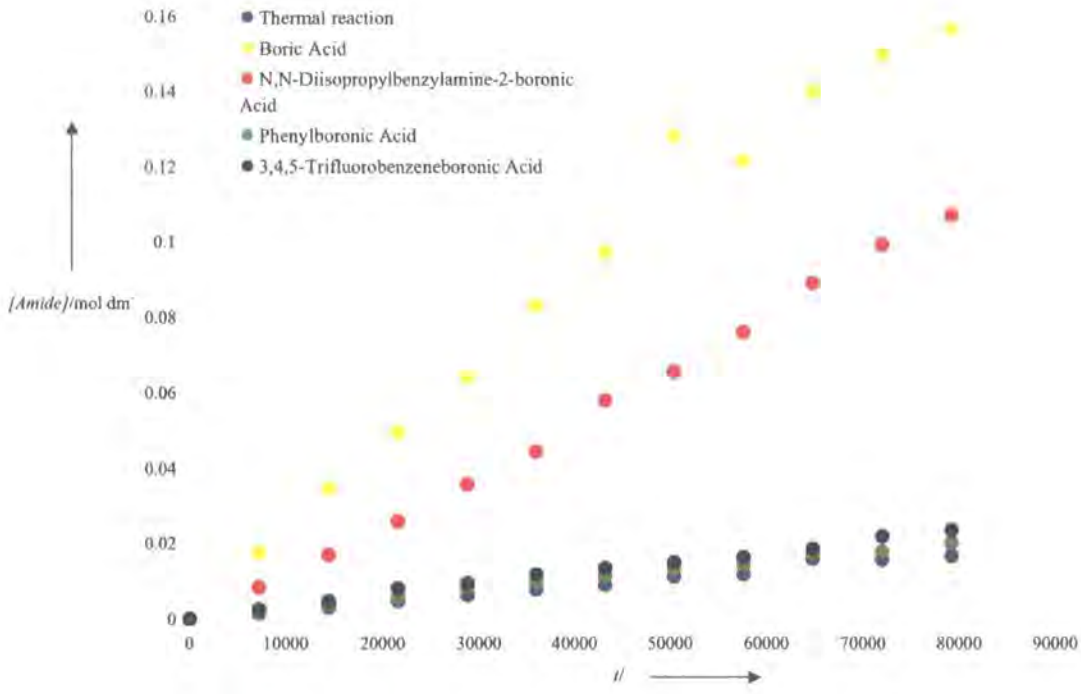

Chart 5: Formation of *N*-benzylbenzamide.

Benzoic acid and benzylamine	Rate constant k_{in} ($moldm^{-3}s^{-1}$)	Conversion 22 h
Thermal reaction	$(2.20 \pm 0.04)\times10^{-7}$	7%
Boric acid	$(2.16 \pm 0.03)\times10^{-6}$	65%
N,*N*-Diisopropylbenzylamine-2-boronic acid	$(1.34 \pm 0.01)\times10^{-6}$	44%
Phenylboronic acid	$(2.60 \pm 0.03)\times10^{-7}$	8%
3,4,5-Trifluorobenzeneboronic acid	$(3.02 \pm 0.05)\times10^{-7}$	10%

Table 21: Rate constants, formation of *N*-benzylbenzamide.

In the formation of *N*-benzylbenzamide (Chart 5, Table 21) the situation changes dramatically. The thermal reaction was slow (*ca.* 7% after 22 hours), with reactions catalysed by **334** and **323** giving similarly poor results. The bifunctional catalyst produced its first relatively impressive result, giving 44% conversion in 22 h, and boric acid produced the most impressive result of 65% over the same timescale. This reaction highlighted the need to investigate the possibility of deboronation of **206** in the presence of benzoic acid.

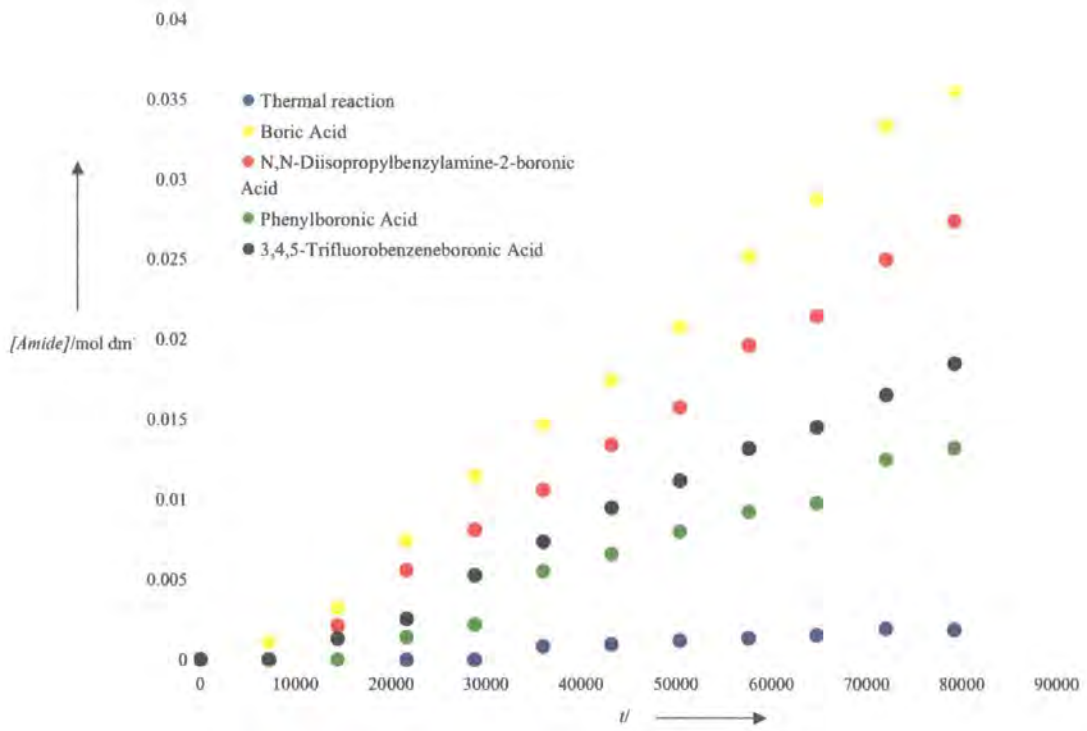

Chart 6: Formation of *N*-morpholinobenzamide.

Benzoic acid and morpholine	Conversion 22 h
Thermal reaction	1%
Boric acid	16%
N,N-Diisopropylbenzylamine-2-boronic acid	12%
Phenylboronic acid	6%
3,4,5-Trifluorobenzeneboronic acid	8%

Table 22: Rate constants, formation of *N*-morpholinobenzamide.

The formation of *N*-morpholinobenzamide (Chart 6, Table 22), both catalysed and uncatalysed, gave poor conversions. The thermal reaction produced only *ca.* 1% amide over 22 hours and the most successful catalysed reaction, with boric acid, produced just 16% amide in 22 hours. The same trend occurs in the formation of *N*-morpholinobenzamide as in the formation of *N*-benzylbenzamide, in that the order of reactivity is thermal < **334** < **323** < **206** < boric acid. What is perhaps surprising is that the reactions with **323** and **334**, which had been almost indistinguishable from the thermal reaction in the formation of *N*-benzylbenzamide, show some evidence of catalytic effect with morpholine as the amine.

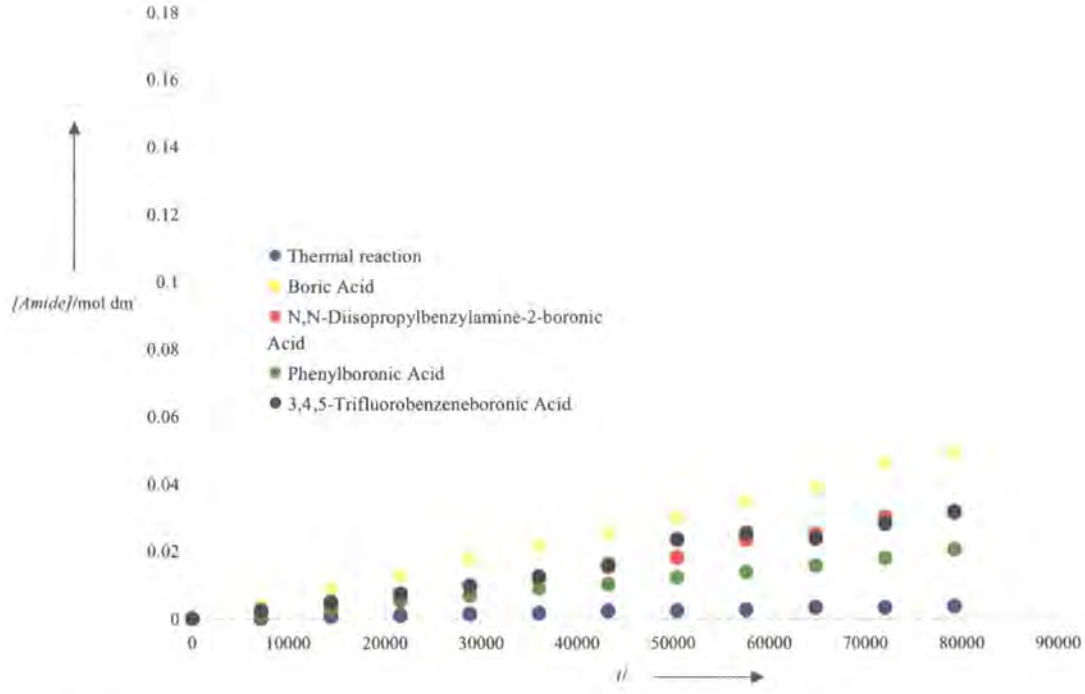

Chart 7: Formation of *N*-4-phenylbutylbenzamide.

Benzoic acid and 4-phenylbutyramine	Rate constant k_{in} ($moldm^{-3}s^{-1}$)	Conversion 22 h
Thermal reaction	(4.69 ± 0.11)×10-8	2%
Boric acid	(6.07 ± 0.05)×10-7	22%
N,*N*-Diisopropylbenzylamine-2-boronic acid	(3.69 ± 0.10)×10-7	14%
Phenylboronic acid	(2.40 ± 0.02)×10-7	9%
3,4,5-Trifluorobenzeneboronic acid	(3.77 ± 0.07)×10-7	14%

Table 23: Rate constants, formation of *N*-4-phenylbutylbenzamide.

The order of reactivity, thermal < **334** < **323** < **206** < boric acid, was again repeated in the formation of *N*-4-phenylbutylbenzamide (Chart 7, Table 23), another reaction where both catalysed and uncatalysed reactions generally produced relatively poor conversions. Here the thermal reaction was very slow, with *ca.* 2% conversion in 22 hours. The reaction with boric acid produced 22% of the amide after 22 hours. The electron deficient boronic acid **323** and the bifunctional boronic acid **206** produced almost identical results, with **334** producing the lowest conversion. All boron acids again produced results significantly better than the uncatalysed reaction.

Dr. C. Grosjean collaborated on the project to convert data for use with Micromath Scientist™, a kinetic data analysis computer program[211] and to perform the rate calculations and where possible to determine the order of the reactions. The change in amide concentration with time was found to follow first order kinetics for the reactions with **320** (Charts 2, 3 and 4, Tables 18, 19 and 20). In the case of the amide formations with **307** (Charts 5, 6 and 7, Table 21, 22 and 23) where the reaction was too slow to be fitted to a particular model, initial rate constants were calculated by regression.[212]

It had been demonstrated in the work of Tang that boric acid was an effective catalyst for the amide bond forming reaction,[209] but the performance of this simple and cheap compound in this study was astounding. In all three reactions with benzoic acid, boric acid proved to be the most effective catalyst. In these reactions there existed a slight excess of a relatively weak carboxylic acid with no α-hydrogens, conditions under which proto-deboronation, of boronic acid catalysts to give boric acid, would be expected to be a slow process. Where the more acidic, α-unsaturated carboxylic acid **320** was used, the performance of monofunctional boronic acids **323**, **334** and boric acid was suspiciously similar, with boronic acids **323** and **334** consistently producing curves broadly of the same profile as the reaction curve of boric acid. It should be noted, however, that in all three cases the reaction curves for the bifunctional boronic acid **206** appear to be distinct from the **334**-**323**-boric acid group. This led us to the conclusion that before the relative efficiencies of the catalysts could be assigned it was necessary to separate the catalytic effects observed due to the boronic acids from the catalytic effect due to the *in situ* formation of boric acid under the reaction conditions. To this end it was decided to investigate proto-deboronation of the boronic acids **323**, **334** and **206** in the presence of carboxylic acids **320** and **307**.

2.6.7 Deboronation studies

As boric acid was an effective catalyst for amide bond formation, and the optimised conditions for bifunctional catalyst **206** and the other boron-mediated amide bond forming catalysts were slightly acidic (*vide supra*), the possibility of generation of boric acid as the active catalyst by *in situ* proto-deboronation had to be investigated.

D_8-Toluene solutions of **320**, **307** or blank D_8-toluene were each combined with catalysts **206**, **323**, **334**, boric acid (at 10 mol%) or no catalyst. Samples were heated for 18 hours at reflux. ^{11}B NMR spectra were recorded before heating and after 1 and 18 hours heating. The 18-hour sample was also subjected to a D_2O shake and reanalysed. All of the experiments were run together at the same time in a single oil bath (Scheme 40). Results are shown below (Table 24). It was hoped that this would enable us to estimate the level of deboronation of the aryl boronic acids and identify the species present.

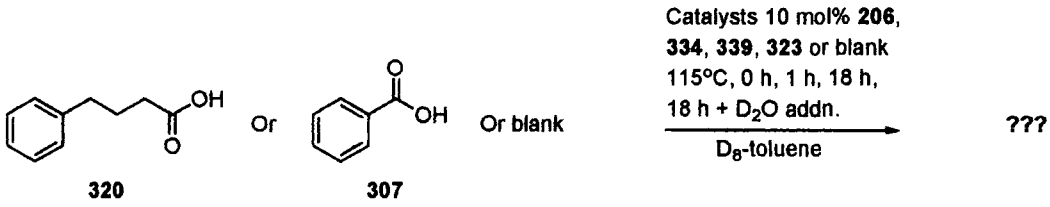

320 307

Scheme 40: Conditions, proto-deboronation experiments.

Entry	Reagents	Timepoint (h) / ^{11}B NMR δ (approx. integration)							
		0 h		1 h		18 h		18 h D_2O shake	
		Major	Minor	Major	Minor	Major	Minor	Major	Minor
1	**339**	No signal		No signal		No signal		19.6 (100%)	
2	**206**	29.1 (100%)		29.1 (100%)		29.5 (weak signal overlapping with 32.0)	32.0 (Weak signal overlapping with 29.5)	8.5 (54%)	29.1 (32%) and 4.1 (14%)
3	**334**	29.1 (100%)		29.1 (100%)		29.1 (100%)		29.1 (94%)	19.6 (4%)
4	**323**	27.4 (100%)		27.4 (100%)		27.2 (80%)	19.6 (20%)	27.4 (94%)	19.6 (6%)
5	**320 + 339**	No signal		No signal		No signal		19.6 (100%)	
6	**320 + 206**	29.2 (100%)		29.9 (60%)	5.1 (40%)	28.15 (very weak signal)		28,3 (98%)	19.7 (2%)
7	**320 + 334**	27.7 (100%)		29.8 (84%)	19.2 (16%)	No signal		19.6 (100%)	
8	**320 + 323**	27.7 (100%)		28.7 (68%)	18.9 (32%)	No signal		19.7 (71%)	28.0 (29%)
9	**307 + 339**	No signal		No signal		No signal		19.6 (100%)	
10	**307 + 206**	No signal		No signal		No signal		No signal	
11	**307 + 334**	29.2 (100%)		30.0 (97%)	19.7 (3%)	No signal		16.8 (100%)	
12	**307 + 323**	No signal		28.03 (35%)	18.03 (65%)	No signal		19.7 (major) and 18.9 (minor) (63% overlapping)	28.09 (37%)

Table 24: ^{11}B NMR data proto-deboronation experiments.

Boric acid is poorly soluble in D_8-toluene and does not appear on any of the anhydrous time-points, but a single strong ^{11}B NMR signal at δ 19.6 ppm appears when D_2O is added after heating at reflux for 18 h (Entry 1, Table 24). When boric acid is heated in the presence of 4-phenylbutyric acid or benzoic acid for 18 hours and then treated with D_2O the sole signal observed in the ^{11}B spectrum appears at δ 19.6 ppm. No signals appear in the ^{11}B NMR

spectra of the anhydrous timepoints with either of the acids (Entries 5 and 9, Table 24).

Bifunctional boronic acid **206**, when heated in solvent in a straight thermolysis reaction, appeared to be consumed to form an insoluble hydride, as evidenced by the disappearance over time of the peak at δ 29 ppm. The D_2O shake revealed three entities: the major product at δ 8.5 ppm, presumably an anhydride or acylated product; the starting material **206** as a minor species; and also a very minor species at around δ 5 ppm (integrations 54, 32 and 14% respectively). This suggests that **206** does not deboronate under these conditions, but instead forms new species. The major product is probably boroxine trimer (Entry 2, Table 24). When heated with 4-phenylbutyric acid for 18 hours, **206** appeared to suffer only approximately 2% deboronation, with 98% of the product apparently unchanged (Entry 6, Table 24). Using benzoic acid **307** there was no evidence of deboronation (Entry 10, Table 24).

When the monofunctional, electron deficient boronic acid **323** was heated in solvent it showed evidence of a small amount of deboronation, with a δ 19.6 ppm ^{11}B NMR integral of 6% after 18 hours and D_2O shake reveal (Entry 4, Table 24). When heated with 4-phenylbutyric acid for 18 hours it appeared to deboronate to form approximately 71% boric acid (Entry 8, Table 24). Deboronation probably also occurred when **323** was heated with benzoic acid, but this is not the only reaction that took place. The 18 hour timepoint with D_2O shake shows two products with similar and overlapping ^{11}B NMR peaks at δ 19.7 and 18.9 ppm (total integral 63%), with unreacted boronic acid making up the remainder of the integral (Entry 12, Table 24).

When the monofunctional boronic acid **334** was heated in solvent it showed evidence of a small amount of deboronation, with a δ 19.6 ppm ^{11}B NMR integral of 4% after 18 hours and D_2O shake reveal (Entry 3, Table 24). When heated with 4-phenylbutyric acid for 18 hours it appeared to deboronate completely, forming 100% boric acid (Entry 7, Table 24). On heating in benzoic acid a new compound, quite possibly a stable acylboron species, was

formed, as evidenced by the appearance of a new signal at 16.8 ppm (Entry 11, Table 24).

In summary, bifunctional boronic acid **206** experiences little or no deboronation in the presence of carboxylic acids **320** and **307** under similar conditions to those used for rate determination (Scheme 39). In contrast, the monofunctional boronic acids tested – 3,4,5-trifluorobenzeneboronic acid **323** and phenylboronic acid **334** – protodeboronate rapidly in the presence of aliphatic acid **320**, converting to mostly boric acid on the reaction timescale, and form new species (not starting material or boric acid) in the presence of benzoic acid **307**. *In situ*-generated boric acid must therefore have contributed a significant part of the catalytic effect observed when catalysts **323** and **334** were used alongside carboxylic acid **320** to form amide bonds. With catalyst **206**, however, the catalytic effect observed was due almost entirely to the bifunctional compound, as little or no deboronation took place.

The process of protodeboronation of boronic acids is well-documented with respect to alkylcarboxylic acids and is recorded as faster for more electron-deficient arylboronic acids.[213, 214] In this case phenylboronic acid **334** showed more deboronation than the more electron deficient **323.** However, this was by no means an exhaustive study.

2.6.8 Initiation temperature determination

Formation of amide **332** with 1 mol% of catalysts **206**, **323** or **334**, as well as the uncatalysed reaction, was investigated at a series of temperatures rising in 10°C increments between 24 and 84°C, and in 6°C increments between 84 and 120°C, with 24 h spent at each temperature increment (Scheme 41). The experiment was run on the SW215 with automated sampling, dilution and injection for analysis on HPLC-UV as described above, but in this case without condensate dehydration. The initiation of all reactions investigated was observed to occur at 84°C by the emergence of the amide peak on the HPLC-UV trace. Hence the initiation point for then formation of amide **332** in

toluene is less than or equal to 84°C and greater than 74°C and the reaction is undetectable by HPLC-UV at room temperature.

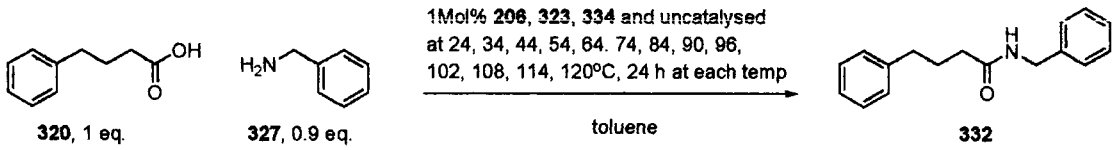

320, 1 eq. **327**, 0.9 eq. **332**

Scheme 41: Initiation temperature determination.

2.6.9 Amide bond cleavage

As catalyst **206** showed activity for amide bond formation, amide bond cleavage was investigated on *N*-benzyl-4-phenylbutyramide **332** (Scheme 42, Table 25). No reactivity was observed in this reaction, either with catalyst **206** or in the uncatalysed reaction in water (Entries 1 and 3, Table 25). Similar lack of reactivity was observed when a water/THF solvent mixture was used in order to prevent biphase formation (Entries 2 and 4, Table 25).

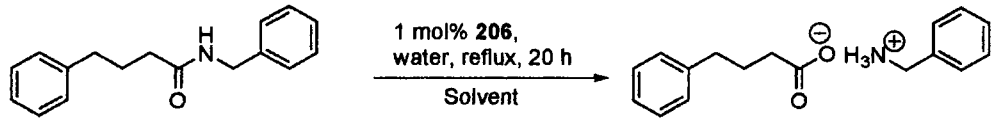

332 **345**

Scheme 42: Conditions, amide bond cleavage.

Entry	Solvent	Catalyst	Conversion
1	Water	None	0%
2	Water:THF, 1:1	None	0%
3	Water	**206**	0%
4	Water:THF, 1:1	**206**	0%

Table 25: Conversions, amide bond cleavage.

2.6.10 Direct ester bond formation

Ester bond formation is directly analogous to the amide bond forming reaction. Catalyst **206** was investigated for activity in the reaction of carboxylic acid **320** with representative alcohols benzyl alcohol **349**, isopropanol **350** and *t*-butanol **351**, using the conditions developed for the amide bond formation reaction (*vide infra*) (Equation 67, Table 26). No reactivity was observed.

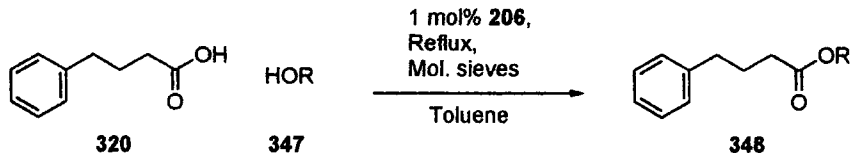

320 **347** **348**

Equation 67: Conditions, ester bond formation.

Entry	Alcohol \ Acid	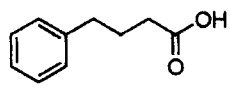 **320**
1	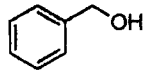 **349**	0%
2	 **350**	0%
3	 **351**	0%

Table 26: Conversions, ester bond formation.

A literature search revealed two examples of boron-mediated ester formation. Houston *et al.* demonstrated that boric acid was effective for the chemoselective esterification of α-hydroxycarboxylic acids, a reaction in which assistance from the neighbouring hydroxyl is postulated to participate in the mechanism by formation of bridge anhydride **354** and its 'ate'-complex **355** (Equation 68).[215] Lowrence has also demonstrated that a synergistic boric acid/sulphuric acid mixture is capable of catalysing the esterification reactions of phenols (Equation 69).[216] These reactions will provide useful starting

points if it is decided to more fully investigate this area of catalysis at a later date.

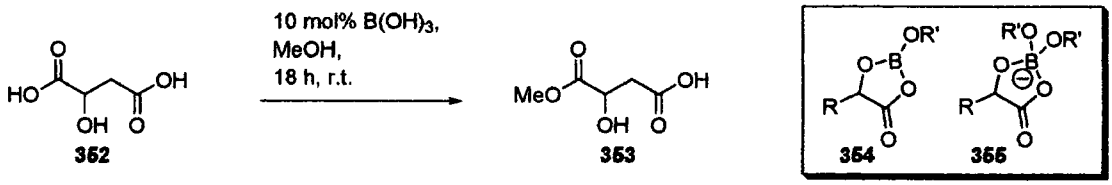

Equation 68: Boric acid-catalysed chemoselective esterification of α-hydroxycarboxylic acids.

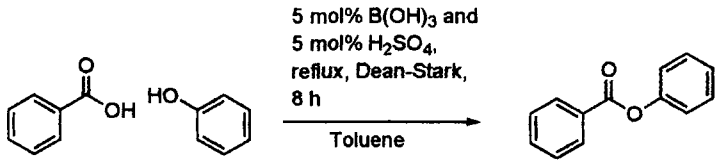

Equation 69: Synergistic boric acid/sulphuric acid-catalysed ester bond formation.

2.6.11 Conclusions – Direct amide bond formation

At the onset of this work the leading compound for amide bond formation catalysis was the electron deficient boronic acid **323**, with Tang reporting the utility of boric acid in 2005 at the midway point of the work, around the same time as the start of our kinetics studies. This gave us the opportunity to design experiments to determine the relative efficiencies of these two boron acids alongside our bifunctional system **206**, which we were able to demonstrate is an amide bond forming catalyst with similar performance to the industry standard compound **323**.

After screening a range of solvents, molarities and dehydration methods we have determined an optimum set of conditions for the amide bond formation reaction catalysed by **206** (*i.e.* reflux in non-polar solvent with dehydration of the condensate and a slight excess of carboxylic acid). These conditions were found to be pretty general for boron-mediated amide bond formation, being

the conditions of choice for reactions catalysed by **323** and related compounds as well as by boric acid.

We have been able to recognise that relatively low temperature thermolysis of carboxylate ammonium salts in non-polar solvent conditions alone does produce amide products. However, the efficiency is highly substrate dependent. Our postulated mechanism is detailed in scheme 43. Presumably there is a critical balance between the ability of the ammonium salt to act as a general Brønsted acid and of the free amine to act as a reasonable nucleophile on either the protonated carboxylic acid or the anhydride (*vide infra*). This balance seems to result in a "benzylic effect", *i.e.* benzylamine shows higher amide bond forming potential than the more nucleophilic amine **340**, especially when coupled with the more reactive acid **320** (Scheme 43).

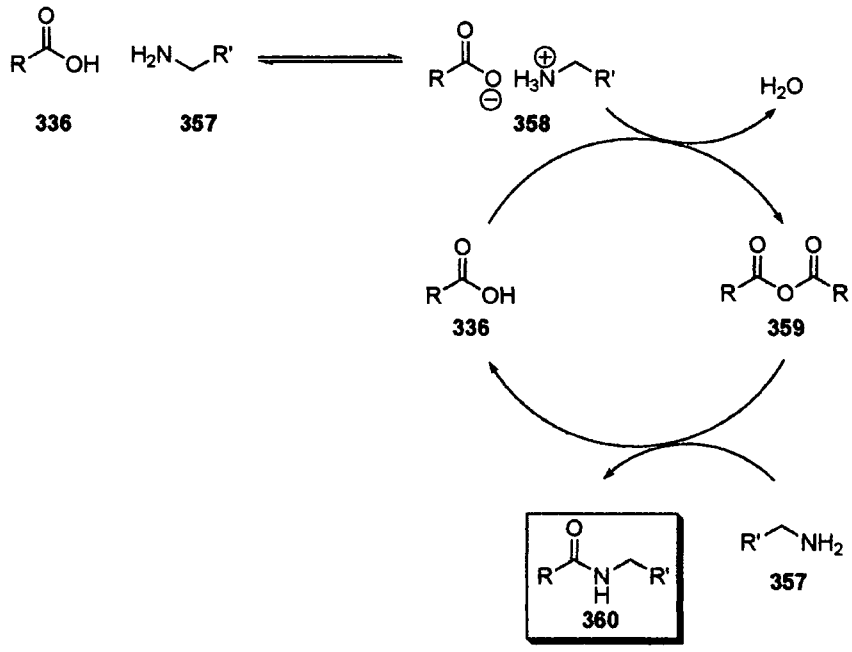

Scheme 43: Postulated mechanism thermal amide bond formation.

We have been able to demonstrate that molecular sieves do not represent an effective catalyst for the amide bond forming reaction, as had been previously claimed in the literature.[210]

Although the industry standard compound, electron-deficient boronic acid **323**, may indeed be an effective catalyst for the amide bond forming reactions at

lower temperatures, under conditions where protodeboronation can compete (*e.g.* with an excess of **320** in refluxing toluene), this system acts predominantly as a source of *in situ* generated boric acid, which is a good general catalyst at higher temperatures. Presumably, at even higher temperatures (*e.g.* refluxing mesitylene, b.p. 165°C), as generally used during the studies of Yamamoto *et al.* on **323** with more difficult substrates (Equations 70 and 71), electron-deficient boronic acids are even more likely to act as a source of boric acid by protodeboronation.

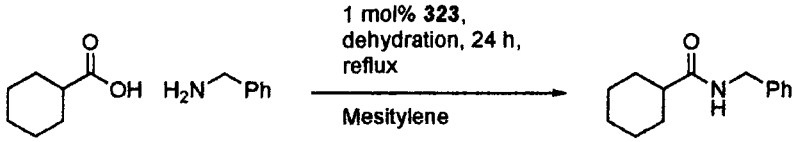

361 **327** **362**, 98%

Equation 70: Yamamoto *et al.*, high temperature amide bond formation.

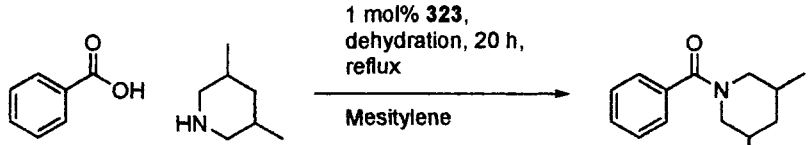

307 **363** **364**, 95%

Equation 71: Yamamoto *et al.*, high temperature amide bond formation.

We note that bifunctional compound **206** was the single outstanding catalyst in one of our six amide bond forming reactions, the formation of **334**. It is perhaps surprising that **206** is effective as a catalyst at all as Yamamoto *et al.* had demonstrated that aryl boronic acids with *ortho*-substituents such as **324** (scheme 31) were very poor amide bond forming catalysts. The extra hindrance provided by the diisopropylbenzyl group appears to be tempered by an advantageous catalytic effect of H-bonding to the B-OH hydroxyl. It should also be noted that the presence of the *o*-diisopropylbenzylamine function significantly reduces protodeboronation, a major problem with both **334** and **323**.

It may well be the case that a new catalyst candidate can be developed in future, which combines greater electron deficiency at boron with the presence

of an intramolecular base. Such a system may well combine the advantages of the bifunctional and the electron deficient systems.

Yamamoto *et al.* claimed that when a 2:1 mixture of **320** and **323** were heated in D_8-toluene for 2 hours, monoacyloxyboronic acid **365** was the major product, with no diacylated boron observed. When **365** was treated with benzylamine at room temperature less than 50% amide was produced, with the remainder of **365** being hydrolysed by the boronic acid generated in the reaction (Scheme 44). The facile reaction of the mixed anhydride **365** with the amine compared with the conditions required for the formation of **365** suggest that the first stage is the rate determining step in this case. Yamamoto then went on to implicate the cyclic boronic acid boroxine anhydride **367** in the reaction mechanism, although no evidence for its formation under the reaction conditions, or its acylation by carboxylic acid, was presented (Scheme 45).[204]

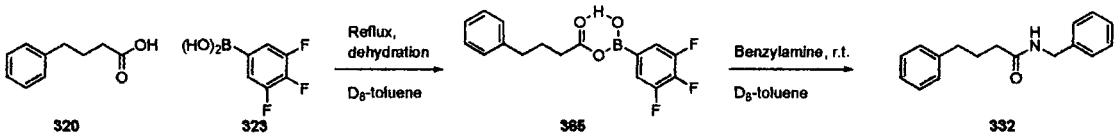

Scheme 44: Yamamoto *et al.*, evidence for acyl boron formation.

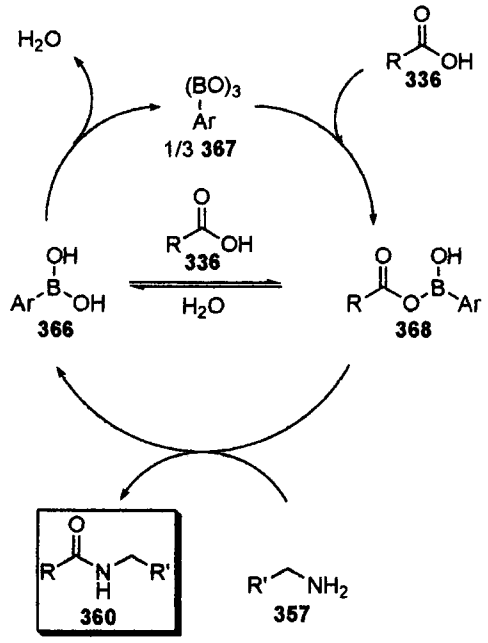

Scheme 45: Yamamoto *et al.*, proposed reaction mechanism for electron-deficient boronic acids.

In the case of the amide bond forming reactions with **320** (Charts 2, 3 and 4, Tables 18, 19 and 20) it has been observed that first order kinetics are followed, which is consistent with the reaction proceeding through an intermediate. This is likely to be **369** or **368**, derived from acylation[217, 218] of either boronic acid or boric acid (Scheme 46). However, for catalyst **323** in toluene both the boronic acid and boric acid-derived intermediates are involved due to proto-deboronation. This contrasts with the thermolysis reaction where the likely intermediate is the carboxylic acid anhydride **359**, which explains the subsequent formation of the amide (Scheme 43). Since the formation of the acyloxyboronates **369** and/or **368** are very likely to be the rate determining step, it is important to understand this reaction. Brown has reported that in the acyloxyboronation of carboxylic acids by boranes, more acidic substrates slow the reaction. This relates to the difference in rate between **320** and **307** (pKa = 4.19 and 4.76 respectively). Similarly, it also suggests that the more electron-deficient the boron the more prone it is to acylation.[217, 218]

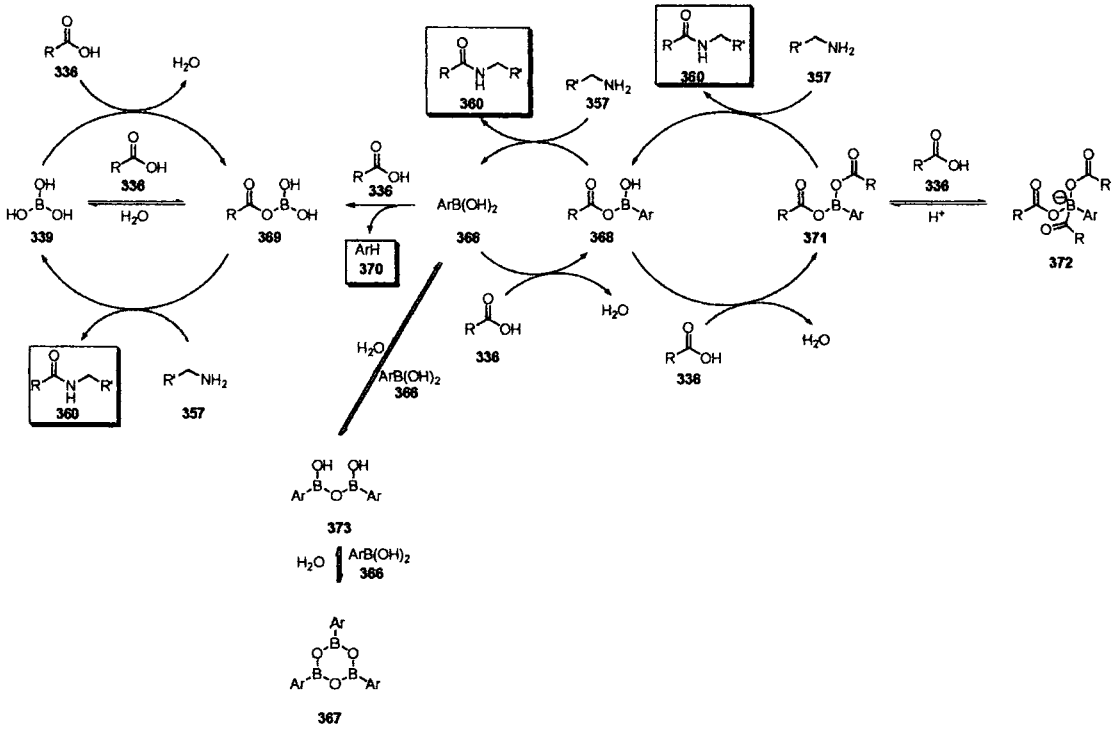

Scheme 46: Proposed mechanism for the boric acid and boronic acid-catalysed routes to amides.

Boric acid was observed to be a much less effective catalyst at lower temperatures (*i.e.* refluxing fluorobenzene b.p. 85°C) during follow-up work within the group by K. Arnold. This raises the question as to why this occurs. It is known that boric acid reacts readily under acylating conditions to form tetraacyldiborate systems of type **374**.[219] However, triacylboranes **375** have also been shown to react *via* amine complex intermediates to provide amides.[220] It is possible that the formation of these species is essential for the catalytic activity of boric acid and that the higher temperature (refluxing toluene) assists catalyst recycling.

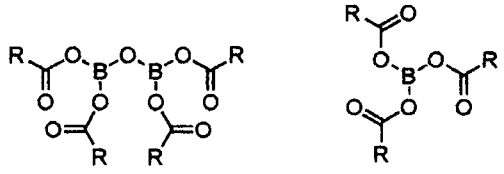

374 **375**

Overall, this gives us three routes for amide bond formation: boronic acid catalysed, boric acid catalysed and thermal (Schemes 45 and 46). The likelihood that the amide formation goes through one particular path rather than another is largely dependent on the nature of the substrates. In the case

of **307**, where the formation of the acid anhydride is not facile, the thermal reaction is virtually non-existent, deboronation is slow, and hence the addition of the correct boronic acid facilitates the reaction. In contrast, when **320** is used, the thermal reaction is reasonable and the addition of arylboronic acid offers only an incremental improvement, caused by boronic acid catalysis and boric acid catalysis (in cases where deboronation is facile).

2.7 Concluding remarks

Before this project was initiated, the study of aminoboronic acids and derivatives as bifunctional catalysts had been, with one exception (i.e. the studies of Letsinger *ca.* 1960), absent from publication in modern chemical literature. In this project, we have accomplished the design, synthesis and characterisation of several series of novel and interesting bifunctional boronic acids and derivatives. We have defined as far as possible the structural details of these molecules and speculated on how these features may allow them to act as bifunctional catalysts. We have designed and implemented a multi-reaction screening program for several of these bifunctional arylaminoborons and identified catalytic direct amide bond formation as an area worthy of further study. Within catalytic amide bond formation we have compared our most successful catalyst, *N*,*N*-diisopropylbenzylamine-2-boronic acid **206**, against the industry standard compound, the electron deficient boronic acid **323**, and found under certain circumstances that the bifunctional compound is the superior catalyst. Most significantly of all we have demonstrated that under certain conditions the direct thermal route to amides is effective. We have also identified that a possible competing reaction in the boronic acid-catalysed direct amide bond formation reaction is the protodeboronation of the arylboronic acid to give boric acid. We noted the work of Tang who demonstrated during the course of this project that boric acid can be an effective catalyst for the amide bond forming reaction. We began work to elucidate this mechanism, but sadly this is where the project ran out of time and passed on to the next student.

Hence we believe that this project has produced a series of potential Lewis acids-Lewis base (or perhaps also Lewis acid-H-bonding or Lewis base-H-bonding) type bifunctional catalysts. We have identified direct amide bond formation as an area in which these compounds function effectively as catalysts and within this area discovered several fundamental facts that serve as interesting points for further investigation.

2.8 Further work

The focus of further efforts in this project is likely to be the investigation of the amide bond forming reaction. Boronic acid **206** has provided a useful lead in that its reactivity differs from electron deficient boronic acid **323** and boric acid and also in the fact it shows much greater resistance to proto-deboronation than **323**. It may well be that by combining the advantageous effects of electron deficiency at boron with a Lewis basic side-arm a superior catalyst can be developed. A catalyst of this type that we had available but never investigated (as we had been focusing on aminoborons) was *o*-nitrobenzeneboronic acid **289**. In this structure the lone pairs of the nitro oxygen are well placed for either intramolecular H-bonding or for interaction with a substrate.

It would be interesting to investigate whether a mixed boron acid-strong Brønsted acid system may work for amide bond formation as it had in Lowrence's work with ester bond formation (Equation 69).[216]

In the phamaceutical industry the use of microwaves in discovery chemistry is very popular. The high temperatures attainable in a microwave synthesiser are almost certain to rapidly accelerate the reaction rate for amide bond formation. Typically, reactions that take ~24 hours in refluxing toluene can be complete in minutes at 200°C, for example. This is due to the temperature dependence of k in the Arrhenius equation. It would be interesting to see if boron acid catalysis is effective with this method of heating. The only potential pitfall in this endeavour would be the choice of solvent system, as non-polar

compounds are microwave transparent it would be necessary to rely on the microwave absorbance of the reagents or to co-add a microwave absorbing ingredient.

Other possible reactions should also not be neglected. A divergent variety of bifunctional catalyst candidates and methods for their synthesis are available within the group. The preferred method for future screenings will be the very close observation of a single reaction type with a range of catalyst candidates and standards, with precise analytical methodology. In this way we will be able to detect evidence of bifunctional effects easily at the screening stage, avoiding the problems of multi-reaction screening.

3 Experimental

3.1 General experimental details

All starting materials were obtained from Aldrich, Lancaster or Frontier Scientific and were used as received unless otherwise stated. Tetrahydrofuran and diethylether were distilled from benzophenone ketyl. Dichloromethane and toluene were distilled from calcium hydride. Dry acetonitrile where used was distilled from activated molecular sieves. Other solvents were used as received unless otherwise stated. Petroleum ether refers to the fraction boiling at 40-60°C. TMEDA and *N,N*-dimethylnaphthyl-1-amine were distilled from calcium hydride. Alkyl lithium reagents were acquired from Aldrich and were titrated immediately prior to each use.[221] Molecular sieves were activated by heating to 450°C *in vacuo* (< 2 mmHg) for at least 6 hours. Air and moisture sensitive reactions were performed under argon using Schlenk techniques and all glassware for use in sensitive reactions was heated for at least 12 hours at 160°C and cooled under a stream of argon. Stirred reactions were stirred using a magnetic stirrer bar unless otherwise stated. Reactions were at room temperature unless otherwise stated. Air and moisture sensitive reagents were stored under argon and were introduced by syringe or canula through rubber septa. Evaporations were carried out at 10-20 mmHg using a Büchi rotary evaporator and water bath followed by evaporation to dryness *in vacuo* (<2 mmHg). All reactions using KHF_2 were carried out in Teflon reaction vessels except where otherwise stated.

All ^{1}H NMR spectra were obtained using either a 250 MHz Varian Oxford, 300 MHz Varian, 400 MHz Varian Mercury or 500 MHz Varian spectrometer, using partially deuterated solvent signals and TMS as the internal standards. ^{13}C NMR spectra were recorded at 100 MHz on a Varian Oxford spectrometer or at 125.5 MHz on a Varian Inova AS500 NMR spectrometer. ^{11}B NMR spectra were recorded at 96 MHz on a Varian Mercury spectrometer or at 128.4 MHz on a Bruker 400 spectrometer. Carbons connected directly to boron were

generally not observed. ^{19}F NMR were recorded at 188.18 MHz on a Varian 200 spectrometer or at 470.26 MHz on a 500 MHz Varian spectrometer. All NMR chemical shifts are quoted in ppm. All NMRs were aquired at room temperature unless otherwise stated. Column chromatography was achieved under medium pressure using fluorochem silica gel 60-200 μ (60 Å). TLC was carried out on Fluka Kieselgel 60-F_{254} aluminium or glass-backed plates and visualistion was achieved using either UV irradiation, phosphomolybdic acid, ethanolic vanillin or alkaline $KMnO_4$. Low resolution ES mass spectra were recorded on a Micromass Autospec. High-resolution ES mass spectra were obtained on a Micromass Autospec spectrometer. Elemental analyses were carried out on an Exeter Analytical CE-440 elemental analyser. Infra red spectra were obtained using a Perkin-Elmer 1615 FTIR operating from a Grams Analyst 1600 and are quoted in cm^{-1}. UV spectra were recorded on an ATI Unicam UV2 UV/Vis spectrometer and are quote in nm. Optical rotations were recorded at the D line of sodium (589 nm) in a 0.05 dm cell. Optical rotation $[\alpha]_D$ values are given in $°cm^3g^{-1}dm^{-1}$. Melting points were determined using an Electrothermal melting point apparatus and are uncorrected.

3.2 Catalyst synthesis and structure

3.2.1 Synthesis of *N,N*-bis-((*S*)-α-methylbenzyl)benzamide 211

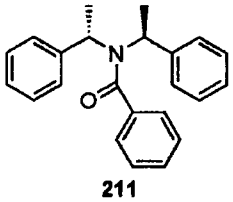

211

To stirred (*S,S*)-(-)-bis(α-methylbenzyl)amine **209** (4.96 g, 22 mmol), DCM (5 ml) and NaOH (aq.) (5% w/v) (23 ml) was added benzoylchloride (3.09 ml, 26.6 mmol) dropwise over a period of 20 minutes. After 1 hour a further dose of NaOH (aq.) (5% w/v) (10 ml) was added. After a further 30 minutes the

reaction was extracted with DCM (2 x 50 ml), dried ($MgSO_4$) and evaporated. Purification by silica gel chromatography (hexane:ethyl acetate, 9:1 to 4:1 as eluant) gave *N,N*-(bis-(*S*)-(α-methylbenzyl)benzamide **211** as an oil, which yielded colourless crystals on standing (5.58 g, 77%): m.p. 69.7°C; $[\alpha]^{20}_D$ = -169.0 (*c* = 0.071 in $CHCl_3$); ^{1}H NMR (400MHz, $CDCl_3$): δ = 7.40-7.20 (m, 5 H; *Ar*), 7.20-7.02 (m, 6 H; *Ar*), 7.02-6.90 (m, 4 H; *Ar*), 4.98-4.62 (br, 2 H; 2 x CH_2), 1.69 (d, *J* = 6.1, 6 H; 2 x CH_3); ^{13}C NMR (100MHz, $CDCl_3$): δ = 171.4 (*C*=O), 140.7 (*Ar*), 138.6 (*Ar*), 128.7 (*Ar*), 128.6 (*Ar*), 128.0 (*Ar*), 127.9 (*Ar*), 127.1 (*Ar*), 125.8 (*Ar*), 55.4 (*Bn*), 18.6 (CH_3); FTIR (thin film) *inter alia*: ν = 3059, 2978, 2362, 1634 (*C*=*O*), 1494, 1429, 1316, 750, 696; HRMS (ES) *m/z*: calcd for $C_{23}H_{24}NO$ $[M+H]^+$: 330.1852; found: 330.1853; Elemental analysis: calcd for $C_{23}H_{23}NO$: C 83.85, H 7.04, N 4.25; found C 83.50, H 7.19, N 4.11.

3.2.2 Synthesis of *N,N*-bis-((*S*)-α-methylbenzyl)benzylamine 227

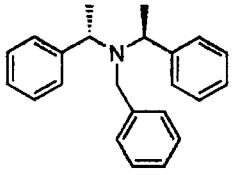

227

To stirred THF (80 ml) was added (*S,S*)-(-)-bis(α-methylbenzyl)amine **209** (2.28 ml, 10 mmol) and 2-formylbenzeneboronic acid **224** (1.50 g, 10 mmol). After 20 minutes sodium triacetoxyborohydride (12.71 g, 60 mmol) was added and the reaction was left to proceed for 20 hours. The THF was evaporated, the resulting mixture was quenched with sat NaCl (aq.) (100 ml). The aqueous layer was extracted with ethyl acetate (4 x 50 ml). The extracts were combined, dried ($MgSO_4$) and evaporated. Purification by silica gel chromatography (hexane:ethyl acetate, 1:1 to ethyl acetate as eluant) gave *N,N*-bis-((S)-α-methylbenzyl)benzylamine **227** as a colourless solid. Amine **227** existed as a 75:25 mixture of rotamers in $CDCl_3$ solution at room temperature. (0.34 g, 11%). m.p. 112.1-112.4°C; $[\alpha]^{20}_D$ = -36.9 (*c* = 0.043 in $CHCl_3$); ^{1}H NMR (400MHz, $CDCl_3$): δ = 7.86 (dd, *J* = 7.0 and 1.7, 1 H; *Ar*),

7.41 (d, *J* = 7.3, 1 H; *Ar*), 7.35-7.21 (m, 4 H; *Ar*), 7.18-7.11 (m, 5 H; *Ar*), 7.03-6.99 (m, 4 H; *Ar*), 4.09 and 3.76 (q, *J* = 7.1 and 7.1 respectively, 1.5 H and 0.5 H respectively; PhC*H*(CH_3)N-), 3.94 (AB q, *J* = 12.9, sep = 41.2, 2 H; PhCH_2N-), 1.81 and 1.47 (each d, *J* = 7.1 and 7.1, 1.5 and 4.5 H respectively; CH_3); ^{13}C NMR (100 MHz, $CDCl_3$): δ = 136.8 (*Ar*), 131.0 (*Ar*), 129.1 (*Ar*), 128.4 (*Ar*), 128.3 (*Ar*), 128.2 (*Ar*), 127.5 (*Ar*), 127.4 (*Ar*), 58.1 (*Bn*), 54.5 (*Bn*), 17.1 (CH_3); FTIR (thin film) *inter alia*: ν = 1602, 1441, 1375, 1275, 1184, 973, 790, 754, 701; HRMS (ES) *m/z*: calcd for $C_{23}H_{26}N$ $[M+H]^+$: 316.2065; found: 316.2066.

3.2.3 Synthesis of *N,N*-diisopropylbenzylamine-2-boronic acid 206

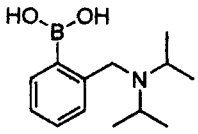

206

To THF (20 ml) and 3 Å activated molecular sieves (4 g) were added 2-formylbenzeneboronic acid **224** (908 mg, 6 mmol) and diisopropylamine (0.854 ml, 6 mmol). After 1 hour stirring sodium triacetoxyborohydride (8 g, 36 mmol) was added, the reaction was stirred for a further 24 hours, then 5% HCl (aq) (10 ml) was added. After 20 minutes the resulting suspension was filtered through a sinter and washed through with water (50 ml) on the sinter. The filtrate THF was removed by azeotroping *in vacuo*. This mixture was then neutralised by the slow addition of sat. $NaHCO_3$ (aq). The filtrate mixture was allowed to stand for 72 h during which time the product crystallised. The mixture was then filtered and washed with cold water (2 x 20 ml) on the filter paper and dried in desiccator to yield *N,N*-diisopropylbenzylamine-2-boronic acid **206** (1.00 g, 71%) as white crystals. Dissolution of the product in DCM followed by slow evaporation produced crystals suitable for single crystal X-ray structure determination. m.p. 152.0-152.9°C; ^{1}H NMR (400 MHz, $CDCl_3$): δ = 9.58 (br, 2 H; -B(O*H*)$_2$), 7.99-7.96 (m, 1 H; *Ar*), 7.38-7.29 (m, 2 H; *Ar*), 7.26-7.22 (m, 1 H; *Ar*), 3.86 (s, 2 H; CH_2), 3.15 (septet, *J* = 6.8, 2 H; 2 x

C*H*(CH_3)$_2$), 1.14 (d, *J* = 6.8, 12 H; 4 x C*H*$_3$), (addition of D_2O caused the peak at δ = 9.58 to disappear); ^{13}C NMR (100 MHz, $CDCl_3$): δ = 142.30 (*Ar*), 136.72 (*Ar*), 130.70 (*Ar*), 130.10 (*Ar*), 127.01 (*Ar*), 51.89 (*Bn*), 47.52 (-NCH(CH_3)), 19.74 (CH_3); ^{11}B NMR (128 MHz, $CDCl_3$): δ = 29 (br); FTIR (nujol) *inter alia*: ν = 2352, 2333, 1376, 970, 752 cm^{-1}; HRMS (ES) *m/z*: calcd for $C_{13}H_{23}BNO_2$ $[M+H]^+$: 236.1822; found: 236.1807; Elemental analysis: calcd for $C_{13}H_{22}BNO_2$: C 66.41, H 9.43, N 5.96; found C 66.26, H 9.45, N 5.78.

On occasions that the product failed to crystallise, solvents were removed *in vacuo* from the neutralised mixture, crude product was extracted into DCM (4 x 50 ml) and solvents were evaporated. The crude material was redissolved into 5% (v/v) aqueous hydrochloric acid, washed (DCM), the pH was adjusted to 10 and the product was extracted into DCM, dried ($MgSO_4$) and solvents evaporated to yield **206** as a white solid. The material produced was spectrocopically and analytically identical to material produced in the above method.

3.2.4 Synthesis of *N*-morpholinobenzylamine-2-boronic acid 235

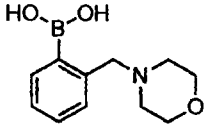

235

To a stirred suspension of 3 Å molecular sieve pellets (12 g) in THF (80 ml) was added morpholine (0.88 ml, 10 mmol) and 2-formylbenzeneboronic acid **224** (1.50 g, 10 mmol). After 20 minutes sodium triacetoxyborohydride (8.48 g, 40 mmol) was added and the reaction was left to proceed for 22 hours. The reaction was quenched by the addition of sat. NaCl (aq.) (50 ml) and filtered immediately to remove sieves. The sieves were washed with DCM (2 x 50 ml), and the combined solvents were evaporated. The mixture was then resuspended in water (100 ml) and extracted with DCM (4 x 50 ml), dried ($MgSO_4$) and solvent evaporated. Purification by solid phase extraction with

Varian Mega bond elut SCX™, a pre-packed column containing silica bonded C18-*p*-benzenesulphonic acid (gradient elution, DCM to methanolic ammonia 10% (w/v)) gave recovery of the product principally as the dimethylborate. The boronic acid was yielded by solvent evaporation with periodic addition of water (3 x 20 ml) to the azeotrope as the volume decreased. The product was redissolved in DCM, dried ($MgSO_4$) and solvent and unreacted morpholine evaporated to give *N*-morpholinobenzylamine-2-boronic acid **235** as a yellow solid. (1.35 g, 61%). m.p. 199-201°C; ^{1}H NMR (400 MHz, $CDCl_3$): δ = 8.49 (br, 2 H; -B(*OH*)$_2$), 7.94 (m, 1 H; *Ar*), 7.36 (m, 2 H; *Ar*), 7.19 (m, 1 H; *Ar*), 3.73 (br, 4 H; -OC*H*$_2$-), 3.66 (s, 2 H; *Bn*), 2.57 (br, 4 H; -NC*H*$_2$CH$_2$-), (addition of D_2O caused peak at δ = 8.49 to disappear); ^{13}C NMR (100 MHz, $CDCl_3$): δ = 140.3 (*Ar*), 136.4 (*Ar*), 130.8 (*Ar*), 130.2 (*Ar*), 127.7 (*Ar*), 66.4 (-OCH_2-), 64.5 (-NCH_2-), 52.4 (*Bn*); ^{11}B NMR (128 MHz, $CDCl_3$): δ = 30 (br); FTIR (thin film) *inter alia*: ν = 2943, 2857, 1598, 1445, 1338, 1307, 1277, 1114, 987, 865, 750, 675, 589, 480; HRMS (ES) *m/z*: calcd for $C_{11}H_{17}BNO_3$ $[M+H]^+$: 222.1301; found: 222.1302.

3.2.5 Synthesis of *N*-methyl-*N*-((*R*)-α-methylbenzyl)benzylamine-2-boronic acid 236

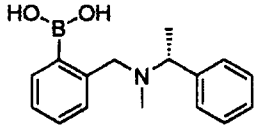

236

To a stirred suspension of 3 Å molecular sieve pellets (12 g) in THF (80 ml), was added (*R*)-(+)-*N*-α-dimethylbenzylamine **231** (1.46 ml, 10 mmol) and 2-formylbenzeneboronic acid **224** (1.50 g, 10 mmol). After 20 minutes, sodium triacetoxyborohydride (8.48 g, 40 mmol) was added and the reaction was left to proceed for 22 hours. The reaction was quenched by the addition of sat NaCl (aq.) (50 ml) and filtered immediately to remove sieves. The sieves were washed with DCM (2 x 50 ml) and combined solvents were evaporated. The mixture was then resuspended in water (100 ml) and extracted with DCM (4 x

50 ml), dried ($MgSO_4$) and solvent evaporated. Purification by solid phase extraction with Varian Mega bond elut SCX™, a pre-packed column containing silica bonded C18-*p*-benzenesulphonic acid (gradient elution, DCM to methanolic ammonia 10% (w/v)) gave principally the dimethylborate, which was not isolated. Instead the boronic acid was produced by solvent evaporation with periodic addition of water (3 x 20 ml) to the azeotrope as the volume decreased. Product was redissolved in DCM and dried ($MgSO_4$) to give *N*-methyl-*N*-((*R*)-α-methylbenzyl)benzylamine-2-boronic acid **236** as an off-white solid. (1.66 g, 62%). m.p. 87.2-90.0°C; $[\alpha]^{20}_D$ = -2.71 (*c* = 0.081 in $CHCl_3$); ^1H NMR (400 MHz, $CDCl_3$): δ = 9.15 (br, 2 H; -B(O*H*)$_2$), 7.93-7.88 (m, 1 H; *Ar*), 7.34-7.20 (m, 7 H; *Ar*), 7.10-7.05 (m, 1 H; *Ar*), 3.73 (q, *J* = 6.7, 1 H; -NC*H*(CH_3)-), 3.62 (AB q br, sep = 160, 2 H; -NCH_2-), 1.47 (d, *J* = 6.7; 3 H), (addition of D_2O caused peak at δ = 9.15 to disappear); ^{13}C NMR (100 MHz, $CDCl_3$): δ = 141.8 (*Ar*), 139.8 (*Ar*), 136.6 (*Ar*), 130.6 (*Ar*), 130.1 (*Ar*), 128.44 (*Ar*), 128.43 (*Ar*), 127.7 (*Ar*), 127.3 (*Ar*), 62.1 (CH_2), 61.2 (-C*H*(CH_3)-), 35.8 (-N(CH_3)-), 17.1 (br; -CH(CH_3)-); ^{11}B NMR (128 MHz, $CDCl_3$): δ = 30.1 (br). FTIR (thin film) *inter alia*: ν = 3271, 1441, 1371, 1145, 1032, 821, 742, 706, 654. HRMS (ES) *m/z*: calcd for $C_{16}H_{21}BNO_2$ $[M+H]^+$: 270.1660; found: 270.1662.

3.2.6 Synthesis of hydrogen *N,N*-diisopropyl-benzylamine-2-trifluoroborate 239

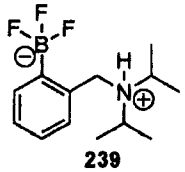

239

To a stirred solution of *N,N*-diisopropylamine-2-boronic acid **206** (0.5 g, 2.13 mmol) in methanol (5 ml) was added potassium hydrogen fluoride (0.714 g, 9.14 mmol) dissolved in a minimum amount of water. After 30 minutes, the precipitated product was removed by filtration, washed with cold methanol and dried. The resulting solid was recrystallised from acetonitrile to give

hydrogen *N,N*-diisopropyl-benzylamine-2-trifluoroborate **239** as a white solid (0.417 g, 75%). All spectroscopic and analytical details were identical to those reported in the literature.[139]

3.2.7 Synthesis of 2-bromo-*N,N*-bis-((*S*)-α-methylbenzyl)benzamide 248

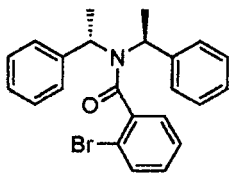

248

To (*S,S*)-(-)-bis(α-methylbenzyl)amine **209** (10 ml, 43.8 mmol) and NaOH (aq.) 5% (w/v) (70 ml, 87 mmol) in DCM (13 ml) was added 2-bromobenzoylchloride (11.47 ml, 43.8 mmol) over 10 minutes with vigorous stirring. After 12 h, DCM (50 ml) was added, the pH was adjusted to 8 with aqueous HCl (10%) and the mixture was filtered to remove starting material HCl salt. The filtrate was washed, NaOH (aq.) 5% (w/v) (4 x 25 ml), HCl (aq.) 5% (w/v) (4 x 25 ml) and sat. NaCl (aq.) (2 x 25 ml), dried ($MgSO_4$) and solvent evaporated to yield 2-bromo-*N,N*-bis-((*S*)-α-methylbenzyl)benzamide **248** as light yellow crystals (12.9 g, 72%). Dissolution of the product in DCM followed by slow evaporation produced crystals suitable for single crystal X-ray structure determination. In the solution phase (both $CDCl_3$ and D_6-DMSO) amide **248** existed as a 60:40 mixture of rotamers at room temperature. m.p. 108.5-109.5°C; $[\alpha]^{20}_D$ = -12.86 (*c* = 1.09 in $CHCl_3$); ^{1}H NMR (400MHz, $CDCl_3$): δ = 7.63 (dd, *J* = 7.7 and 4.9, 1 H; *Ar*), 7.46 – 7.18 (m, 8 H; *Ar*), 7.16 - 7.05 (m, 4 H; *Ar*), 6.95 – 6.86 (m, 1 H; *Ar*), 4.97 (q, *J* = 7.1, 0.6 H; *Bn*), 4.87 (q, *J* = 7.1, 0.4 H; *Bn*), 4.75 (q, *J* = 7.1, 0.4 H; *Bn*), 4.60 (q, *J* = 7.1, 0.6 H; *Bn*), 2.01 (d, *J* = 7.0, 1.8 H; CH_3), 1.92 (d, *J* = 7.0, 1.2 H; CH_3), 1.83 (d, *J* = 7.0, 1.2 H; CH_3), 1.65 (d, *J* = 7.0, 1.8 H; CH_3); ^{13}C NMR (100MHz, $CDCl_3$): δ = 168.2 (*C*=O), 168.4 (*C*=O), 141.3 (*Ar*), 139.9 (*Ar*), 139.6 (*Ar*), 133.3 (*Ar*), 133.2 (*Ar*), 129.8 (*Ar*), 128.7 (*Ar*), 128.5 (*Ar*), 128.2 (*Ar*), 128.1 (*Ar*), 127.9 (*Ar*), 127.5 (*Ar*), 127.1 (*Ar*), 127.0 (*Ar*), 126.5 (*Ar*), 119.3 (*Ar*), 57.7 (*Bn*), 57.6 (*Bn*), 53.9 (*Bn*),

53.7 (*Bn*), 19.4 (CH_3), 18.4 (CH_3), 18.1 (CH_3), (several ^{13}C (*Ar*) atoms and 1 ^{13}C (CH_3) atom not observed due to insufficient linear resolution); FTIR (thin film) *inter alia*: ν = 2362, 1633 (*C*=*O*), 1428, 1317, 1157, 1022, 770, 746, 695, 546; HRMS (ES) m/z: calcd for $C_{23}H_{23}BrNO$ $[M+H]^+$: 408.0958; found: 408.0959.

3.2.8 Synthesis of 3-bromo-*N*,*N*-bis-((*S*)-α-methylbenzyl)benzamide 250

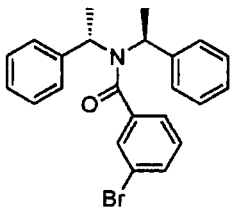

250

To (*S*,*S*)-(-)-bis(α-methylbenzyl)amine **209** (8.1 ml, 35.5 mmol) and NaOH (aq.) 10% (w/v) (15.6 ml, 39 mmol) in diethylether (10 ml) was added 3-bromobenzoylchloride (5.16 ml, 35.5 mmol) was over 30 minutes. After 12 h pH was adjusted to 8 with aqueous HCl 10% (w/v). Some amine starting material HCl salt precipitated and was collected by filtration. The filtrate was washed with NaOH (aq.) 5% (w/v) (4 x 25 ml), HCl (aq.) 5% (w/v) (4 x 25 ml) and sat. NaCl (aq.) (4 x 25 ml). The solution was then dried ($MgSO_4$) and solvents evaporated. Purification was by recrystalisation from hexane. During the cooling phase of recrystalisation, an oil separated and was discarded. 3-Bromo-*N*,*N*-bis-((*S*)-α-methylbenzyl)benzamide **250** was collected by filtration as white crystals which were suitable for single crystal X-ray structure determination (and consisted of a 50:50 mixture of amide rotamers) (12.3 g, 85%). $[\alpha]^{20}_D$ = -124.8 (*c* = 0.070 in $CHCl_3$); m.p. 86.6-86.8°C; ^1H NMR (500 MHz, $CDCl_3$): δ = 7.51 (dt, *J* = 7.7 and 1.7, 1 H; *Ar*), 7.47 (br, 1 H; *Ar*), 7.32-7.25 (m, 2 H; *Ar*), 7.21 (br, 6 H; *Ar*), 7.05 (br, 4 H; *Ar*), 4.80 (br, 2 H; *Bn*), 1.75 (br, 6 H; CH_3); ^{13}C NMR (125 MHz, $CDCl_3$): δ = 170.0 (*C*=O), 140.5 (*Ar*), 133.4 (*Ar*), 132.1 (*Ar*), 130.4 (*Ar*), 129.2 (*Ar*), 128.3 (*Ar*), 128.1 (*Ar*), 127.6 (*Ar*), 124.6 (*Ar*), 122.9 (*Ar*), 55.5 (br) (*Bn*),18.8 (CH_3); FTIR (thin film) *inter*

alia: ν = 1636 (*C*=*O*), 1429, 1314, 1204, 1162, 1069, 766, 695, 663, 598, 546; HRMS (ES) *m/z*: calcd for $C_{23}H_{22}ONBrNa$ $[M+Na]^+$: 430.0777; found: 430.0778.

3.2.9 Synthesis of hydrogen quinoline-8-trifluoroborate 254

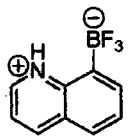

254

To quinoline-8-boronic acid (2.14 g, 12.4 mmol) in methanol (3 ml) was added potassium hydrogendifluoride (4.08 g, 49.6 mmol) dissolved in the minimal amount of distilled water. After 30 mins, solvent were evaporated. The resulting crude solid was extracted with dry acetonitrile (2 x 20 ml) and then with hot dry acetonitrile (2 x 20 ml) and filtered. The organic extracts were combined and evaporated. Recrystallisation from dry acetonitrile gave hydrogen quinoline-8-trifluoroborate **254** as white crystals (1.37 g, 99%). m.p. > 300°C; ^{1}H NMR (400 MHz, CD_3CN) δ = 8.74 (dd, *J* = 4.1 and 1.6, 1 H; *Ar*), 8.08 (dd, *J* = 8.4 and 2.0, 1 H; *Ar*), 7.82 (d, *J* = 7.2, 1 H; *Ar*), 7.60 (dd, *J* = 8.4 and 1.6, 1 H; *Ar*), 7.35 (t, *J* = 7.2, 1 H; *Ar*), 7.25 (dd, *J* = 8.0 and 4.0, 1 H; *Ar*), 2.13 (s, 1 H, N*H*); ^{11}B NMR (128.38 MHz, D_6DMSO) δ = 3.6 (br); ^{19}F NMR (282.2 MHz, CD_3CN) δ = -139.58 (q, *J* = 34.0); FTIR (thin film) *inter alia*: ν = 3241, 3040, 1571, 1495, 1249, 1162, 1083, 1069, 981, 933, 789, 606, 473; HRMS (ES) *m/z*: calcd for $C_9H_7BF_3N$ $[M-H]^-$: 196.0551; found: 196.0549.

3.2.10 Synthesis of 2-phenylpyridine 258

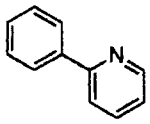

258

To stirred 2'-bromo-2-phenylpyridine (0.244 g, 1.04 mmol) in THF (10 ml) at -40°C was added dropwise a 1.63 M solution of *t*-butyllithium in pentane (1.276 ml, 2.08 mmol). After 40 minutes trimethylborate (0.236 ml, 2.08 mmol) was added rapidly and the reaction was allowed to warm to room temperature. TMSCl (0.132 ml, 1.03 mmol) was added and solvents were evaporated. Crude mixture was redissolved in DCM (5 ml) and (+/-)-2-methyl-2,4-pentanediol (0.144 ml, 1.14 mmol) was added, solvents were evaporated. Purification by silica column chromatography (petroleum ether:ethyl acetate, 4:1 as eluant) yielded 2-phenylpyridine **258** as a clear liquid (0.140 g, 87%). All spectroscopic and analytical details were identical to those reported in the literature.[174, 175]

3.2.11 Synthesis of dimethyl-[8-(diisopropyloxyborolyl)-naphthalen-1-yl]amine 271

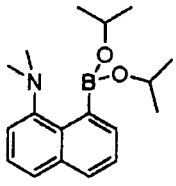

271

To a solution of *N,N*-dimethylnapthyl-1-amine **267** (10.5 ml, 0.064 mol) in diethyl ether (180 ml) was added a 1.2 M solution of *n*-butyllithium in hexanes (50.25 ml, 0.064 mol). After 125 hours the reaction mixture was cooled to -78°C and triisopropyl borate (10.18 ml, 0.071 mol) was added as rapidly as possible without raising the reaction temperature above -70°C. After 1 hour at -78°C the reaction was allowed to warm to room temperature over 3 hours.

The mixture was then filtered and rinsed through with diethyl ether (2 x 50 ml). The solvent was evaporated to yield the crude borate. This was then distilled by Kugelröhr (135°C, 0.7 mmHg) to produce dimethyl-[8-(diisopropyl oxyborolyl)-naphthalen-1-yl]amine **271** as a colourless liquid (12.8 g, 48%). b.p. 135°C, 0.7 mmHg; ^{1}H NMR (300 MHz, $CDCl_3$): δ = 7.76 (d, *J* = 7.8, 1 H; *Ar*), 7.67 (d, *J* = 8.1, 1 H; *Ar*), 7.40-7.58 (m, 3 H; *Ar*), 7.33 (d, *J* = 7.2 Hz, 1H; *Ar*), 4.07 (sept, *J* = 6, 2 H; -OC*H*(CH_3)$_2$), 2.73 (s, 6 H; -N(CH_3)$_2$), 1.21 (d, *J* = 6, 6 H; -OCH(C*H*$_3$)(CH_3)), 1.14 (d, *J* = 6, 6 H; -OCH(CH_3)(C*H*$_3$)); ^{13}C NMR (75 MHz, $CDCl_3$): δ = 152.0 (*Ar*), 134.6 (*Ar*) 133.8 (*Ar*), 129.8 (*Ar*), 126.9 (*Ar*), 126.8 (*Ar*), 125.8 (*Ar*), 125.7 (*Ar*), 116.5 (*Ar*), 65.2 (-OCH(CH_3)$_2$), 47.8 (-N(CH_3)$_2$), 25.4 (-OCH(C*H*$_3$)(CH_3), 25.2 (-OCH(CH_3)(C*H*$_3$); ^{11}B NMR (128.4 MHz, MeCN) δ = 18 (br); FTIR (thin film) *inter alia*: ν = 1455, 1170 (s, C-O), 1150, 1120, 1050, 971, 890, 750; HRMS (ES) m/z: calcd for $C_{18}H_{28}BNO_2$ $[M+H]^+$: 301.1988; found: 301.1986;

3.2.12 Synthesis of 1,3,5-tris(1-*N*,*N*-dimethylamino)-8-naphthylboroxine 270

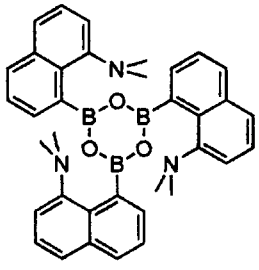

270

To *N*,*N*-dimethylnapthyl-1-amine **267** (24.5 ml, 0.149 mol) in diethyl ether (450 ml) was added a 2.5 M solution of *n*-butyllithium in hexanes (59.6 ml, 0.149 mol). After 125 hours the reaction mixture was cooled to -78°C and trimethylborate (50 ml 0.48 mol) was added as rapidly as possible without raising the temperature of the reaction above -70°C. After 1 hour at -78°C the reaction was allowed to warm to room temperature over 3 hours. NaOH (aq.) 5% (w/v) (400 ml) was added to the reaction. After 30 minutes the white precipitate was collected by filtration, washed, diethyl ether (2 x 100 ml) and

5% (w/v) NaOH (2 x 50 ml). Solvent was evaporated to yield 1,3,5-tris(1-*N*,*N*-dimethylamino)-8-naphthylboroxine **270** as a white powder (20.14 g, 69%). m.p. > 280°C; ^{1}H NMR (300 MHz, $CDCl_3$): δ = 7.81 (d, *J* = 6.3, 1 H; *Ar*), 7.70-7.54 (m, 3 H; *Ar*), 7.37 (dd, *J* = 8.1 and 8.1, 1 H; *Ar*), 7.25 (dd, *J* = 7.5 and 0.9, 1 H; *Ar*), 2.91 (s, 6 H; -N(CH_3)$_2$); ^{13}C NMR (100 MHz, CD_3CN): δ = 149.9 (*Ar*), 133.6 (*Ar*), 131.8 (*Ar*), 126.6 (*Ar*), 126.4 (*Ar*), 125.1 (*Ar*), 124.24 (*Ar*), 124.15 (*Ar*), 115.2 (*Ar*), 45.3 (-N(CH_3)$_2$); ^{11}B (96 MHz, $CDCl_3$): δ = 19 (br); FTIR (thin film) *inter alia*: ν = 1452, 1254, 1204, 1116, 1056, 828, 780 (s), 760, 665; HRMS (ES) *m/z*: calcd for $C_{36}H_{37}B_3N_3O_3$ $[M+H]^+$: 592.3114; found: 592.3101.

In order to obtain single crystals of 1,3,5-tris-(1-*N*,*N*-dimethylamino)-8-naphthylboroxine an alternative procedure was followed. Over a solution of *N*,*N*-dimethylnaphthyl-1-aminediisopropylborate **271** (1.0 g, 3.34 mmol) in diethylether (9 ml) was floated water (10 ml). The mixture was left to stand for 48 hours and colourless crystals were formed at the biphasic interface, which were identical to boroxine **270** (0.59 g, 90%) and were suitable for X-ray analysis.

3.2.13 Synthesis of dimethyl-[8-(4,4,5,5-tetramethyl-[1,3,2]dioxaborolan-2-yl)-amine 272

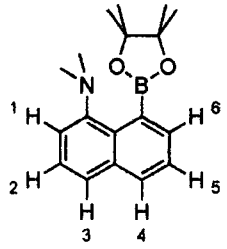

272

A mixture of boroxine **270** (1.01 g, 1.69 mmol), pinacol (0.66 g, 5.07 mmol), *para*-toluenesulfonic acid (0.66 g, 3.4 mmol), ethyl acetate (100 ml) and water (100 ml) was vigorously stirred for 3 days. The organic layer was separated, the water layer re-extracted with diethyl ether (4 x 100 ml), the combined organic extracts partially evaporated, the resulting solution absorbed on to

silica gel (~2 g) and the remaining solvent evaporated. The resulting solid was added to a silica gel column and the product was eluted (hexane: ethyl acetate, 4: 1 as eluant) to yield white crystals of dimethyl-[8-(4,4,5,5-tetramethyl-[1,3,2]dioxaborolan-2-yl)-amine **272** (0.908 g, 60%) which were suitable for single crystal X-ray structure determination. m.p. 77.4-78.2°C; ^{1}H NMR (500 MHz, $CDCl_3$): δ = 7.75 (d, *J* = 8.5, 1 H; *H*^{4}), 7.69 (d, *J* = 8.0, 1 H; *H*^{3}), 7.65 (d, *J* = 6.5, 1 H; *H*^{6}), 7.56 (dd, *J* = 8.5 and 6.5, 1 H; *H*^{5}), 7.45 (dd, *J* = 8.0 and 7.5, 1 H; *H*^{2}), 7.33 (d, *J* = 7.5, 1 H; *H*^{1}), 2.86 (s, 6 H; -N(CH_3)$_2$), 1.43 (s, 12 H; -C(CH_3)$_2$); ^{13}C NMR (125.7 MHz, $CDCl_3$): δ = 150.4 (*Ar*), 134.7 (*Ar*), 132.7 (*Ar*), 129.1 (*Ar*), 128.3 (*Ar*), 125.95 (*Ar*), 125.77 (*Ar*), 125.75 (*Ar*), 115.0 (*Ar*), 81.7 (-O*C*(CH_3)$_2$-), 47.8 (-N(*C*H$_3$)$_2$), 26.6 (-OC(*C*H$_3$)$_2$-); ^{11}B NMR (96 MHz, $CDCl_3$): δ = 22 (br); FTIR (thin film) *inter alia*: ν = 1460, 1181 (s), 1149, 1122, 1051, 971, 884, 821, 773 (s); MS (ES, MeCN): *m/z* (%): 297.3 (100) [M+H]$^+$; Elemental analysis: calcd for $C_{18}H_{24}BNO_2$: C 72.74, H 8.14, N 4.71; found C 72.93, H 8.24, N 4.53.

3.2.14 Synthesis of *N,N*-dimethyl-[8-(difluoroborolyl)-naphthalen-1-yl]-amine 273

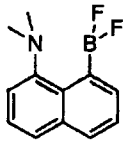

273

1,3,5-Tris-(1-*N,N*-dimethylamino)-8-naphthylboroxine **270** (1.0 g, 1.69 mmol) was dissolved in THF (450 ml) in an 1 L glass flask, potassium hydrogen difluoride (1.58 g, 20.2 mmol) dissolved in water (50 ml) was added and the reaction was heated at reflux for 5 hours. Solvents were evaporated and the product was extracted from the crude with chloroform (2 x 50 ml), followed by filtration through a very fine glass sinter. Evaporation gave *N,N*-dimethyl-[8-(difluoroborolyl)-naphthalen-1-yl]-amine **273** as light red-brown solid (0.58 g, 52%). m.p. 137.9-138.3°C; ^{1}H NMR (400 MHz, $CDCl_3$): δ = 7.76 – 7.85 (m, 3 H; *Ar*), 7.67 (dt, *J* = 8.4 and 1.6, 1 H; *Ar*), 7.53 (dt, *J* = 7.6 and 0.6, 1 H; *Ar*),

7.36 (dd, *J* = 7.6 and 1.6, 1 H; *Ar*), 2.95 (s, 6 H; -N(CH_3)$_2$); ^{13}C NMR (125.7 MHz, $CDCl_3$): δ = 148.4 (*Ar*), 134.2 (*Ar*), 131.7 (*Ar*), 129.3 (*Ar*), 127.5 (*Ar*), 126.5 (*Ar*), 125.8 (*Ar*), 125.2 (*Ar*), 112.8 (*Ar*), 48.1 (-N(CH_3)$_2$); ^{11}B NMR (128 MHz, $CDCl_3$): δ = 9.82 (br t, *J* = 58 Hz); ^{19}F NMR (470.26 MHz, $CDCl_3$) δ = -148.3 (unsymmetric q, *J* = 58 Hz); FTIR (nujol) *inter alia*: ν = 2922 (s), 1126, 1080, 780, 699; MS (ES, MeCN): *m/z* (%): 243.1 (100) [MNa]$^+$; Elemental analysis: calcd for $C_{12}H_{12}BF_2N$: C 65.80, H 5.52, N 6.39; found C, 65.55, H 5.59, N 6.23.

3.2.15 Synthesis of 3-(4,4,5,5-tetramethyl-[1,3,2]dioxaborolan-2-yl)-phenylamine 280

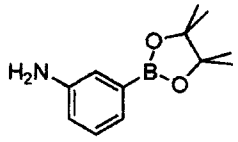

280

Aniline-3-boronic acid (1.00 g, 6.45 mmol) and pinacol (0.763 g, 6.45 mmol) were added to ethyl acetate (150 ml). After 20 hours the solution was dried ($MgSO_4$), filtered and evaporated to yield a brown solid, which was dissolved in a minimal amount of ethyl acetate and absorbed onto silica gel. Purification by silica gel chromatography (hexane:ethyl acetate, 1:1 as eluant) gave an orange oil which crystallised on standing for 48 hours to give large orange crystals of 3-(4,4,5,5-tetramethyl-[1,3,2]dioxaborolan-2-yl)-phenylamine **280** (1.31 g, 93%) which were suitable for single crystal X-ray structure determination. m.p. 90.0°C (lit. 93°C)[222]; Elemental analysis: calcd for $C_{12}H_{19}BNO_2$: C 65.70, H 8.28, N 6.39; found: C 65.77, H 8.31, N 6.31. All other spectroscopic and analytical details were identical to those reported in the literature.[222]

3.2.16 Synthesis of hydrogen 3-aminobenzenetrifluoroborate 281

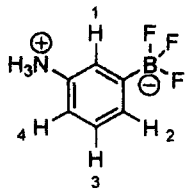

281

To a stirred solution of 3-aminobenzeneboronic acid (1.00 g, 6.45 mmol) in methanol (12 ml) was added potassium hydrogendifluoride (1.66g, 21.28 mmol) dissolved in minimal water. After 30 minutes solvents were evaporated (including 36 hours under high vacuum) and the product extracted with dry acetonitrile (2 x 20 ml) and hot, dry acetonitrile (2 x 20 ml). The organic extracts were combined, filtered and the solvent evaporated to yield hydrogen 3-aminobenzenetrifluoroborate **281** as amorphous brown solid (1.31 g, 80%). Decomposition at 171°C; ^{1}H NMR (400MHz, D_6-DMSO): δ = 6.78 (br dd, J = 7.3 and 7.3, 1 H; H^3), 6.67 (br s, 1 H; H^1), 6.61 (br d, J = 7.3, 1 H; H^2), 6.32 (dq, J = 7.3 and 1.1, 1 H; H^4), 4.94 (br, 2 H; -NH_2), 3.36 (br, 1 H; [D_6DMSO-H]$^+$); (addition of D_2O caused the peak at δ = 4.94 to disappear); ^{13}C NMR (100MHz, D_6-DMSO): δ = 145.0 (*Ar*), 126.5 (*Ar*), 120.9 (*Ar*), 118.8 (*Ar*), 111.8 (*Ar*); ^{11}B NMR (160 MHz, D_6-DMSO): δ = 3 (br); ^{19}F (188 MHz, D_6-DMSO): δ = -139.15 (br); FTIR (thin film) *inter alia*: ν = 1578, 1434, 1271, 1182, 931, 789, 706, 600, 470; HRMS (ES) *m/z*: calcd for $C_6H_6BF_3N$ [M-H]$^-$: 160.0551; found: 160.0552.

3.3 Complexation studies of fluorinated boron Lewis acids

3.3.1 Synthesis of potassium *o*-nitrobenzenetrifluoroborate 290

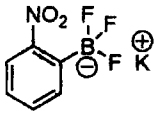

290

To a stirred solution of *o*-nitrobenzeneboronic acid (1.00 g, 6 mmol) in methanol (3 ml) was added potassium hydrogen difluoride (1.876g, 0.024 mol) dissolved in minimal distilled water. A precipitate was immediately observed. Solvents were evaporated. Product was extracted from the crude solid with dry acetonitrile (2 x 20 ml) and hot dry acetonitrile (2 x 20 ml) and filtered. Solvent was evaporated and the crude product recrystalised from acetonitrile to yield potassium *o*-nitrobenzenetrifluoroborate **290** (1.37 g, 100%) as light orange crystals which were suitable for single crystal X-ray structure determination. m.p. > 250°C; ^{1}H NMR (300 MHz, CD_3CN): δ = 7.66 (br d, *J* = 6.3, 1 H; *Ar*), 7.48-7.39 (m, 2 H; *Ar*), 7.28 (dt, *J* = 1.5 and 6.9, 1H; *Ar*); ^{13}C NMR (125 MHz, CD_3CN): δ = 135.21 (*Ar*), 135.18 (*Ar*), 131.2 (*Ar*), 127.6 (*Ar*), 122.2 (*Ar*); ^{19}F NMR (376 MHz, CD_3CN): δ = -141.68 (q, *J* = 48);^{11}B NMR (96 MHz, CD_3CN): δ = 2.33 (q, *J* = 48); FTIR (thin film) *inter alia*: ν = 1522 (s, NO_2), 1344 (s, NO_2), 1300, 1168, 970, 940, 730, 607; MS (ES, MeCN): *m/z* (%): 190.2 (100) $[M]^-$; HRMS (ES) *m/z*: calcd for $C_6H_4BF_3K_2NO_2$ $[M+K]^+$: 267.9556; found: 267.9558.

3.3.2 Representative procedure for NMR shift experiments

D_3-acetonitrile solvent for NMR studies was dried by filtration through activated 3Å molecular sieve pellets onto activated 3Å molecular sieve pellets. Measurement of liquids was by volumetric pipette from an argon-flushed container.

In a dry NMR tube under argon Lewis acid **298** (0.4 ml of a 0.37M solution) was added alongside equimolar substrate **160**, **291**, **26**, **292**, **293**, **294**, **295** or **296** (0.148 mmol). The tube was then shaken for 20 seconds and the NMR spectra (^{11}B, ^{19}F, ^{1}H, ^{1}H-cosy, ^{13}C, ^{13}C-DEPT 135) were recorded. Reference spectra of all substrates and Lewis acids were recorded individually at the same concentration.

3.4 Catalyst *vs* Reaction screening

3.4.1 Microdart operation

All experiments were undertaken on a Gilson SK-233 Microdart liquid handling workstation controlled by Reactarray software, equipped with 96 position heating block. The reaction vessels were 2 ml HPLC vials. In the water-free reaction screens, the vials were dried in a desiccator for 3 days over P_2O_5 *in vacuo*, complete with stirring bars and crimpable lids. Vials and lids were flushed with nitrogen and removed to an Atmosbag™ (disposable glove box filled with nitrogen), and sealed. Reagents were stored under argon and were introduced by syringe through Teflon-rubber septa. Reactions were stirred. HPLC-UV analysis was obtained on an Agilent 1100 HPLC apparatus. Solvents were degassed by integrated Teflon membrane vacuum degasser. Column was held at a constant 40°C by the integrated column heater. UV detection was provided by a Waters 996 Photodiode array UV detector, set to record absorbance over a wavelength range of 211-212 nm. The HPLC-UV apparatus was controlled by Millenium32 software.

To THF (0.75 ml) or THF: H2O, 80: 20 in a 2 ml vial was added nucleophile **38**, **304**, **295**, **305**, **160** or **306** (1 mmol) and electrophile **160**, **26**, **293** or **307** In the case where reagent was a solid a THF solution was added and the solvent was reduced accordingly. A 1 M solution of catalyst or standard **270**, **279**, **253**, **308**, **309**, **310**, (**308** and **309**) or THF (0.1 ml, 0.1 mmol w.r.t. B) was then added. After 1 hour and 12 hours, 100 μl aliquots were removed from each reaction to an analytical vial to which acetonitrile (900 μl) was added. The solution was mixed (by aspiration and dispensing from needle) and serially diluted in two stages down to 1/1000 the reaction concentration. (A sample (100 μl) was taken from the first analytical vial, transferred to second, mixed with acetonitrile (900 μl), a sample (100 μl) was taken from the second vial and the process was repeated) Diluted samples were transferred to an HPLC machine for analysis.

HPLC method was gradient elution, (injection volume 20 μl, total loop fill, 5 x multiplier, gradient elution; 100% water/TFA 0.05% (v/v) to 100% MeCN/TFA 0.05% (v/v), 1 $mlmin^{-1}$, over 8 mins followed by 2 minutes equilibration at 100% water/TFA 0.05% (v/v), prior to next injection) on a Phenomenex Luna™ C18 (2) column (50 mm x 2 mm particle size 3 μ) without a guard cartridge. Peak area data was exported to a spreadsheet and processed manually.

3.5 Direct amide bond formation

3.5.1 Synthesis of *N*-methylbenzylamine benzoate 333

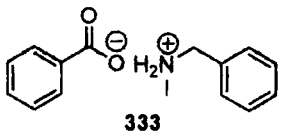

333

To benzoic acid **307** (122 mg, 1 mmol) in diethyl ether (50 ml) was added *N*-methylbenzylamine **305** (121 mg, 1 mmol) and solvents evaporated to give *N*-methylbenzylamine benzoate **333** as a white solid (243 mg, 100%). m.p. 79.2-80°C; ^{1}H NMR (400 MHz, $CDCl_3$): δ = 9.30 (br, 2 H; -N*H*$_2$(CH$_3$)), 7.93 (dt, *J* = 6.9 and 1.5, 2 H; *Ar*), 7.38-7.34 (m, 3 H; *Ar*), 7.30 (tt, *J* = 7.1 and 1.6, 2 H, *Ar*), 7.24-7.20 (m, 3 H; *Ar*), 4.43 (s, 3 H; C*H*$_3$), 3.93 (s, 2 H; *Bn*), (addition of D_2O caused the peak at δ = 9.30 to disappear); ^{13}C NMR (100 MHz, $CDCl_3$): δ = 173.0 (*C*=O), 136.2 (*Ar*), 132.6 (*Ar*), 130.8; *Ar*), 129.8 (*Ar*), 129.4 (*Ar*), 128.9 (*Ar*), 128.7 (*Ar*), 127.8 (*Ar*), 52.7 (*C*H$_2$), 32.0 (*C*H$_3$); FTIR (thin film) *inter alia*: ν = 3305, 2590 (br), 1627, 1534, 1372, 826, 710, 700, 671; Elemental analysis: calcd for $C_{17}H_{19}NO$: C 74.05, H 7.04, N 5.76; found C 74.04, H 7.07, N 5.77.

3.5.2 Representative procedures – Amide bond forming experiments

Decribed below are the methods used to access amides during the course of this project.

Method A: To toluene (40 ml) was added *N,N*-diisopropylbenzylamine-2-boronic acid **206** (23.5 mg, 0.1 mmol), carboxylic acid (10 mmol) and amine (9 mmol). The mixture was heated at reflux for 20 hours, allowed to cool and solvents evaporated. Crude was dissolved in DCM (200 ml) and washed with HCl (aq.) 5% (w/v) (2 x 100 ml), sat. NaCl (aq.) (100 ml), NaOH (aq.) 5% (w/v)

(2 x 100 ml), sat. NaCl (aq.) (100 ml), dried ($MgSO_4$) and solvents evaporated to give amide.

Method B: As method A, except with Sohxlet dehydration of the condensate stream, with CaH_2 as dessicant.

Method C: As method A, except with Sohxlet dehydration of the condensate stream, activated 3 Å molecular sieves pellets as dessicant.

Method D: As method A, except activated 3 Å molecular sieves pellets (12 g) were added at start of reaction.

Other relative molarities and solvents were investigated during optimisation using **332** as model.

3.5.2.1 Synthesis of *N*-benzyl-4-phenylbutyramide 332

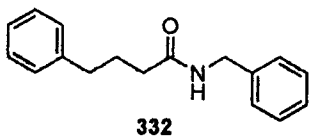

332

Method A (2.91 g, 91%). All spectroscopic and analytical details were identical to those reported in the literature.[209]

3.5.2.2 Synthesis of *N*-4-phenylbutylbenzamide 341

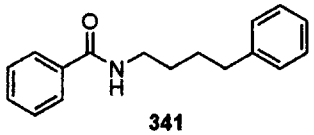

341

Method C, 3.27 mmol scale, (116 mg, 14%). m.p. 73.8-80°C; ^{1}H NMR (400 MHz, $CDCl_3$): δ = 7.67 (t, *J* = 1.3, 1 H; *Ar*), 7.66 (t, *J* = 1.5, 1 H; *Ar*), 7.42 (tt, *J*

= 7.4 and 2.4, 1 H; *Ar*), 7.34 (tt, *J* = 7.4 and 2.4, 2 H; *Ar*), 7.24-7.18 (m, 2 H; *Ar*), 7.14-7.08 (m, 3 H; *Ar*), 6.05, (br, 1 H; N*H*), 3.40 (dt, *J* = 6.0 and 7.0, 2 H; CH_2), 2.59 (t, *J* = 7.4, 2 H; CH_2),1.70-1.45 (m, 4 H; CH_2), (addition of D_2O caused the peak at δ = 6.05 to disappear); ^{13}C NMR (75 MHz, $CDCl_3$): 167.8 (*C*=O), 142.3 (*Ar*), 135.0 (*Ar*), 131.6 (*Ar*), 130.1 (*Ar*), 128.78 (*Ar*), 128.65 (*Ar*), 128.60 (*Ar*), 127.1 (*Ar*), 126.1 (*Ar*), 40.1 (CH_2), 35.7 (CH_2), 29.5 (CH_2), 29.0 (CH_2); FTIR (thin film) *inter alia*: ν = 3302, 2935, 2861, 2360, 2340, 1636 (s, *C*=*O*), 1540, 1452, 1371, 741, 694; HRMS (ES) *m/z*: calcd for $C_{17}H_{20}NO$ $[M+H]^+$: 254.1539; found: 254.1537; Elemental analysis: calcd for $C_{17}H_{19}NO$: C 80.60, H 7.56, N 5.53; found C 79.92, H 7.49, N 5.27.

3.5.2.3 Synthesis of *N*-4-phenylbutyl-4-phenylbutyramide 342

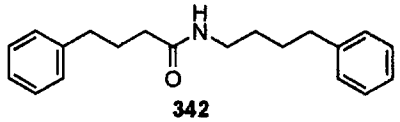

342

Method C, 3.27 mmol scale, (0.85 g, 88%). m.p. 57.1-60.4°C; ^1H NMR (400 MHz, $CDCl_3$): δ = 7.23-7.17 (m, 4 H; *Ar*), 7.14-7.05 (m, 6 H; *Ar*), 5.35 (br, 1 H; N*H*), 3.18 (dt, *J* = 5.9 and 7.0, 2 H; CH_2), 2.60-2.52 (m, 4 H; CH_2), 2.07 (t, *J* = 7.3, 2 H; CH_2), 1.94-1.84 (m, 2 H; CH_2), 1.62-1.51 (m, 2 H; CH_2), 1.49-1.39 (m, 2 H; CH_2), (addition of D_2O caused the peak at δ = 5.35 to disappear); ^{13}C NMR (100 MHz, $CDCl_3$): δ = 172.6 (*C*=O), 142.1 (*Ar*), 141.5 (*Ar*), 128.49 (*Ar*), 128.39 (*Ar*), 128.35 (*Ar*), 126.0 (*Ar*), 125.8 (*Ar*), 39.3 (CH_2), 35.9 (CH_2), 35.5 (CH_2), 35.2 (CH_2), 29.2 (CH_2), 28.6 (CH_2), 27.1 (CH_2), (1 C (*Ar*) not observed due to insufficient linear resolution); FTIR (thin film) *inter alia*: ν = 3305 (*N-H*), 2932, 2857, 2349, 1636 (s, *C*=*O*), 1537 (s, *N-H*), 1453, 1371, 741, 694; HRMS (ES) m/z: calcd for $C_{20}H_{26}NO$ $[M+H]^+$: 296.2009; found: 296.2008; Elemental analysis: calcd for $C_{20}H_{25}NO$: C 81.31, H 8.53, N 4.74; found C 81.09, H 8.56, N 4.70.

3.5.2.4 Synthesis of *N*-morpholinobenzamide 343

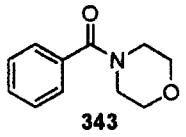

343

Method C, 3.27 mmol scale, (75 mg, 12%). All spectroscopic and analytical details were identical to those reported in the literature.[223, 224]

3.5.2.5 Synthesis of *N*-morpholino-4-phenylbutyramide 344

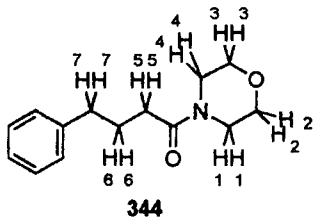

344

Method D, (0.59 g, 28%). b.p. 72°C; ^{1}H NMR (400 MHz, $CDCl_3$): δ = 7.31-7.25 (m, 2 H; *Ar*), 7.22-7.16 (m, 3 H; *Ar*), 3.62 (br s, 6 H; H^2 and H^3), 3.36 (br s, 2 H; H^1), 2.68 (t, *J* = 7.4, 2 H^7), 2.30 (t, *J* = 7.5, 2 H^5); 1.98 (tt, *J* = 7.4 and 7.5; H^6); ^{13}C NMR (100 MHz, $CDCl_3$): δ = 171.4 (*C*=O), 141.57 (*Ar*), 128.47, (*Ar*), 128.38 (*Ar*), 126.0 (*Ar*), 66.88 (-*C*H_2O-), 66.61 (-*C*H_2O-), 45.9 (-N*C*H_2-), 41.9 (-N*C*H_2-), 35.2 (*C*H_2), 32.1 (*C*H_2), 26.7 (*C*H_2); FTIR (thin film) *inter alia*: ν = 2914, 2854, 2361, 2338, 1637 (s, *C*=*O*), 1430, 1232, 1113, 1024, 848, 747, 700, 560; HRMS (ES) *m/z*: calcd for $C_{14}H_{19}NO_2$ $[M+H]^+$: 234.1489, found; 234.1487.

3.5.2.6 Synthesis of *N*-benzylbenzamide 328

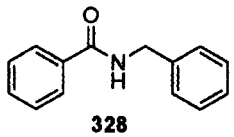

328

Method D, (0.32 g, 17%). All spectroscopic and analytical details were identical to those reported in the literature.[225]

3.5.2.7 Synthesis of *N*-morpholinotrimethylacetamide 376

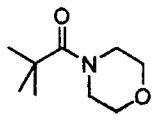

376

Method D, (92 mg, 6%). All spectroscopic and analytical details were identical to those reported in the literature.[226]

3.5.2.8 Synthesis of *N*-benzyltrimethylacetamide 377

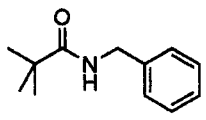

377

Method D, (0.26 g, 15%). All spectroscopic and analytical details were identical to those reported in the literature.[225]

3.5.3 Direct amide bond formation – Kinetics experiments

All experiments were undertaken on a Gilson 215SW liquid handling workstation equipped with 10 place heating block with on-line HPLC analysis and controlled using Gilson 735 software. HPLC system consisted of a Phenomenex or Degassex Teflon membrane vacuum degasser followed by a Gilson 322 pump connected to a Gilson 819 injection module connected via the column to an Agilent 1100 series diode array detector with a back pressure regulator placed after the detector and before the waste bottle. Post injector piping was ultra low volume PEEK and was used in minimal quantity to reduce system dead volume. The HPLC system was controlled by Gilson Unipoint software vers. 5.11 through a Gilson GSIOC server.

3.5.3.1 Representitive procedure – Amide bond forming kinetics experiments

Reaction tubes was charged with catalyst **206**, **334**, **339**, **323** (0.0375 mmol) or no catalyst and assembled under micro Soxhlet apparatus loaded with activated 3Å molecular sieves. Benzylamine **327** (0.385 ml, 3.27 mmol) and toluene (5.625 ml) were added and the mixture heated to 120°C under reflux and argon. A 2 M solution of carboxylic acid acid **320** in toluene (1.875 ml, 3.75 mmol) was added and immediately a sample (100 µl) of the reaction mixture was taken. Further samples were taken once every 2 hours up until 22 hours. Immediately a sample was removed from the reaction, the reaction was quenched by the addition of room teparature MeCN (900 µl), mixed, and further diluted serially in 2 x 10 fold dilution steps (total 1000 fold dilution). The 1000 fold diluted sample was then analysed using on-line HPLC-UV.

An analysis wavelength of 210 nm was found to be efficacious for all acids and amides studied. Amines were generally not readily observed by reverse phase HPLC as they tended to elute on the injection peak. Elution was provided by one or both of methods A and B (Scheme 27).

A) Isocratic elution, (injection volume 20 μl, total loop fill, 5 x multiplier, 70: 30, MeCN/TFA 0.05% (v/v): water/TFA 0.05% (v/v), 1 $mlmin^{-1}$, 10 mins) on a Phenomenex Gemini™ C-18 column (150 mm x 4.60 mm, particle size 5 μm) guarded by a single 0.5 mm cartridge of the same material as the column.

B) Gradient elution, (injection volume 20 μl, total loop fill, 5 x multiplier, analysis: 100% water/TFA 0.05% (v/v) to 100% MeCN/TFA 0.05% (v/v), 1 $mlmin^{-1}$, 15 mins; reequilbration of column: 100% MeCN/TFA 0.05% (v/v) to 100% water/TFA 0.05% (v/v), 1 $mlmin^{-1}$, 2 mins, followed by 100% water/TFA 0.05% (v/v), 1 $mlmin^{-1}$, 2 mins, on a Phenomenex Gemini™ C-18 column (150 mm x 4.60 mm, particle size 5 μm) guarded by a single 0.5 mm cartridge of the same material as the column.

Entry	Amide formed	Elution method(s) used
1	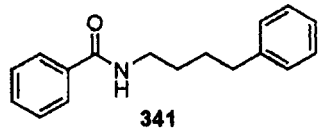 **341**	A and B
2	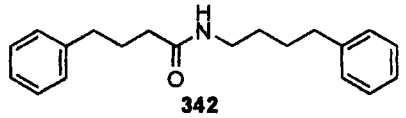 **342**	B
3	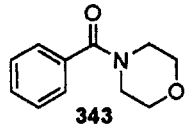 **343**	B
4	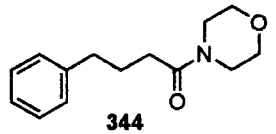 **344**	B
5	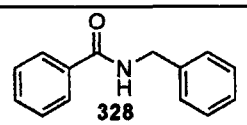 **328**	B
6	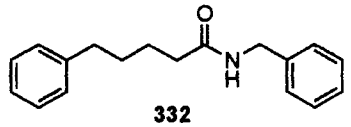 **332**	B

Table 27: Elution methods for amide bond kinetics experiments with dehydration.

Calibration of HPLC-UV response was achieved using external calibration curves and checked by normalisation of starting material consumption against product formation.

Four or more (typically six) solutions of analyte acid and analyte amide with graduated concentrations covering the concentration range of the amide bond forming experiment in question were produced. Samples were analysed by the same method as used in the original acquisition and the results plotted to give a calibration curve against which the samples could be calibrated.

Peak area data was extracted using Unipoint peak recognition software and data was exported to Excel spreadsheet software for analysis. Grosjean collaborated in this work to apply calculations within Micromath Scientist™ to extract the kinetics data from suitable reactions.[211]

All data produced as well as calibration curve data is provided in appendix B.

3.5.4 Deboronation studies

To an NMR tube was added 0.66 M solution of 4-phenylbutyric acid in D_8-toluene (0.75 ml, 0.5 mmol) and catalyst **206**, **334**, **323**, boric acid **339** (0.05 mmol) or no catalyst. NMR spectra, ^{1}H, ^{13}C, ^{11}B and ^{11}B - ^{1}H decoupled were acquired post mixing and after the samples had been heated at 115°C for 1 hour and 18 hours. After analysis the 18 hour samples were exposed to a D_2O shake and reanalysed by NMR, ^{1}H, ^{13}C, ^{11}B and ^{11}B-^{1}H decoupled.

3.5.5 Initiation temperature determination

Reaction tubes was charged with catalyst (0.0375 mmol) and assembled under reflux apparatus. Benzylamine (0.385 ml, 3.27 mmol) and toluene (5.625 ml) were added and the mixture heated to 84°C under reflux and argon. A 2 M solution of acid in toluene (1.875 ml, 3.75 mmol) was added. After 24 hours a sample (100 μl) of the reaction mixture was taken. Immediately a sample was removed from the reaction, the reaction was quenched by the addition of room temperature MeCN (900 μl), mixed, and further diluted sequentially in 2 x 10 fold dilution steps (total 1000 fold dilution). The 1000 fold diluted sample was then analysed using on-line HPLC-UV. The temperature was increased by 6°C and the, wait 24 hours, sample, quench, dilute, increase temperature was repeated 7 times.

The experiment was repeated with modifications. The starting temperature was 24°C and the incremental temperature increase was 10°C.

HPLC conditions were as follows: Analysis wavelength, 210 nm: Gradient elution, (injection volume 20 μl, total loop fill, 5 x multiplier, analysis: 100% H_2O/TFA 0.05% (v/v) to 100% MeCN/TFA 0.05% (v/v), 1 $mlmin^{-1}$, 20 mins; reequilibration of column: 100% H_2O/TFA 0.05% (v/v), 1 $mlmin^{-1}$, 2 mins) on a Phenomenex Luna™ C-18(2) column (150 mm x 4.60 mm, particle size 3 μm) guarded by a single 0.5 mm cartridge of the same material as the column.

4 References

[1] S. Takayama, G. J. McGarvey, C. H. Wong, *Chem. Soc. Rev.* **1997**, *26*, 407.

[2] H. Tye, P. J. Comina, *J. Chem. Soc. Perkin Trans. 1.* **2001**, 1729.

[3] H. Tye, *J. Chem. Soc. Perkin Trans. 1.* **2000**, 275.

[4] G. J. Rowlands, *Tetrahedron.* **2001**, *57*, 1865.

[5] J. A. Ma, D. Cahard, *Angew. Chem. Int. Ed.* **2004**, *43*, 4566.

[6] P. I. Dalko, L. Moisan, *Angew. Chem. Int. Ed.* **2001**, *40*, 3726.

[7] B. List, *Synlett.* **2001**, 1675.

[8] L. Liu, R. Breslow, *Bioorg. Med. Chem.* **2004**, *12*, 3277.

[9] L. Liu, R. Breslow, *J. Am. Chem. Soc.* **2002**, *124*, 4978.

[10] J. M. Yan, R. Breslow, *Tetrahedron Lett.* **2000**, *41*, 2059.

[11] M. Shibasaki, N. Yoshikawa, *Chem. Rev.* **2002**, *102*, 2187.

[12] M. Shibasaki, H. Sasai, T. Arai, *Angew. Chem. Int. Ed.* **1997**, *36*, 1237.

[13] E. K. van den Beuken, B. L. Feringa, *Tetrahedron.* **1998**, *54*, 12985.

[14] A. C. Spivey, D. P. Leese, F. Zhu, S. G. Davey, R. L. Jarvest, *Tetrahedron.* **2004**, *60*, 4513.

[15] A. de Maijere, F. E. Meyer, *Angew. Chem. Int. Ed.* **1994**, *33*, 2379.

[16] E. J. Corey, C. J. Helal, *Angew. Chem. Int. Ed.* **1998**, *37*, 1987.

[17] E. J. Corey, *Pure Appl. Chem.* **1990**, *62*, 1209.

[18] E. J. Corey, S. Shibata, R. K. Bakshi, *J. Org. Chem.* **1988**, *53*, 2861.

[19] E. J. Corey, R. K. Bakshi, S. Shibata, C. P. Chen, V. K. Singh, *J. Am. Chem. Soc.* **1987**, *109*, 7925.

[20] E. J. Corey, R. K. Bakshi, S. Shibata, *J. Am. Chem. Soc.* **1987**, *109*, 5551.

[21] S. Itsuno, K. Ito, A. Hirao, S. Nakahama, *Chem. Commun.* **1983**, 469.

[22] A. Hirao, S. Itsuno, S. Nakahama, N. Yamazaki, *Chem. Commun.* **1981**, 315.

[23] M. P. Sibi, G. R. Cook, P. R. Liu, *Tetrahedron Lett.* **1999**, *40*, 2477.

[24] M. P. Gamble, J. R. Studley, M. Wills, *Tetrahedron Lett.* **1996**, *37*, 2853.

[25] A. Hayes, G. Clarkson, M. Wills, *Tetrahedron Asymmetry.* **2004**, *15*, 2079.

[26] M. P. Gamble, A. R. C. Smith, M. Wills, *J. Org. Chem.* **1998**, *63*, 6068.

[27] B. Burns, N. P. King, H. Tye, J. R. Studley, M. Gamble, M. Wills, *J. Chem. Soc. Perkin Trans. 1.* **1998**, 1027.

[28] M. Kitamura, S. Suga, K. Kawai, R. Noyori, *J. Am. Chem. Soc.* **1986**, *108*, 6071.

[29] L. Pu, H. B. Yu, *Chem. Rev.* **2001**, *101*, 757.

[30] M. Yamakawa, R. Noyori, *J. Am. Chem. Soc.* **1995**, *117*, 6327.

[31] B. Goldfuss, K. N. Houk, *J. Org. Chem.* **1998**, *63*, 8998.

[32] M. Yamakawa, R. Noyori, *Organometallics.* **1999**, *18*, 128.

[33] J. Vazquez, M. A. Pericas, F. Maseras, A. Lledos, *J. Org. Chem.* **2000**, *65*, 7303.

[34] B. Goldfuss, M. Steigelmann, S. I. Khan, K. N. Houk, *J. Org. Chem.* **2000**, *65*, 77.

[35] M. C. Kozlowski, S. L. Dixon, M. Panda, G. Lauri, *J. Am. Chem. Soc.* **2003**, *125*, 6614.

[36] R. Noyori, S. Suga, H. Oka, M. Kitamura, *Chem. Rec.* **2001**, *1*, 85.

[37] M. Kitamura, S. Suga, M. Niwa, R. Noyori, *J. Am. Chem. Soc.* **1995**, *117*, 4832.

[38] K. Funabashi, M. Jachmann, M. Kanai, M. Shibasaki, *Angew. Chem. Int. Ed.* **2003**, *42*, 5489.

[39] Y. F. Kang, L. Liu, R. Wang, W. J. Yan, Y. F. Zhou, *Tetrahedron Asymmetry.* **2004**, *15*, 3155.

[40] E. F. DiMauro, M. C. Kozlowski, *Org. Lett.* **2001**, *3*, 3053.

[41] B. L. Pagenkopf, E. M. Carreira, *Tetrahedron Lett.* **1998**, *39*, 9593.

[42] Y. Hamashima, D. Sawada, M. Kanai, M. Shibasaki, *J. Am. Chem. Soc.* **1999**, *121*, 2641.

[43] M. Kanai, Y. Hamashima, M. Takamura, M. Shibasaki, *J. Synth. Org. Chem. Jpn.* **2001**, *59*, 766.

[44] Y. Hamashima, D. Sawada, H. Nogami, M. Kanai, M. Shibasaki, *Tetrahedron.* **2001**, *57*, 805.

[45] M. Takamura, Y. Hamashima, H. Usuda, M. Kanai, M. Shibasaki, *Angew. Chem. Int. Ed.* **2000**, *39*, 1650.

[46] H. Nogami, S. Matsunaga, M. Kanai, M. Shibasaki, *Tetrahedron Lett.* **2001**, *42*, 279.

[47] J. Casas, C. Najera, J. M. Sansano, J. M. Saa, *Org. Lett.* **2002**, *4*, 2589.

[48] J. Casas, C. Najera, J. M. Sansano, J. M. Saa, *Tetrahedron.* **2004**, *60*, 10487.

[49] J. Casas, A. Baeza, J. M. Sansano, C. Najera, J. M. Saa, *Tetrahedron Asymmetry.* **2003**, *14*, 197.

[50] A. Baeza, J. Casas, C. Najera, J. M. Sansano, J. M. Saa, *Angew. Chem. Int. Ed.* **2003**, *42*, 3143.

[51] M. Takamura, K. Funabashi, M. Kanai, M. Shibasaki, *J. Am. Chem. Soc.* **2000**, *122*, 6327.

[52] E. Ichikawa, M. Suzuki, K. Yabu, M. Albert, M. Kanai, M. Shibasaki, *J. Am. Chem. Soc.* **2004**, *126*, 11808.

[53] K. Funabashi, H. Ratni, M. Kanai, M. Shibasaki, *J. Am. Chem. Soc.* **2001**, *123*, 10784.

[54] Y. C. Shen, X. M. Feng, G. L. Zhang, Y. Z. Jiang, *Synlett.* **2002**, 1353.

[55] Y. C. Shen, X. M. Feng, Y. Li, G. L. Zhang, Y. Z. Jiang, *Tetrahedron.* **2003**, *59*, 5667.

[56] Y. C. Shen, X. M. Feng, Y. Li, G. L. Zhang, Y. Z. Jiang, *Eur. J. Org. Chem.* **2004**, 129.

[57] J. R. Porter, W. G. Wirschun, K. W. Kuntz, M. L. Snapper, A. H. Hoveyda, *J. Am. Chem. Soc.* **2000**, *122*, 2657.

[58] C. A. Krueger, K. W. Kuntz, C. D. Dzierba, W. G. Wirschun, J. D. Gleason, M. L. Snapper, A. H. Hoveyda, *J. Am. Chem. Soc.* **1999**, *121*, 4284.

[59] N. S. Josephsohn, K. W. Kuntz, M. L. Snapper, A. H. Hoveyda, *Abs. Pap. Am. Chem. Soc.* **2002**, *224*, 439.

[60] N. S. Josephsohn, K. W. Kuntz, M. L. Snapper, A. H. Hoveyda, *J. Am. Chem. Soc.* **2001**, *123*, 11594.

[61] H. B. Deng, M. R. Isler, M. L. Snapper, A. H. Hoveyda, *Angew. Chem. Int. Ed.* **2002**, *41*, 1009.

[62] A. E. Taggi, A. M. Hafez, H. Wack, B. Young, D. Ferraris, T. Lectka, *J. Am. Chem. Soc.* **2002**, *124*, 6626.

[63] S. France, H. Wack, A. M. Hafez, A. E. Taggi, D. R. Witsil, T. Lectka, *Org. Lett.* **2002**, *4*, 1603.

[64] A. E. Taggi, A. M. Hafez, T. Lectka, *Acc. Chem. Res.* **2003**, *36*, 10.

[65] S. France, M. H. Shah, A. Weatherwax, H. Wack, J. P. Roth, T. Lectka, *J. Am. Chem. Soc.* **2005**, *127*, 1206.

[66] S. France, A. Weatherwax, A. E. Taggi, T. Lectka, *Acc. Chem. Res.* **2004**, *37*, 592.

[67] P. M. Pihko, *Angew. Chem. Int. Ed.* **2004**, *43*, 2062.

[68] P. R. Schreiner, *Chem. Soc. Rev.* **2003**, *32*, 289.

[69] A. Wittkopp, P. R. Schreiner, *Chem. Eur. J.* **2003**, *9*, 407.

[70] P. R. Schreiner, A. Wittkopp, *Org. Lett.* **2002**, *4*, 217.

[71] T. Okino, Y. Hoashi, Y. Takemoto, *J. Am. Chem. Soc.* **2003**, *125*, 12672.

[72] T. Okino, Y. Hoashi, T. Furukawa, X. N. Xu, Y. Takemoto, *J. Am. Chem. Soc.* **2005**, *127*, 119.

[73] B. Vakulya, S. Varga, A. Csampai, T. Soos, *Org. Lett.* **2005**, *7*, 1967.

[74] B. J. Li, L. Jiang, M. Liu, Y. C. Chen, L. S. Ding, Y. Wu, *Synlett.* **2005**, 603.

[75] T. Okino, S. Nakamura, T. Furukawa, Y. Takemoto, *Org. Lett.* **2004**, *6*, 625.

[76] Y. Hoashi, T. Yabuta, Y. Takemoto, *Tetrahedron Lett.* **2004**, *45*, 9185.

[77] A. Berkessel, F. Cleemann, S. Mukherjee, T. N. Muller, J. Lex, *Angew. Chem. Int. Ed.* **2005**, *44*, 807.

[78] A. Berkessel, S. Mukherjee, F. Cleemann, T. N. Muller, J. Lex, *Chem. Commun.* **2005**, 1898.

[79] M. S. Taylor, E. N. Jacobsen, *J. Am. Chem. Soc.* **2004**, *126*, 10558.

[80] P. Vachal, E. N. Jacobsen, *J. Am. Chem. Soc.* **2002**, *124*, 10012.

[81] M. S. Sigman, E. N. Jacobsen, *Abs. Pap. Am. Chem. Soc.* **1998**, *216*, 231.

[82] A. V. Malkov, A. Mariani, K. N. MacDougall, P. Kocovsky, *Org. Lett.* **2004**, *6*, 2253.

[83] T. Hayashi, K. Kishi, A. Yamamoto, Y. Ito, *Tetrahedron Lett.* **1990**, *31*, 1743.

[84] T. Hayashi, A. Yamamoto, Y. Ito, E. Nishioka, H. Miura, K. Yanagi, *J. Am. Chem. Soc.* **1989**, *111*, 6301.

[85] T. Hayashi, K. Kanehira, T. Hagihara, M. Kumada, *J. Org. Chem.* **1988**, *53*, 113.

[86] T. Hayashi, A. Yamamoto, T. Hagihara, Y. Ito, *Tetrahedron Lett.* **1986**, *27*, 191.

[87] T. Hayashi, *Pure Appl. Chem.* **1988**, *60*, 7.

[88] M. Schinnerl, C. Bohm, M. Seitz, O. Reiser, *Tetrahedron Asymmetry.* **2003**, *14*, 765.

[89] Y. Ito, M. Sawamura, T. Hayashi, *J. Am. Chem. Soc.* **1986**, *108*, 6405.

[90] M. Sawamura, Y. Nakayama, T. Kato, Y. Ito, *J. Org. Chem.* **1995**, *60*, 1727.

[91] A. Togni, S. D. Pastor, *J. Org. Chem.* **1990**, *55*, 1649.

[92] M. Sawamura, Y. Ito, T. Hayashi, *Tetrahedron Lett.* **1990**, *31*, 2723.

[93] T. Hayashi, M. Sawamura, Y. Ito, *Tetrahedron.* **1992**, *48*, 1999.

[94] Y. Ito, M. Sawamura, H. Hamashima, T. Emura, T. Hayashi, *Tetrahedron Lett.* **1989**, *30*, 4681.

[95] M. Sawamura, Y. Ito, T. Hayashi, *Tetrahedron Lett.* **1989**, *30*, 2247.

[96] A. Togni, S. D. Pastor, *Tetrahedron Lett.* **1989**, *30*, 1071.

[97] V. K. Aggarwal, H. AbdelRahman, L. Fan, R. V. H. Jones, M. C. H. Standen, *Chem. Eur. J.* **1996**, *2*, 1024.

[98] V. K. Aggarwal, L. Bell, M. P. Coogan, P. Jubault, *J. Chem. Soc. Perkin Trans. 1.* **1998**, 2037.

[99] P. I. Dalko, L. Moisan, *Angew. Chem. Int. Ed.* **2004**, *43*, 5138.

[100] J. Seayad, B. List, *Org. Biomol. Chem.* **2005**, *3*, 719.

[101] W. Notz, F. Tanaka, C. F. Barbas, *Acc. Chem. Res.* **2004**, *37*, 580.

[102] B. List, *Acc. Chem. Res.* **2004**, *37*, 548.

[103] Z. G. Hajos, D. R. Parrish, *J. Org. Chem.* **1974**, *39*, 1615.

[104] U. Eder, G. Sauer, R. Wiechert, *Angew. Chem. Int. Ed.* **1971**, *10*, 496.

[105] B. List, R. A. Lerner, C. F. Barbas, *J. Am. Chem. Soc.* **2000**, *122*, 2395.

[106] A. B. Northrup, D. W. C. MacMillan, *J. Am. Chem. Soc.* **2002**, *124*, 6798.

[107] A. Cordova, W. Notz, C. F. Barbas, *Chem. Commun.* **2002**, 3024.

[108] Y. Sekiguchi, A. Sasaoka, A. Shimomoto, S. Fujioka, H. Kotsuki, *Synlett.* **2003**, 1655.

[109] A. Bogevig, N. Kumaragurubaran, K. A. Jorgensen, *Chem. Commun.* **2002**, 620.

[110] H. E. Zimmerman, M. D. Traxler, *J. Am. Chem. Soc.* **1957**, *79*, 1920.

[111] W. Notz, B. List, *J. Am. Chem. Soc.* **2000**, *122*, 7386.

[112] C. Pidathala, L. Hoang, N. Vignola, B. List, *Angew. Chem. Int. Ed.* **2003**, *42*, 2785.

[113] A. Cordova, W. Notz, C. F. Barbas, *J. Org. Chem.* **2002**, *67*, 301.

[114] N. S. Chowdari, D. B. Ramachary, A. Cordova, C. F. Barbas, *Tetrahedron Lett.* **2002**, *43*, 9591.

[115] P. Pojarliev, W. T. Biller, H. J. Martin, B. List, *Synlett.* **2003**, 1903.

[116] Y. Hayashi, W. Tsuboi, M. Shoji, N. Suzuki, *J. Am. Chem. Soc.* **2003**, *125*, 11208.

[117] Y. Hayashi, W. Tsuboi, I. Ashimine, T. Urushima, M. Shoji, K. Sakai, *Angew. Chem. Int. Ed.* **2003**, *42*, 3677.

[118] B. List, P. Pojarliev, W. T. Biller, H. J. Martin, *J. Am. Chem. Soc.* **2002**, *124*, 827.

[119] B. List, *J. Am. Chem. Soc.* **2000**, *122*, 9336.

[120] W. Notz, F. Tanaka, S. Watanabe, N. S. Chowdari, J. M. Turner, R. Thayumanavan, C. F. Barbas, *J. Org. Chem.* **2003**, *68*, 9624.

[121] A. Cordova, *Synlett.* **2003**, 1651.

[122] Y. Hayashi, J. Yamaguchi, T. Sumiya, K. Hibino, M. Shoji, *J. Org. Chem.* **2004**, *69*, 5966.

[123] G. F. Zhong, *Angew. Chem. Int. Ed.* **2003**, *42*, 4247.

[124] A. Cordova, H. Sunden, A. Bogevig, M. Johansson, F. Himo, *Chem. Eur. J.* **2004**, *10*, 3673.

[125] A. Bogevig, H. Sunden, A. Cordova, *Angew. Chem. Int. Ed.* **2004**, *43*, 1109.

[126] Y. Hayashi, J. Yamaguchi, T. Sumiya, M. Shoji, *Angew. Chem. Int. Ed.* **2004**, *43*, 1112.

[127] Y. Hayashi, J. Yamaguchi, K. Hibino, M. Shoji, *Tetrahedron Lett.* **2003**, *44*, 8293.

[128] M. Engqvist, J. Casas, H. Sunden, I. Ibrahem, A. Cordova, *Tetrahedron Lett.* **2005**, *46*, 2053.

[129] H. Sunden, M. Engqvist, J. Casas, I. Ibrahem, A. Cordova, *Angew. Chem. Int. Ed.* **2004**, *43*, 6532.

[130] A. Bogevig, K. Juhl, N. Kumaragurubaran, W. Zhuang, K. A. Jorgensen, *Angew. Chem. Int. Ed.* **2002**, *41*, 1790.

[131] N. Kumaragurubaran, K. Juhl, W. Zhuang, A. Bogevig, K. A. Jorgensen, *J. Am. Chem. Soc.* **2002**, *124*, 6254.

[132] B. List, *J. Am. Chem. Soc.* **2002**, *124*, 5656.

[133] N. Vignola, B. List, *J. Am. Chem. Soc.* **2004**, *126*, 450.

[134] B. List, P. Pojarliev, H. J. Martin, *Org. Lett.* **2001**, *3*, 2423.

[135] D. Enders, A. Seki, *Synlett.* **2002**, 26.

[136] M. Shi, L. H. Chen, C. Q. Li, *J. Am. Chem. Soc.* **2005**, *127*, 3790.

[137] R. L. Letsinger, S. H. Dandegaonker, *J. Am. Chem. Soc.* **1959**, *81*, 498.

[138] M. Lauer, G. Wulff, *J. Organomet. Chem.* **1983**, *256*, 1.

[139] S. W. Coghlan, R. L. Giles, J. A. K. Howard, L. G. F. Patrick, M. R. Probert, G. E. Smith, A. Whiting, *J. Organomet. Chem.* **2006**, *690*, 4784.

[140] B. J. Bunn, P. J. Cox, N. S. Simpkins, *Tetrahedron.* **1993**, *49*, 207.

[141] P. J. Cox, N. S. Simpkins, *Tetrahedron Asymmetry.* **1991**, *2*, 1.

[142] B. J. Bunn, N. S. Simpkins, *J. Org. Chem.* **1993**, *58*, 533.

[143] J. Clayden, C. C. Stimson, M. Keenan, A. E. H. Wheatley, *Chem. Commun.* **2004**, 228.

[144] J. Clayden, F. E. Knowles, C. J. Menet, *Tetrahedron Lett.* **2003**, *44*, 3397.

[145] J. Clayden, C. J. Menet, *Tetrahedron Lett.* **2003**, *44*, 3059.

[146] J. Clayden, M. N. Kenworthy, M. Helliwell, *Org. Lett.* **2003**, *5*, 831.

[147] J. Clayden, Y. J. Y. Foricher, H. K. Lam, *Eur. J. Org. Chem.* **2002**, 3558.

[148] J. Clayden, C. J. Menet, K. Tchabanenko, *Tetrahedron.* **2002**, *58*, 4727.

[149] R. A. Bragg, J. Clayden, C. J. Menet, *Tetrahedron Lett.* **2002**, *43*, 1955.

[150] J. Clayden, S. Purewal, M. Helliwell, S. J. Mantell, *Angew. Chem. Int. Ed.* **2002**, *41*, 1049.

[151] R. A. Bragg, J. Clayden, M. Bladon, O. Ichihara, *Tetrahedron Lett.* **2001**, *42*, 3411.

[152] J. Clayden, R. P. Davies, M. A. Hendy, R. Snaith, A. E. H. Wheatley, *Angew. Chem. Int. Ed.* **2001**, *40*, 1238.

[153] R. A. Bragg, J. Clayden, *Tetrahedron Lett.* **1999**, *40*, 8323.

[154] R. A. Bragg, J. Clayden, *Tetrahedron Lett.* **1999**, *40*, 8327.

[155] A. Ahmed, J. Clayden, S. A. Yasin, *Chem. Commun.* **1999**, 231.

[156] D. S. Matteson, *J. Organomet. Chem.* **1999**, *581*, 51.

[157] R. J. Mattson, K. M. Pham, D. J. Leuck, K. A. Cowen, *J. Org. Chem.* **1990**, *55*, 2552.

[158] A. F. Abdel-Magid, K. G. Carson, B. D. Harris, C. A. Maryanoff, R. D. Shah, *J. Org. Chem.* **1996**, *61*, 3849.

[159] J. Knowles, *Unpublished results*, **2005**.

[160] http://www.ccdc.cam.ac.uk.

[161] E. Vedejs, R. W. Chapman, S. C. Fields, S. Lin, M. R. Schrimpf, *J. Org. Chem.* **1995**, *60*, 3020.

[162] H. Günther, *NMR spectroscopy*, 2nd ed., Wiley, Stutgart, **2001**.

[163] T. Ishiyama, M. Murata, N. Miyaura, *J. Org. Chem.* **1995**, *60*, 7508.

[164] A. Suzuki, *J. Organomett. Chem.* **1999**, *576*, 147.

[165] K. Wada, T. Mizutani, S. Kitagawa, *J. Org. Chem.* **2003**, *68*, 5123.

[166] W. Q. Yang, J. Yan, G. Springsteen, S. Deeter, B. H. Wang, *Bioorg. Med. Chem. Lett.* **2003**, *13*, 1019.

[167] A. P. Lightfoot, G. Maw, C. Thirsk, S. J. R. Twiddle, A. Whiting, *Tetrahedron Lett.* **2003**, *44*, 7645.

[168] J. A. Zoltewicz, C. D. Dill, *Tetrahedron.* **1996**, *52*, 14469.

[169] E. C. Butterworth, I. M. Heilbron, D. H. Hey, *J. Chem. Soc.* **1940**, 355.

[170] A. Beeby, A. Congreve, *Unpublished results,* **2002**.

[171] Abramovi.Ra, M. Saha, *J. Chem. Soc. B Phys. Org.* **1966**, 733.

[172] W. E. Parham, C. K. Bradsher, *Acc. Chem. Res.* **1982**, *15*, 300.

[173] W. F. Bailey, J. J. Patricia, *J. Organomet. Chem.* **1988**, *352*, 1.

[174] P. J. Steel, G. B. Caygill, *J. Organomet. Chem.* **1987**, *327*, 101.

[175] P. Sett, S. Chattopadhyay, P. K. Mallick, *Spectrochim. Acta A Mol. Biomol. Spectrosc.* **2000**, *56*, 855.

[176] J. T. B. H. Jastrzebski, G. van Koten, K. Goubitz, C. Arlen, P. M., *J. Organomet. Chem.* **1983**, *246*, 75.

[177] C. Chuit, R. J. P. Corriu, P. Monforte, C. Reye, J. P. Declercq, A. Dubourg, *J. Organomet. Chem.* **1996**, *511*, 171.

[178] M. F. de la Torre, M. C. Caballero, A. Whiting, *Tetrahedron.* **1999**, *55*, 8547.

[179] S. Darses, G. Michaud, J. P. Genet, *Eur. J. Org. Chem.* **1999**, 1875.

[180] E. Vedejs, S. C. Fields, R. Hayashi, S. R. Hitchcock, D. R. Powell, M. R. Schrimpf, *J. Am. Chem. Soc.* **1999**, *121*, 2460.

[181] G. Conole, A. Clough, A. Whiting, *Acta Cryst. Sect. C Cryst. Struct. Commun.* **1995**, *51*, 1056.

[182] E. Vedejs, S. C. Fields, M. R. Schrimpf, *J. Am. Chem. Soc.* **1993**, *115*, 11612.

[183] P. W. Fowler, A. Soncini, *Chem. Phys. Lett.* **2004**, *383*, 507.

[184] P. V. Schleyer, H. J. Jiao, N. Hommes, V. G. Malkin, O. L. Malkina, *J. Am. Chem. Soc.* **1997**, *119*, 12669.

[185] P. W. Fowler, E. Steiner, *J. Phys. Chem. A* **1997**, *101*, 1409.

[186] K. Jug, *J. Org. Chem.* **1983**, *48*, 1344.

[187] G. Alcaraz, L. Euzenat, O. Mongin, C. Katan, I. Ledoux, J. Zyss, M. Blanchard-Desce, M. Vaultier, *Chem. Commun.* **2003**, 2766.

[188] M. Lauer, H. Bohnke, R. Grotstollen, M. Salehnia, G. Wulff, *Chem. Ber.* **1985**, *118*, 246.

[189] M. Bielecki, H. Eggert, J. C. Norrild, *J. Chem. Soc. Perkin Trans. 2* **1999**, 449.

[190] S. Toyota, M. Asakura, T. Futakawa, M. Oki, *Bull. Chem. Soc. Jpn.* **1999**, 72, 1879.

[191] H. Noth, B. Wrackmeyer, P. Diehl, E. Fluck, R. Kosfield, *N.M.R. Spectroscopy of Boron Compounds*, Springer-Verlag, Berlin, **1978**.

[192] A. Gryff-Keller, *Bull. Pol. Ac. Sci. Chem.* **1998**, *46*, 105.

[193] B. A. Deore, I. Yu, M. S. Freund, *J. Am. Chem. Soc.* **2004**, *126*, 52.

[194] S. J. Gaskell, F. L. Brancia, S. J. Oliver, *Rapid Commun. Mass Spectrom.* **2000**, *14*, 2070.

[195] R. T. Hawkins, A. U. Blackham, *J. Am. Chem. Soc.* **1967**, *32*, 597.

[196] C. Najera, *Synlett.* **2002**, 1388.

[197] G. H. Coleman, A. M. Alvarado, *Org. Synth.* **1923**, *3*, 3.

[198] C. N. Webb, *Org. Synth.* **1927**, *7*, 6.

[199] B. S. Jursic, Z. Zdravkovski, *Synth. Commun.* **1993**, *23*, 2761.

[200] L. F. Fieser, J. E. Jones, *Org. Synth.* **1941**, *20*, 66.

[201] M. Mader, P. Helquist, *Tetrahedron Lett.* **1988**, *29*, 3049.

[202] K. Ishihara, Y. Kuroki, N. Hanaki, S. Ohara, H. Yamamoto, *J. Am. Chem. Soc.* **1996**, *118*, 1569.

[203] R. Nomura, T. Nakano, Y. Yamada, H. Matsuda, *J. Org. Chem.* **1991**, *56*, 4076.

[204] K. Ishihara, S. Ohara, H. Yamamoto, *J. Org. Chem.* **1996**, *61*, 4196.

[205] K. Ishihara, S. Ohara, H. Yamamoto, *Macromolecules.* **2000**, *33*, 3511.

[206] K. Ishihara, S. Ohara, H. Yamamoto, D. T. Amos, R. L. Danheiser, *Org. Synth.*, *79*, 176.

[207] K. Ishihara, S. Kondo, H. Yamamoto, *Synlett.* **2001**, 1371.

[208] R. Latta, G. Springsteen, B. H. Wang, *Synthesis.* **2001**, 1611.

[209] P. Tang, H. Krause, A. Furstner, *Org. Syn.* **2004**, *81*, 262.

[210] J. Cossy, C. Palegrosdemange, *Tetrahedron Lett.* **1989**, *30*, 2771.

[211] Micromath, 2.02 ed.

[212] Microsoft, **2003**.

[213] L. H. Toporcer, R. E. Dessy, S. I. E. Green, *J. Am. Chem. Soc* **1965**, *87*, 1236.

[214] K. V. Nahabedian, H. G. Kuivila, *J. Am. Chem. Soc* **1961**, *83*, 2167.

[215] T. A. Houston, B. L. Wilkinson, J. T. Blanchfield, *Org. Lett.* **2004**, *6*, 679.

[216] W. W. Lowrence, *Tetrahedron Lett.* **1971**, 3453.

[217] H. C. Brown, T. P. Stocky, *J. Am. Chem. Soc.* **1977**, *99*, 8218.

[218] A. Pelter, M. G. Hutchings, T. E. Levitt, K. W. Smith, *Chem. Commun.* **1970**, 347.

[219] A. Dal Negro, L. Ungaretti, A. Perotti, *J. Chem. Soc., Dalton Trans.* **1972**, 1639.

[220] A. Pelter, T. E. Levitt, P. Nelson, *Tetrahedron.* **1970**, *26*, 1899.

[221] A. F. Burchat, J. M. Chong, N. Nielsen, *J. Organomet. Chem.* **1997**, *542*, 281.

[222] C. M. Vogels, H. L. Wellwood, K. Biradha, M. J. Zaworotko, S. A. Westcott, *Can. J. Chem.* **1999**, *77*, 1196.

[223] A. Tillack, I. Rudloff, M. Beller, *Eur. J. Org. Chem.* **2001**, 523.

[224] M. Jedrzejczak, R. E. Motie, D. P. N. Satchell, *J. Chem. Soc. Perkin Trans. 2.* **1993**, 599.

[225] C. T. Chen, J. H. Kuo, V. D. Pawar, Y. S. Munot, S. S. Weng, C. H. Ku, C. Y. Liu, *J. Org. Chem.* **2005**, *70*, 1188.

[226] D. Barillier, M. P. Strobel, L. Morin, D. Paquer, *New J. Chem.* **1982**, *6*, 201.